

Aus dem  
CharitéCentrum 13 für Innere Medizin mit Gastroenterologie und Nephrologie  
Medizinische Klinik mit Schwerpunkt Nephrologie und Internistische Intensivmedizin  
Charité Universitätsmedizin Berlin

Direktor: Professor Dr. med. Kai-Uwe Eckardt

# **Habilitationsschrift**

**Einfluss der pulmonalen Zirkulation und Variablen der Hämostase  
auf das akute Lungenversagen des Erwachsenen  
unter besonderer Berücksichtigung von COVID-19**

zur Erlangung der Lehrbefähigung

für das Fach Innere Medizin

vorgelegt dem Fakultätsrat der Medizinischen Fakultät

Charité - Universitätsmedizin Berlin

von

Dr. med. Jan Kruse

Eingereicht: September 2021

Dekan: Prof. Dr. med. R. Pries

1. Gutachter\* in: Prof Dr Sascha David

2. Gutachter\* in Prof Dr Carsten Willam

# Inhaltsverzeichnis

Abkürzungsverzeichnis.....	3
1. Einleitung.....	4
2. Wissenschaftliche Fragestellungen .....	8
3. Eigene Arbeiten .....	10
3.1. Welche Rolle spielt die Perfusion für den Gasaustausch der Lunge? Einfluss von inhalativem Stickstoffmonoxid in niedrigen Konzentrationen.....	10
3.2. Lässt sich das pulmonalvaskuläre Kapillarleck im ARDS Quantifizieren? Die Rolle der Sonographie. ....	18
3.3. Welche Rolle spielt die Gerinnungskaskade im COVID-ARDS? .....	29
3.3.1 <i>Hypofibrinolyse bei Patienten mit schwerer COVID-19-Erkrankung</i> .....	29
3.3.2 <i>Die Hypofibrinolyse nach schwerer COVID 19-Erkrankung ist reversibel</i> .....	43
3.4. Wie beeinflusst die Gerinnungs- und Perfusionsstörung der Lungen Morphologie und Verlauf des ARDS? Lungenkavitationen im C-ARDS.....	56
4. Diskussion .....	68
5. Zusammenfassung .....	71
6. Literatur .....	72
7. Danksagung .....	75
8. Erklärung .....	76

## 1. Abkürzungsverzeichnis

ARDS	Adult Respiratory Distress Syndrome
C-ARDS	COVID-19 assoziiertes akutes Lungenversagen
COVID-19	Durch das Coronavirus SARS-CoV-2 ausgelöste Erkrankung
EVLWI	Extravaskulärer Lungenwasserindex
DIC	Disseminierte intravasale Gerinnung
ML	Maximum lysis
NO	Stickstoffmonoxid
N <sub>2</sub> O	Lachgas
PEEP	Positive endexpiratory pressure
Ppb	Parts per billion
ROTEM®	Rotationsthrombelastometrie, Firma Tem Innovations GmbH, München

## 1. Einleitung

Seit der Erstbeschreibung des akuten Lungenversagens oder Adult Respiratory Distress Syndrome (ARDS) im Jahre 1967 <sup>1</sup> hat sich das Verständnis für die Ursachen und die Pathogenese dieses Symptomkomplexes enorm weiterentwickelt. Dennoch bleibt sowohl die Prävalenz als auch die Mortalität des akuten Lungenversagens unverändert hoch <sup>2</sup>

Es scheint ausgeprägte Gemeinsamkeiten in der Pathophysiologie dieses Symptomkomplexes zu geben, beispielhaft seien die zentrale Bedeutung der inflammatorischen Kaskaden und den entsprechenden Mediatoren genannt und die Bedeutung die dem Zusammenbruch der alveolo-kapillären Barrieren zukommt <sup>3</sup>. Dennoch ist in den letzten Jahren auch immer klarer geworden, dass die Pathophysiologie im Detail ebenso vielfältig ist wie die Ursachen, die zu einem akuten Lungenversagen führen können. Diese Tatsache kann auch zur Erklärung der Schwierigkeiten angeführt werden, trotz teilweise großer, randomisierter multizentrischer Studien die zu diesem Thema durchgeführt wurden, effektive therapeutische Strategien zu entwickeln, um die Prognose der betroffenen Patienten nachhaltig zu verbessern.

Lediglich für die lungenschonende Beatmung, die restriktive Flüssigkeitsbilanzierung und die Bauchlagerung konnte in großen Studien ein nachhaltiger Effekt auf die Prognose eines heterogenen Kollektivs von ARDS-Patienten gezeigt werden<sup>4,5,6</sup> Für andere vielversprechende therapeutische Ansätze wie den Einsatz von Muskelrelaxantien und die extrakorporale Lungenersatztherapie ist die Datenlage weiterhin nicht eindeutig.<sup>7 8 9</sup>

Die Ursachen eines akuten Lungenversagens sind vielfältig.

Neben Pneumonien und Pneumonitiden durch unterschiedlichste Erreger und Noxen, zählen Sepsis, Pankreatitiden, Traumata und Verbrennungen zu den häufigeren Auslösern.

Natürlich steht die Behandlung der auslösenden Grunderkrankung immer im Vordergrund der therapeutischen Bemühungen.

Dennoch muss bei diesen schweren Erkrankungen nicht selten das gesamte Spektrum der therapeutischen Möglichkeiten der modernen Intensivmedizin zum Einsatz kommen, um eine ausreichend lange Stabilisierung der Vitalfunktionen zu ermöglichen, die eine kausale Therapie des Grundleidens überhaupt erst ermöglicht.

Traditionell steht hierbei die Beatmungstherapie und deren Feinjustierung weit im Vordergrund des Interesses. Störungen der Belüftung, der Ventilation, der Lungen scheinen therapeutischen Interventionen vergleichsweise leicht zugänglich.

Sauerstoffapplikation, nicht-invasive Beatmungsstrategien und die endotracheale Intubation und gegebenenfalls auch Tracheotomie sind Standardinterventionen der Intensivmedizin und die radiologisch in schweren Fällen des Lungenversagens nahezu immer nachweisbaren teilweise ausgedehnten Belüftungsstörungen der Lungen unterstreichen die Bedeutung einer Sicherstellung der Lungenventilation oftmals eindrucksvoll.

Entsprechend ist in den vergangenen Jahren und Jahrzehnten ein Großteil des wissenschaftlichen Fokus auf diesen Aspekt des akuten Lungenversagens und seiner Therapie gerichtet worden.

Viele Fragestellungen aus diesem Bereich sind entsprechend mit randomisierten, teilweise multizentrischen Fragestellungen untersucht worden.

Das „Open-Lung“-Konzept sei hier beispielhaft genannt und eine Vielzahl von wissenschaftlichen Untersuchungen widmete sich seither der Frage, durch welche

Feineinstellung der Überdruckbeatmung eine ausreichende Eröffnung und Offenhalten der kollabierten Lungenareale und damit einer Verbesserung des Gasaustausches erreicht werden könne.

Insbesondere der Einstellung des optimalen positiven endexpiratorischen Druckes (PEEP) kam hierbei ein hoher Grad an Aufmerksamkeit zu.

Dass letztlich ein adäquates Verhältnis zwischen Ventilation und Perfusion für den Erfolg der Maßnahmen, gemessen an der Sauerstoffversorgung und der Kohlendioxidentfernung des Patienten entscheidend ist, wird nicht immer im gleichen Maße bedacht.

Weder der klinischen Untersuchung am Patientenbett, noch den gängigen radiologischen Verfahren wie dem bettseitigen Röntgenbild der Thoraxorgane oder der Computertomographie ist die Lungenperfusion in gleichem Ausmaße zugänglich. Die Lungenperfusion ist deutlich schwerer mit diesen Verfahren beurteilbar als das Lungenparenchym und Faktoren wie der Gerinnungssituation der Patienten wird häufig deutlich weniger Beachtung geschenkt als dem Ausmaß der Belüftung.

Seit Dezember 2019 führte die Verbreitung eines neuartigen Coronavirus, SARS-CoV-2, das erstmals in der chinesischen Provinz Wuhan nachgewiesen wurde zu einer weltweiten Pandemie. Die durch dieses Virus ausgelöste Erkrankung wird als COVID-19 bezeichnet und ist in ihrem Verlauf unter anderem durch eine hohe Rate von schweren akuten Formen des Lungenversagens charakterisiert (C-ARDS). Mittlerweile hat sie sich über alle Kontinente verbreitet und bislang und über 4 219 000 Todesopfer gefordert.<sup>10</sup>

Bereits früh im Verlauf der Pandemie wurde über Besonderheiten im Verlauf des C-ARDS berichtet, was die mechanischen Eigenschaften der Lungen der betroffenen

Patienten betrifft und postuliert, dass diese sich substantiell von denen anderer Patienten im akuten Lungenversagen unterscheiden <sup>11</sup>.

Gleichermaßen wurde bereits früh eine besondere prothrombotische Disposition von Patienten die an COVID-19 erkrankten postuliert<sup>12</sup>

In der Folge wurde immer wieder über deutlich erhöhte Inzidenzen thromboembolischer Ereignissen und über deutliche Erhöhung der Marker des Gerinnungssystems wie des Fibrinogens und von Fibrinogenspaltprodukten berichtet<sup>13</sup>.

Welche Rolle die Lungenperfusion in der Pathogenese des akuten Lungenversagens im Allgemeinen und des C-ARDS im Besonderen spielt ist Gegenstand dieser Untersuchung.

## 2. Wissenschaftliche Fragestellungen

Die Tatsache, dass das Verhältnis von Ventilation zu Perfusion der Lungen eine der entscheidenden Determinanten für den pulmonalen Gasaustausch darstellt ist seit langem weitgehend unumstritten <sup>14</sup>

Im Allgemeinen scheint jedoch einer Verbesserung der Ventilation in diesem Kontext traditionell ein höherer Grad an Aufmerksamkeit geschenkt zu werden, wenn es um eine Verbesserung dieses Missverhältnisses geht. Beispielhaft seien die internationalen großen und häufig multizentrisch angelegten Studien genannt, die sich über Jahrzehnte mit der Frage des optimalen Niveaus des positiven endexpiratorischen Druckes (PEEP) und sogenannten Rekrutierungsmanövern befasst haben um die Situation des Patienten mit ARDS auf der Intensivstation zu verbessern. <sup>15-18</sup>

Vergleichsweise wenig beachtet ist demgegenüber die Frage, welchen Einfluss Alterationen des vaskulären und des Gerinnungssystems auf Pathogenese und Verlauf des akuten Lungenversagens ausüben. Die vaskuläre Hyperpermeabilität im Sinne eines schweren Kapillarlecks ist ein bekannter Faktor, die adäquate Diagnostik zur Einschätzung des Schweregrades ist jedoch weiterhin Gegenstand der Forschung. <sup>3,19</sup>

Betrachtet man das COVID-ARDS (C-ARDS) im Besonderen, so können sowohl die Beobachtung gehäufte thromboembolischer Ereignisse als auch die Darstellung zum Teil ausgedehnter In-Situ-Thrombosen in der pulmonalen Strombahn in Obduktionsserien als Hinweis auf eine herausragende Bedeutung der Lungenperfusion in der Pathogenese dieser Erkrankung gewertet werden. <sup>20,21</sup>

Es ergeben sich folgende wissenschaftliche Fragestellungen:

1. Wie stark ist die vaskuläre Komponente an Veränderungen des Gasaustausches.
2. Lässt sich das pulmonalvaskuläre Kapillarleck im ARDS quantifizieren
3. Welche Rolle spielt die Gerinnungskaskade im ARDS und C-ARDS
4. Wie beeinflussen Perfusionsstörungen die Morphologie und Pathogenese des C-ARDS

### 3. Eigene Arbeiten

#### 3.1. Welche Rolle spielt die Perfusion für den Gasaustausch der Lunge? Einfluss von inhalativem Stickstoffmonoxid in niedrigen Konzentrationen

Inhalatives Stickstoffmonoxid (NO) wird seit 1991 in der klinischen Behandlung von Patienten mit akutem Lungenversagen eingesetzt<sup>22</sup>. Das Molekül wirkt vasodilatierend und aufgrund seiner kurzen Halbwertszeit und hohen Reagibilität bewirkt es bei inhalativer Aufnahme eine selektive Vasodilatation in den ventilerten Lungenarealen mit der Folge einer homogeneren Verteilung von Ventilation und Perfusion und einer Verringerung des Missverhältnisses dieser beiden essentiellen Komponenten des Gasaustausches.<sup>23</sup>

Eine Metaanalyse aus dem Jahr 2017 kann zu dem Schluss, dass inhalatives Stickstoffmonoxid zwar den pulmonalen Gasaustausch zumindest vorübergehend in vielen Fällen verbessern kann, dass es aber keinen Beweis für einen positiven Effekt auf klinisch relevante Endpunkte gibt während sich Hinweise für eine Häufung akuter Nierenschädigungen fanden<sup>24</sup>.

Dennoch findet Stickstoffmonoxid weiterhin breite Verwendung als Therapie in schweren Fällen des akuten Lungenversagens.

In einer Untersuchung konnten wir an Patienten, die sich einem elektiven kardiochirurgischen Eingriff unterzogen, dass bereits NO-Konzentrationen im Bereich von wenigen parts per billion (ppb) einen signifikanten Effekt auf den Gasaustausch der Patienten hatten und die Oxygenierung signifikant verbesserten.

Hierfür wurden die Patienten, die sich einem elektiven kardio-chirurgischen operativen Eingriff unterzogen nach Einleitung der Narkose und Implementierung eines erweiterten hämodynamischen Monitorings einschließlich pulmonalarteriellen

Einschwemmkatheter nacheinander mit komprimierter Luft, synthetischer Luft und einem Gemisch aus Lachgas ( $\text{N}_2\text{O}$ ) und synthetischer Luft beatmet.

Gleichzeitig wurde die Stickstoffmonoxidkonzentration im In- und Expirationsschenkel des Beatmungssystems gemessen.

Während die Stickstoffmonoxidkonzentration in der komprimierten Luft, die aus der Umgebung des Krankenhauses in einer urbanen Gegend angesogen wurde, abhängig von Witterung und Verkehrsaufkommen, Konzentrationen im einstelligen bis niedrig-zweistelligen ppb Bereich enthielt, war die synthetische Luft erwartungsgemäß  $\text{NO}$ -frei. Für Lachgas ist eine Kontamination mit Stickstoffmonoxid, bedingt durch den Herstellungsprozess bekannt. Entsprechend bewegte sich die gemessene Stickstoffmonoxidkonzentration im Inspirationsschenkel im gleichen Bereich, wie in der komprimierten Luft.

Nach einer Einwaschphase nach Wechsel des Beatmungsgemisches waren die registrierten arteriellen Sauerstoffpartialdrücke ( $\text{paO}_2$ ) unter Beatmung mit synthetischer Luft signifikant niedriger als unter Beatmung mit komprimierter Luft oder besagtem Lachgasgemisch. Diese Beobachtungen lassen den Schluss zu, dass sich die beobachteten Effekte auf den Gasaustausch auf die im Gasgemisch enthaltenen niedrigen Stickstoffmonoxidkonzentrationen und den mit ihrer Zufuhr verbundenen selektiven vasodilatatorischen Effekte zurückzuführen ist.

Hier zeigt sich eindrucksvoll, wie ausgeprägt die vaskuläre Komponente die Effektivität des pulmonalen Gasaustauschs ist und lässt darauf schließen dass Veränderungen im pulmonalvaskulären System, in Perfusion und Gerinnungssystem auch in der Situation eines akuten Lungenversagens eine substantielle Bedeutung für den Gasaustausch der Patienten zukommt.<sup>25</sup>

**W.Hess, J. Kannmacher, J. Kruse: Contamination of anaesthetic gases with nitric oxide and its influence on oxygenation: study in patients undergoing open heart surgery; Br J Anaesth 2004; 93: 629-33**

## CLINICAL INVESTIGATIONS

## Contamination of anaesthetic gases with nitric oxide and its influence on oxygenation: study in patients undergoing open heart surgery<sup>†</sup>

W. Hess\*, J. Kannmacher and J. Kruse

Department of Anaesthesiology and Operative Intensive Care, AK St Georg Hospital, Lohmühlenstraße 5, 20099 Hamburg, Germany

\*Corresponding author. E-mail: hessana@g-email.de

**Background.** Nitric oxide is important in vasomotor regulation. Contamination of anaesthetic gases with nitric oxide could affect gas exchange.

**Methods.** We measured oxygenation and nitric oxide concentrations in the inspiratory and expiratory limb of the ventilator circuit in patients about to have cardiac surgery. Measurements were made before surgery when the circulation and respiratory conditions were stable.  $F_{I_{O_2}}$  was set at 0.35. The breathing circuit was supplied with a fresh gas flow greater than the minute volume so that exhaled gas was not re-used. Three gas mixtures were given in sequence to each patient: oxygen and compressed air (AIRc), oxygen and nitrous oxide, and oxygen and synthetic air (AIRs) that was free from nitric oxide. All patients were given AIRs as the second gas and the other two gas mixtures (AIRc and nitrous oxide) were given randomly as the first and third gases.

**Results.** During ventilation with oxygen–AIRc, the median nitric oxide concentration was 5.6 ppb, during ventilation with oxygen–nitrous oxide it was 5.0 ppb and using oxygen–AIRs it was 1.5 ppb. When AIRc and nitrous oxide were used,  $P_{a_{O_2}}$  was greater and venous admixture was less than when AIRs was used. The different gas mixtures did not affect pulmonary vascular pressures or cardiac output.

**Conclusions.** Compressed air and nitrous oxide contain very low concentrations of nitric oxide (<10 ppb). This can affect pulmonary oxygen transfer during anaesthesia.

*Br J Anaesth* 2004; **93**: 629–33

**Keywords:** anaesthetics gases; complications, nitric oxide contamination; oxygen, inspired concentration, partial pressure

Accepted for publication: June 22, 2004

Nitric oxide is an important substance involved in many biological processes, including neurotransmission, cellular host defence and gastrointestinal motility, and is a key substance in vasomotor regulation.<sup>1,2</sup>

Inhaled nitric oxide has been used to treat infants with pulmonary artery hypertension (PAH) and adults with acute lung injury (ALI).<sup>3</sup> Nitric oxide concentrations of 100–2000 ppb can improve arterial oxygenation in patients with ALI,<sup>4</sup> and concentrations of 5–40 ppm are used for treating PAH.

Compressed air (AIRc) is used in generic anaesthetic machines or ventilators. This AIRc contains variable amounts of nitric oxide as a result of air pollution,<sup>5–7</sup> and this may affect lung function. In addition, ventilation with a mixture of nitrous oxide and oxygen is common in general

anaesthesia. Little is known about the effects of contamination of nitrous oxide by nitric oxide.

We investigated pulmonary artery pressure and oxygen exchange in patients before cardiac surgery. We used a constant  $F_{I_{O_2}}$  of 0.35 and mixtures of oxygen with compressed air, nitrous oxide and synthetic air which contains less nitric oxide.

### Methods

After approval from the ethics committee (Ethik-Kommission der Ärztekammer Hamburg) and with written

<sup>†</sup>This article is accompanied by Editorial I.

consent we studied 37 patients (NYHA II–III) who were about to have elective cardiac surgery. We excluded patients with known lung disease or poor left ventricular function (ejection fraction <0.3).

The patients were premedicated with flunitrazepam 1–2 mg orally. An ECG lead II and a pulse oximeter probe were attached. A pulmonary artery catheter (Baxter, Irvine, CA, USA) and arterial and venous cannulae were placed before induction of anaesthesia. Anaesthesia was induced with etomidate 0.2 mg kg<sup>-1</sup>, fentanyl 5 µg kg<sup>-1</sup> and pancuronium 0.1 mg kg<sup>-1</sup>. Anaesthesia was maintained with propofol 0.5 mg kg<sup>-1</sup> h<sup>-1</sup> i.v.

After tracheal intubation, the lungs were ventilated with a set volume (Cicero Machine, Dräger, Lübeck, Germany). The fresh gas flow was set to be greater than the respiratory minute volume to avoid rebreathing of alveolar gas. In a correctly functioning system without leaks, the fresh gas flow can be reduced to the alveolar minute volume so that only fresh and dead-space gas are present in the system at the start of the next inspiration. The respiratory minute volume was first adjusted to obtain an end-tidal carbon dioxide fraction of 3.5–4.0 vol %. Later, ventilation was adjusted to obtain an arterial pressure between 4.4 and 5.4 kPa (see Table 3 below). The inspiratory and expiratory concentrations of oxygen, nitrous oxide and end-tidal carbon dioxide were measured with an anaesthetic gas analyzer (Cardiocard, Datex, Finland).

When the circulation and respiratory state were stable, three different gas mixtures were used successively for ventilation:

- (i) oxygen plus compressed air (AIRc) with  $F_{I_{O_2}}=0.35$ ;
- (ii) oxygen plus synthetic air (AIRs) with  $F_{I_{O_2}}=0.35$ ;
- (iii) oxygen plus nitrous oxide with  $F_{I_{O_2}}=0.35$ .

During the use of each gas mixture we measured the inspiratory (NO<sub>insp</sub>) and expiratory (NO<sub>exp</sub>) concentrations of nitric oxide 20 cm away from the Y-piece in the inspiratory and expiratory limbs of the breathing circuit. We used a chemiluminescent analyzer (TE24C-Chemiluminescens-NO-NO<sub>2</sub>-NOx-Analysator, Thermo Instruments GmbH, Dortmund, Germany). This device measures nitric oxide concentrations down to 0.4 ppb and is linear to within 1% over the range 0.4 ppb to 100 ppm. We calibrated the analyzer periodically using three calibrating gases: pure nitrogen, nitrogen containing 180 ppb nitric oxide and nitrogen containing 320 ppb nitric oxide.

During ventilation with each gas mixture, we measured the following: inspiratory and expiratory oxygen concentration, inspiratory and expiratory nitrous oxide concentration, end-tidal carbon dioxide concentration, heart rate, mean arterial pressure, mean central venous pressure, mean pulmonary arterial pressure, mean pulmonary artery wedge pressure, cardiac output (thermodilution method), and arterial and mixed venous blood gases.

The pulmonary vascular resistance and the total peripheral resistance were calculated using standard formulae.

The alveolar–arterial oxygen partial pressure difference  $P(A-a)_{O_2}$  was calculated using the alveolar air equation:

$$P_{A_{O_2}} = F_{I_{O_2}}(P_{\text{bar}} - P_{H_2O}) - P_{A_{CO_2}}/R + ([P_{A_{CO_2}}/R] \times [F_{I_{O_2}} - R])$$

where  $R$  is the respiratory quotient. Values of  $P_{\text{bar}}=101.08$  kPa,  $P_{H_2O}=6.25$  kPa and  $R=0.8$  were assumed. The shunt fraction  $Q_s/Q_T$  was calculated using the equation:

$$Q_s/Q_T = (C_c'O_2 - C_aO_2) / (C_c'O_2 - C_vO_2)$$

Arterial, venous and capillary oxygen saturation were obtained from line charts representing the oxyhaemoglobin dissociation curve (Kelman and Nunn) after correction of saturation for pH using the nomogram given by Kelman and Nunn.<sup>8</sup>

The oxygen content  $Co_2$  was calculated using the formula:

$$Co_2 = Hb \times 1.37 So_2 + Po_2 \alpha$$

where  $\alpha$  is the solubility coefficient (Bunsen) and has a value of 0.0228 ml dl<sup>-1</sup> kPa<sup>-1</sup> for oxygen, and each gram of haemoglobin can bind 1.37 ml of oxygen. The oxygen content of end-capillary blood was calculated from the ideal alveolar  $PO_2$ .

After the study was completed, anaesthesia appropriate for the subsequent surgery was started.

### Statistical analysis

Data are expressed as the median with the (25, 75) quartile or as the mean and standard deviation (SD). The data distributions are displayed using box and whisker plots of the inspiratory and expiratory nitric oxide concentrations. Histograms of the AIRc and nitrous oxide–nitric oxide values were used to determine whether the distribution of the measured concentrations was normal.

Comparisons of values obtained during AIRs–oxygen ventilation with those obtained in the other two periods were made using the Wilcoxon test.

## Results

We studied 37 patients (13 male, 24 female) with a mean age of 66 yr (range 41–80), a mean height of 169 (SD 9) cm and a mean weight of 78 (13) kg. Coronary bypass grafts were planned in 29 patients, aortic valve replacements in three patients, mitral valve replacements in three patients, and aortic and mitral valve replacements in two patients.

The nitric oxide concentrations of the inspired and exhaled gases in the three measurement periods are given in Table 1 as median and quartile values and are shown graphically as box and whisker plots in Figure 1. Differences between oxygen–AIRs and the other gas mixtures are all significant ( $P < 0.0001$ ). Figure 2 shows the distribution of nitric oxide values in the oxygen–AIRc and oxygen–nitrous oxide mixtures. In the oxygen–AIRc mixture the nitric oxide values are nearly normally distributed, but in the

**Table 1** Median and quartile values (25, 75) of the nitric oxide concentrations in the three gas mixtures (AIRc/oxygen, AIRs/oxygen and nitrous oxide (N<sub>2</sub>O)/oxygen) during inspiration and expiration. \*Significantly different from AIRs ( $P < 0.01$ ). \*\*Significantly different from AIRs ( $P < 0.001$ )

	Nitric oxide (ppb)		
	O <sub>2</sub> /AIRc	O <sub>2</sub> /AIRs	O <sub>2</sub> /N <sub>2</sub> O
Inspired			
Median	5.6**	1.5	5.0**
Quartile (25, 75)	(3.8, 8.2)	(1.0, 1.7)	(3.6, 6.4)
Expired			
Median	4.2**	2.8	3.3*
Quartile (25, 75)	(2.9, 5.6)	(2.1, 3.5)	(2.8, 3.8)

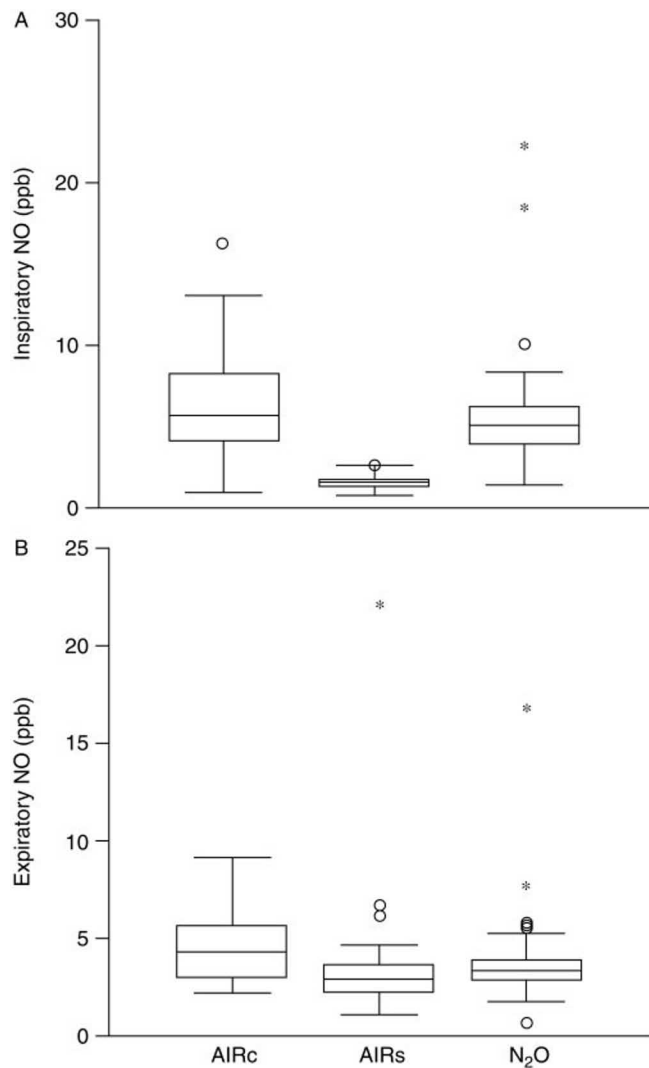


**Fig 1** Box and whisker plots (median, quartile, range) for (A) inspired and (B) expired nitric oxide concentrations during ventilation with the three gas mixtures. ○ Adjacent values; \*outlier.

oxygen–nitrous oxide mixture the values for two patients fall outside the normal distribution curve.

Figure 3 shows the individual values of the arterial  $P_{O_2}$  during ventilation with compressed air, synthetic air and the

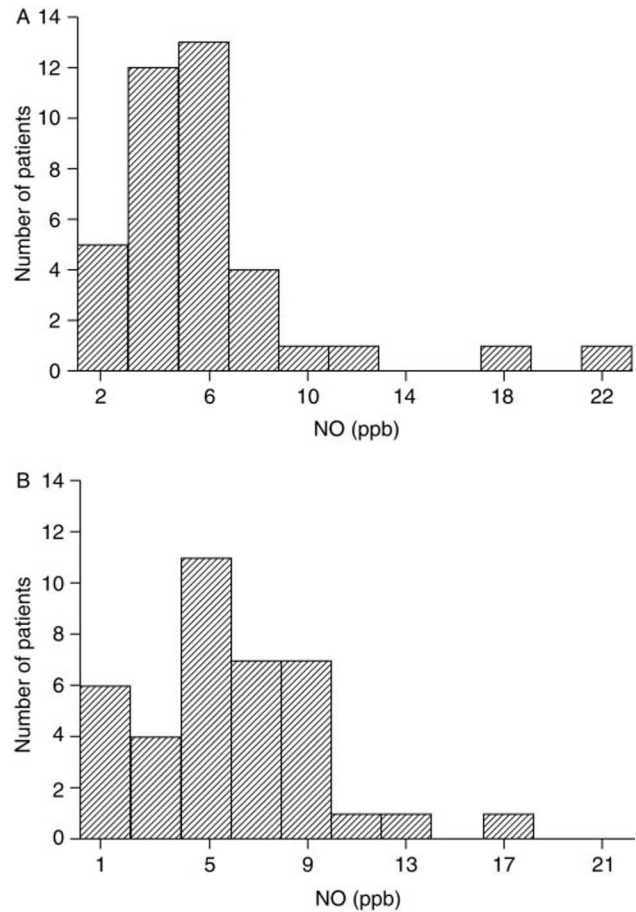


**Fig 2** Histograms of the nitric oxide values showing the distribution during ventilation with (A) nitrous oxide–oxygen and (B) AIRc–oxygen mixtures.

nitrous oxide mixture. Lines link values for the same patient. The dotted line indicates that the gas mixture was given first (AIRc,  $n=20$ ; nitrous oxide,  $n=17$ ); the solid line indicates that the gas mixture was given last.

Table 2 presents the oxygenation data as medians and quartile values. Measures of oxygenation were significantly different during ventilation with AIRc and nitrous oxide mixtures:  $P_{a_{O_2}}$  was greater and  $P_{(A-a)_{O_2}}$  and  $Q_S/Q_T$  were less with the nitrous oxide mixture than with AIRs. The mixed venous oxygen partial pressure was significantly greater during ventilation with AIRc than with AIRs, but the difference was not significant during ventilation with nitrous oxide.

The haemodynamic values obtained during the study are listed in Table 3. The heart rate, the cardiac output and the arterial, atrial and pulmonary pressures did not differ significantly in the three study periods.

The arterial carbon dioxide pressure was 4.7 (0.4) during ventilation with AIRc, 4.6 (0.5) during ventilation with AIRs and 4.6 (0.5) during ventilation with nitrous oxide. The pulmonary vascular resistance and total peripheral resistance did not change substantially with any of the different gas mixtures.

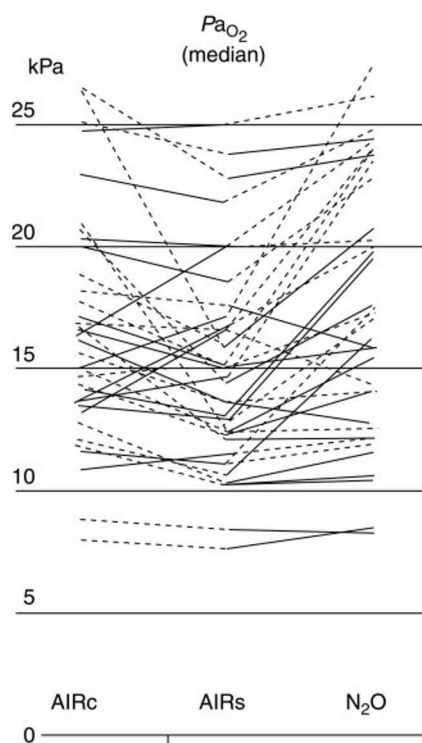


**Fig 3** Individual  $Pa_{O_2}$  values for patients during the three study periods. Lines link values for the same patient. The dotted line indicates that the gas mixture was given first (AIRc,  $n=20$ ; nitrous oxide,  $n=17$ ); the solid line indicates that it was given last. The AIRs–oxygen mixture was always given second.

**Table 2** Arterial oxygen partial pressure ( $Pa_{O_2}$ ), alveolar–arterial oxygen partial pressure difference ( $P(A-a)_{O_2}$ ), mixed venous oxygen tension ( $Pv_{O_2}$ ) and calculated values of venous admixture (in %). The data are presented as median and quartile values (25, 75). \*Significantly different from AIRs ( $P<0.01$ ). \*\*Significantly different from AIRs ( $P<0.001$ ). NS, not significant;  $N_2O$ , nitrous oxide

	AIRc	AIRs	$N_2O$
$Pa_{O_2}$ (kPa)			
Median	14.9*	14.4	16.6**
Quartile (25, 75)	(12.9, 19.3)	(11.8, 16.9)	(12.5, 23.1)
$P(A-a)_{O_2}$ (kPa)			
Median	12.2*	13.0	10.3*
Quartile (25, 75)	(8.4, 14.5)	(10.2, 15.9)	(4.9, 15.3)
$Pv_{O_2}$ (kPa)			
Median	4.9*	4.7	4.8 (NS)
Quartile (25, 75)	(4.6, 5.5)	(4.5, 5.1)	(4.4, 5.3)
$Q_s/Q_t$ (%)			
Median	9.7**	12.7	8.4**
Quartile (25, 75)	(5.8, 12.1)	(8.1, 18.6)	(5.5, 14.0)

## Discussion

Compressed air and nitrous oxide are used commonly in combination with oxygen to ventilate patients during general anaesthesia. We found that both gases contained low concentrations of nitric oxide. The contamination of compressed air with nitric oxide is well known. Low concentrations of nitric oxide in compressed air can improve

**Table 3** Haemodynamic values during the three study periods (mean, (SD)). HR, heart rate; mAP, mean arterial pressure; mPAP, mean pulmonary artery pressure; mPCWP, mean pulmonary capillary wedge pressure; mRAP, mean right atrial pressure; CO, cardiac output; SVR, systemic vascular resistance; PVR, pulmonary vascular resistance;  $N_2O$ , nitrous oxide. Arterial partial pressure of carbon dioxide ( $Pa_{CO_2}$ ) is indicated as mean (SD)

	AIRc	AIRs	$N_2O$
HR (beats $min^{-1}$ )	63 (14)	63 (15)	63 (15)
mAP (mm Hg)	70 (9)	69 (10)	68 (10)
mPAP (mm Hg)	21.2 (7.9)	21.2 (7.5)	21.7 (7.2)
mPCWP (mm Hg)	12.7 (6.0)	12.9 (6.1)	13.3 (5.6)
mRAP (mm Hg)	8.6 (3.2)	8.6 (3.2)	9.2 (3.4)
CO ( $l\ min^{-1}$ )	4.1 (1.0)	4.0 (1.1)	3.7 (1.2)
SVR ( $dyn\ s\ cm^{-5}$ )	1296 (474)	1319 (539)	1369 (544)
PVR ( $dyn\ s\ cm^{-5}$ )	189 (137)	189 (129)	207 (146)
$Pa_{CO_2}$ (kPa)	4.7 (0.4)	4.6 (0.5)	4.7 (0.5)

arterial oxygenation in adult and paediatric ICU patients.<sup>6,7,9</sup> The mean nitric oxide concentrations used in those studies (70–140 ppb) were greater than in the present study (median 5.6 ppb). We checked our measurement device by measuring nitric oxide concentrations at a control point for air pollution near the hospital on the same day (median 4.0 (3.2–7.8) ppb). The lower level of air pollution is due to the location of Hamburg near the North Sea.

We found that the concentration of nitric oxide in nitrous oxide was similar to that in compressed air. Nitrous oxide is produced by heating ammonium nitrate to 240°C. After cleaning, it is liquefied under pressure. Overheating can result in contamination with nitric oxide and nitrogen dioxide. German standards require that nitric oxide contamination of nitrous oxide must not exceed 1 ppm. The concentrations we found were much less than this value (the highest concentration was 22.3 ppb).

The inspiratory nitric oxide values in nitrous oxide were not normally distributed. In our hospital nitrous oxide is stored in large tanks. When a tank is empty, nitrous oxide is taken from the next tank. The tanks do not contain supplies from the same batch. In contrast, synthetic air is obtained from small tanks, and this gas is highly purified for analytical use.

Surprisingly, these very low concentrations of nitric oxide in AIRc and nitrous oxide had significant effects on oxygenation in intubated and ventilated patients. Physiologically, nitric oxide is produced in the respiratory tract, with the largest contribution coming from the upper airways.<sup>10–12</sup> Intubation deprives the inspired gas of its natural source of nitric oxide. Ventilation with nitric oxide free AIRs significantly affected oxygenation. We did not find a correlation between concentrations of nitric oxide in the inspiratory gas mixture and the effects on oxygenation. This supports previous findings.<sup>6,7</sup>

The increase in arterial  $PO_2$  and the decrease in  $P(A-a)_{O_2}$  and the venous admixture during ventilation with nitrous oxide, relative to the values obtained during ventilation with AIRs, were obviously more pronounced than those during ventilation with AIRc. Nitrous oxide can

cause vasoconstriction.<sup>13–15</sup> In combination with nitric oxide this effect of nitrous oxide could reduce shunt, as has been shown with the vasoconstrictor almitrine. We should also consider the second-gas effect.<sup>16</sup> At the onset of ventilation with nitrous oxide, this gas is absorbed from the alveoli into the blood more rapidly than nitrogen diffuses from blood to the alveoli. This increases the alveolar partial pressures of oxygen and nitric oxide. When nitrogen is washed out and the body is saturated with nitrous oxide the second-gas effect ceases. This process takes about 10 min. We did not start our measurements until the expiratory nitrous oxide concentration had reached the inspiratory value. Thus it is unlikely that the second-gas effect was important. Further study would be needed to determine whether nitrous oxide has an additional effect on oxygenation and matching of ventilation and perfusion.

We measured the nitric oxide concentration in both the inspiratory and the expiratory limbs of the ventilation circuit. The concentration of exhaled nitric oxide should correspond to the production of nitric oxide in the lower airways when ventilated with AIRs. It was between 1.5 and 2.8 ppb. Some of the nitric oxide inspired with AIRc and nitrous oxide was taken up. Assuming an endogenous production of 2.8 ppb, the share of exhaled nitric oxide was calculated as 26% during ventilation with AIRc. Therminarias and colleagues<sup>17</sup> found that about a third of the inspired nitric oxide was re-exhaled. During ventilation with nitrous oxide the calculated uptake of nitric oxide was greater and the percentage of exhaled nitric oxide was only 7%. This could be caused by the second-gas effect.

In summary, our data demonstrate the following. Intubation deprives the patient, at least partially, of the natural source of nitric oxide during inspiration. Nitric oxide free synthetic air impairs pulmonary oxygen exchange. Compressed air and nitrous oxide often contain very low concentrations of nitric oxide (<10 ppb). However, these concentrations can increase oxygenation. There is no correlation between the concentration of nitric oxide and the decrease in  $P_{(A-a)O_2}$ . An individual value between 3 and 5 ppb nitric oxide is probably necessary to obtain physiological matching of ventilation with perfusion.

In our study we found that the nitric oxide concentrations in nitrous oxide were similar to those found in compressed air.

## References

- 1 Palmer RM, Ferrige AG, Moncada S. Nitric oxide release accounts for the biological activity of endothelium-derived relaxing factor. *Nature* 1987; **327**: 524–6

- 2 Ignarro LJ, Buga GM, Wood KS, Byrns RE, Chaudhuri G. Endothelium-derived relaxing factor produced and released from artery and vein is nitric oxide. *Proc Natl Acad Sci USA* 1987; **84**: 9265–9
- 3 Steudel W, Hurford WE, Zapol WM. Inhaled nitric oxide. Basic biology and clinical applications. *Anesthesiology* 1999; **91**: 1090–1121
- 4 Gerlach H, Pappert D, Lewandowski K, Rossaint R, Falke KJ. Long-term inhalation with evaluated low doses of nitric oxide for selective improvement of oxygenation in patients with adult respiratory distress syndrome. *Intensive Care Med* 1993; **19**: 443–9
- 5 Pinsky MR, Genc F, Lee KH, Delgado E. Contamination of hospital compressed air with nitric oxide. *Chest* 1997; **111**: 1759–63
- 6 Lee KH, Tan PS, Rico P, Delgado E, Kellum JA, Pinsky MR. Low levels of nitric oxide contaminant in hospital compressed air: physiologic significance? *Crit Care Med* 1997; **25**: 1143–6
- 7 Benzing A, Loop T, Mols G, Geiger K. Unintended inhalation of nitric oxide by contamination of compressed air. *Anesthesiology* 1999; **91**: 945–50
- 8 Nunn JF (ed.) *Nunn's Applied Respiratory Physiology*, 4th Edn. Oxford: Butterworth Heinemann, 1993; p. 573
- 9 Gerlach H, Rossaint R, Pappert D, Knorr M, Falke KJ: Autoinhalation of nitric oxide after endogenous synthesis in nasopharynx. *Lancet*, 1994; **343**: 518–19
- 10 Schedin U, Frostell C, Persson MG, Jakobsson J, Andersson G, Gustafsson LE. Contribution from upper and lower airways to exhaled endogenous nitric oxide in humans. *Acta Anaesthesiol Scand* 1995; **39**: 327–32
- 11 Lundberg JOM, Weitzberg E, Lundberg JM, Alving K. Nitric oxide in exhaled air. *Eur Respir J* 1996; **9**: 2671–80
- 12 Smith N, Eger E, Stoelting R. The cardiovascular and sympathomimetic responses to the addition of nitrous oxide to halothane in man. *Anesthesiology* 1970; **324**: 10–21
- 13 Eiserle J, Smith N. Cardiovascular effects of 40 percent nitrous oxide in man. *Anesth Analg* 1973; **51**: 956–61
- 14 Lappas D, Mortimer J, Laver M. Left ventricular performance and pulmonary circulation following addition of nitrous oxide to morphine during coronary artery surgery. *Anesthesiology* 1975; **43**: 61–9
- 15 Lu Q, Mourgeon E, Law-Koune JD, et al. Dose–response curves of inhaled nitric oxide with and without almitrine in nitric oxide responding patients with acute respiratory distress syndrome. *Anesthesiology* 1995; **83**: 929–43
- 16 Epstein RM, Rackow H, Salanitro E, Wolf GL. Influence of the concentration effect on the uptake of anesthesia mixtures: the second gas effect. *Anesthesiology* 1964; **25**: 364–71
- 17 Therminarias A, Flore P, Favre-Juvin A, Oddou M, Delaire M, Grimbert F. Air contamination with nitric oxide: effect on exhaled nitric oxide response. *Respir Crit Care Med* 1998; **157**: 791–5

### **3.2. Lässt sich das pulmonalvaskuläre Kapillarleck im ARDS Quantifizieren? Die Rolle der Sonographie.**

Neben den Effekten, die pulmonalvaskuläre Dilatation bzw. – Konstriktion auf den Gasaustausch hat, übt das vaskuläre System auch über sein Endothel und dessen Barrierefunktion entscheidende Einflüsse auf die Pathogenese und den klinischen Verlauf des ARDS aus.<sup>26</sup>

Jede Veränderung, die zu einer Verlängerung der Diffusionsstrecke zwischen Alveolarraum und Blutkompartiment in der pulmonalkapillären Strombahn führt, muss zwangsläufig zu einer deutlichen Einschränkung des pulmonalen Gasaustausches führen, der nur aufgrund der kurzen Distanz der Gasaustauschstrecke effektiv möglich ist<sup>27</sup>. So müssen sich durch ein Kapillarleck bedingte Flüssigkeitseinlagerungen mit einer Verschlechterung der Gasaustauschsituation manifestieren.

Kommt es durch Aktivierung der inflammatorischen Kaskaden zu einer Störung der endothelialen Barrierefunktion, kann zwar die interstitielle Flüssigkeitsakkumulation noch für eine gewisse Zeit durch das lymphatische System und Rücktransport in den vaskulären Raum kompensiert werden, führt jedoch bei Fortschreiten des Prozesses unweigerlich zu vermehrter Flüssigkeitsansammlung im Alveolarraum und zum Lungenödem<sup>28</sup>

Die Ultraschalluntersuchung der Lungen hat in den letzten Jahrzehnten eine zunehmende Bedeutung in der Intensivmedizin erfahren, da sie bettseitig einsetzbar und damit nicht mit dem Risiko eines Transportes des kritisch kranken Patienten behaftet ist.<sup>29</sup>

Kommt es durch interstitielle und alveoläre Flüssigkeitsansammlung zu einer Verdickung der interlobären Septen lassen sich sonographisch vermehrte B-Linien als diagnostisch wertvolle Artefakte darstellen.<sup>30</sup>

Wir stellten uns die Frage, ob die Menge der sonographisch darstellbaren B-Linien im Vergleich zur Referenzmethode des mittels transpulmonaler Thermodilution gemessenen extravaskulären Lungenwasserindex (EVLWI) verlässlich das Ausmaß der pulmonalen Überwässerung darstellen kann um damit die Schwere des Kapillarlecks zu quantifizieren und wie die Korrelation des Ultraschalls im Vergleich zur röntgenologischen Untersuchung der Thoraxorgane am liegenden Patienten mit der Thermodilution als Standardmethode ist .

Wir konnten eine starke Korrelation unseres B-Line-Scores in einem vereinfachten Viersektorenprotokoll des Thorax mit dem extravaskulären Lungenwasserindex in der transthorakalen Thermodilution zeigen. Der Spearmankoeffizient erreichte einen Wert von 0,9 mit statistischer Signifikanz ( $p < 0,001$ ).

Demgegenüber zeigte die Befundung der Röntgenuntersuchung der Thoraxorgane am liegenden Patienten durch eine erfahrene Fachärztin für Radiologie eine deutlich schwächere Korrelation mit dem EVLWI, die auch keine statistische Signifikanz erreichte.

Um die Interobservervariabilität zu überprüfen, wurden die Ultraschallbilder und Videosequenzen durch zwei geblindete Untersucher nachbefundet mit einer ebenfalls statistisch signifikanten und guten Korrelation Grad an Übereinstimmung mit einem (Spearman Koeffizient von 0,72; p-Wert  $< 0.0001$ ).

Unsere Untersuchung führte damit zu der Schlussfolgerung, dass die bettseitige Sonographie der Lunge ein nützliches Instrument zur Einschätzung des Schweregrades der pulmonalen Überwässerung bei Patienten mit ARDS darstellt und Aufschlüsse über den Schweregrad der Schädigung der endothelialen Funktion und damit einer der wesentlichen vaskulären Komponenten in der Pathogenese des Lungenversagens zulässt<sup>31</sup>.

**P. Enghard , S. Rademacher<sup>1</sup> , J. Nee , D. Hasper. , U. Engert , A. Jörre and J. M. Kruse: Simplified lung ultrasound protocol shows excellent prediction of extravascular lung water in ventilated intensive care patients; Crit Care ; 2015; 9:36**

RESEARCH

Open Access

# Simplified lung ultrasound protocol shows excellent prediction of extravascular lung water in ventilated intensive care patients

Philipp Enghard<sup>1</sup>, Sibylle Rademacher<sup>1</sup>, Jens Nee<sup>1</sup>, Dietrich Hasper<sup>1</sup>, Ulrike Engert<sup>2</sup>, Achim Jörres<sup>1</sup> and Jan M Kruse<sup>1\*</sup>

## Abstract

**Introduction:** Ultrasound of the lung and quantification of B lines was recently introduced as a novel tool to detect overhydration. In the present study, we aimed to evaluate a four-region protocol of lung ultrasound to determine the pulmonary fluid status in ventilated patients in the intensive care unit.

**Methods:** Fifty patients underwent both lung ultrasound and transpulmonary thermodilution measurement with the PiCCO system. An ultrasound score based on number of single and confluent B lines per intercostal space was used to quantify pulmonary overhydration. To check for reproducibility, two different intensivists who were blinded as to the ultrasound pictures reassessed and classified them using the same scoring system. The results were compared with those obtained using other methods of evaluating hydration status, including extravascular lung water index (EVLWI) and intrathoracic blood volume index calculated with data from transpulmonary thermodilution measurements. Moreover, chest radiographs were assessed regarding signs of pulmonary overhydration and categorized based on a numeric rating scale.

**Results:** Lung water assessment by ultrasound using a simplified protocol showed excellent correlation with EVLWI over a broad range of lung hydration grades and ventilator settings. Correlation of chest radiography and EVLWI was less accurate. No correlation whatsoever was found with central venous pressure measurement.

**Conclusion:** Lung ultrasound is a useful, non-invasive tool in predicting hydration status in mechanically ventilated patients. The four-region protocol that we used is time-saving, correlates well with transpulmonary thermodilution measurements and performs markedly better than chest radiography.

## Introduction

Ultrasound is readily available at the bedside and is non-invasive, making it an ideal diagnostic tool in the hand of the intensivist. The detection of B lines by ultrasound of the lung to diagnose pulmonary edema in the setting of emergency medicine has previously been reported [1]. Changes in pulmonary hydration status before and after hemodialysis were detectable using ultrasound [2]. B lines can be described as vertical, narrow-based artefacts spreading up to the edge of the screen. In previous studies, researchers found B lines to be

a surrogate of acute interstitial syndrome and confluent B lines to correspond to alveolar edema [3]. In animal studies, a good correlation between lung ultrasound and lung water assessment using gravimetry was found [4]. A steep learning curve has been reported for lung ultrasound, making it a promising tool for the intensivist [5]. Various protocols have been used to assess extravascular lung water (EVLW) in patients in the intensive care unit (ICU) and in outpatients, but to date no agreement has been reached about the best protocol to use in the ICU setting [5]. In a consensus conference, a 28-zone protocol was suggested following studies in which a 28-sector approach was applied in a cardiology setting and in patients undergoing hemodialysis [2,6]. In the ICU setting, simplified models with an eight-sector protocol, and even a two-sector protocol, have been evaluated in comparison with pulmonary

\* Correspondence: jan-matthias.kruse@charite.de

<sup>1</sup>Medizinische Klinik mit Schwerpunkt Nephrologie und Internistische Intensivmedizin, Charité-Universitätsmedizin Berlin, Augustenburger Platz 1, 13353 Berlin, Germany

Full list of author information is available at the end of the article

capillary wedge pressure (PCWP) and EVLW [2,7,8]. In the critical care population, a good prediction of EVLW through ultrasound using an eight-zone protocol has been reported. Additionally, in a study in which a four-zone approach was evaluated in comparison with PCWP, researchers reported promising results [7,9].

Currently, various methods are used to diagnose pulmonary overhydration and guide fluid therapy in the critically ill patient. Transpulmonary thermodilution as a method to measure extravascular lung water index (EVLWI) has become a standard tool in many ICUs, and it has been shown to have a significant correlation to lung gravimetry as the standard *ex vivo* method to assess EVLW [10]. EVLWI was demonstrated to be an independent marker of outcome in acute respiratory distress syndrome (ARDS) and in a population of mixed ICU patients [11,12]. Chest radiography, computed tomography, and measurement of central venous pressure (CVP) or PCWP are also commonly used to gain information about pulmonary water content. Nevertheless, all these methods have their own drawbacks and pitfalls. Exposure to radiation is unavoidable when serial chest radiography is conducted, and ordering chest radiography and waiting for it to be conducted and processed leads to significant delay in decision-making. Transfer to the computed tomography scanner adds the risk of transport of the critically ill patient. Pulmonary artery catheterization and introduction of central venous and arterial lines are invasive procedures that carry their own risks.

At present, little information is available regarding the use of lung ultrasound for EVLW assessment in mechanically ventilated patients in the ICU. In the critical care setting, it is of key importance to receive the necessary information about pulmonary hydration status on the spot to guide further therapy. Lung ultrasound at the bedside is a promising tool to use to achieve this goal, and a simplified approach may be of great value. Here we report the results of 50 ventilated patients who underwent four-sector lung ultrasound and transpulmonary dilution measurements, chest radiography and CVP measurements for comparison of the utility of the different methods for lung water assessment in the ICU.

## Material and methods

### Patients

We enrolled all patients 18 years of age or older who were admitted to our medical ICUs for various diagnoses and underwent lung ultrasound and transpulmonary thermodilution measurements with the PiCCO device (PULSION Medical Systems, Munich, Germany) (Table 1).

The study was approved by the local ethics committee of Charité Universitätsmedizin Berlin (EA4/005/14). No formal consent from the patients was needed according to the ethics committee decision. The study was

**Table 1 Clinical features<sup>a</sup>**

Demographics	Data
Age, yr	62 (21 to 88)
Sex, M/F	29/21
APACHE II score	27 (11 to 47)
Duration of ventilation, hr	343 (23 to 1,836)
EVLWI score	10.0 (5.0 to 31.0)
ITBVI score	941.5 (535.0 to 1,600.0)
PaO <sub>2</sub> /FiO <sub>2</sub>	205.5 (70.0 to 373.0)
Sepsis	17
Pneumonia	6
Acute respiratory distress syndrome	6
Cardiopulmonary resuscitation	6
Acute myocardial infarction	5
Pancreatitis	2
Liver failure	2
Other	6

<sup>a</sup>APACHE II, Acute Physiology and Chronic Health Evaluation II; EVLWI, Extravascular lung water index; ITBVI, Intrathoracic blood volume index; PaO<sub>2</sub>/FiO<sub>2</sub>, Index of arterial partial pressure of oxygen and inspiratory oxygen concentration. Values are reported as medians (minimum to maximum) or counts.

conducted according to the principles of the Declaration of Helsinki [13].

### Ultrasound measurements

A Vivid S6 ultrasound machine and a 3.5-MHz curved array probe (GE Healthcare, Chalfont St Giles, UK) were used for all examinations. A single measurement was recorded for each patient. Patients were scanned while in supine position, and four intercostal spaces (ICSs) were examined: the ICS between the third and fourth ribs and the ICS between the sixth and seventh ribs to the left and right of the sternum and between the parasternal and midclavicular line (Figure 1). The number of single and confluent B lines was recorded, and a score ranging from 0 to 32 was calculated to summarize the B lines of the four ICSs (Table 2). Screenshots of every ICS examined were recorded, and two intensivists who were blinded to the details of the images analyzed them using the same scoring system. The averaged result is presented in Figure 2.

### Transpulmonary thermodilution measurements

All measurements were performed using the PiCCO device. The PiCCO device was applied only for clinical reasons and independently from the study protocol.

Examinations were performed by application a 20-ml bolus of 0.9% saline at 4°C. At least three single measurements were performed with the patient in supine position. If there was a significant variability in the results, further measurements were performed until three conclusive results were obtained.

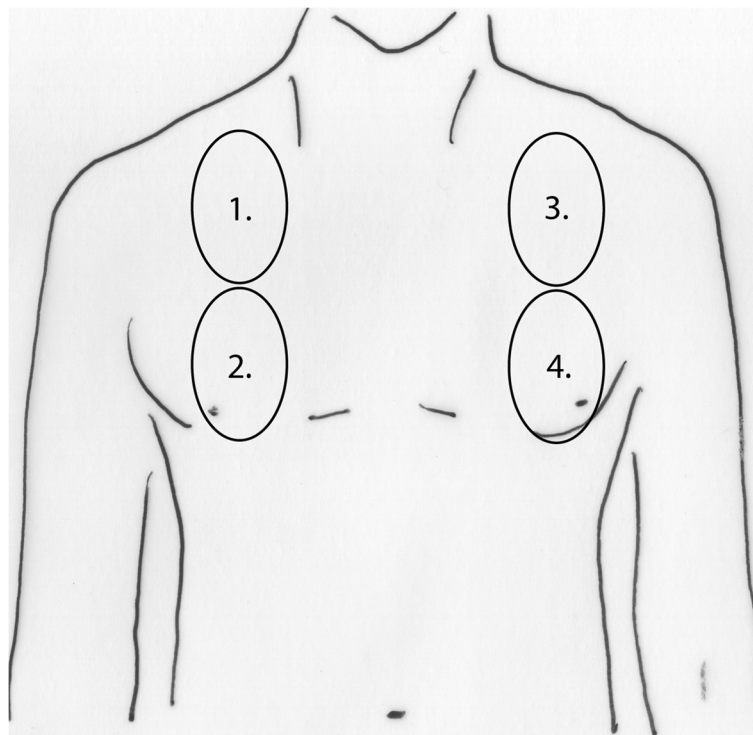


**Figure 1** Scheme of the four parasternal views corresponding to the intercostal spaces between the third and fourth ribs and between the sixth and seventh ribs used to calculate the ultrasound score.

**Radiography**

Anteroposterior chest radiographs with the patient in supine position were obtained within a 24-hour period before or after the ultrasound measurements were recorded. A senior radiology consultant who was blinded as to their details evaluated them for pulmonary fluid burden using a numeric rating scale ranging from 0 to 32 (low = 0 to 10, moderate = 11 to 20 and high = 21+). Kerley A and B lines, grade and distribution of vascular dilatation and opacities, effusions and cardiac enlargement were assessed.

**Table 2** Ultrasound scoring system

Ultrasound finding	Score
No B line/ICS <sup>a</sup>	0
One B line/ICS <sup>a</sup>	1
Two B lines/ICS <sup>a</sup>	2
Three B lines/ICS <sup>a</sup>	3
Four B lines/ICS <sup>a</sup>	4
Five B lines/ICS <sup>a</sup>	5
Confluent B lines >50% ICS <sup>a</sup>	6
Confluent B lines >75% ICS <sup>a</sup>	7
Confluent B lines 100% ICS <sup>a</sup>	8

<sup>a</sup>ICS, Intercostal space.

**Central venous pressure**

The central venous catheter had to be placed in either the internal jugular or subclavian vein, and correct position had to be confirmed by chest radiography. Measurements were taken with the patient in supine position after controlling for the correct positioning of the pressure transducer and zeroing of the transducer. Values were taken retrospectively from the patient’s electronic medical record.

**Statistical analysis**

The Spearman coefficient was used to determine correlations, and a Bland-Altman plot was generated to check for possible bias. Analysis was performed and graphs were generated using GraphPad Prism 6.0 (GraphPad Software, La Jolla, CA, USA) and SPSS (IBM SPSS, Chicago, IL, USA) software.

**Results**

**Presence and extent of B lines intimately correlate with pulmonary water status as assessed by extravascular lung water index**

The EVLWI was measured using the PICCO technology and compared with the lung ultrasound findings. The median duration of the lung ultrasound examination was 2 minutes, with a range from 1.5 to 7 minutes.

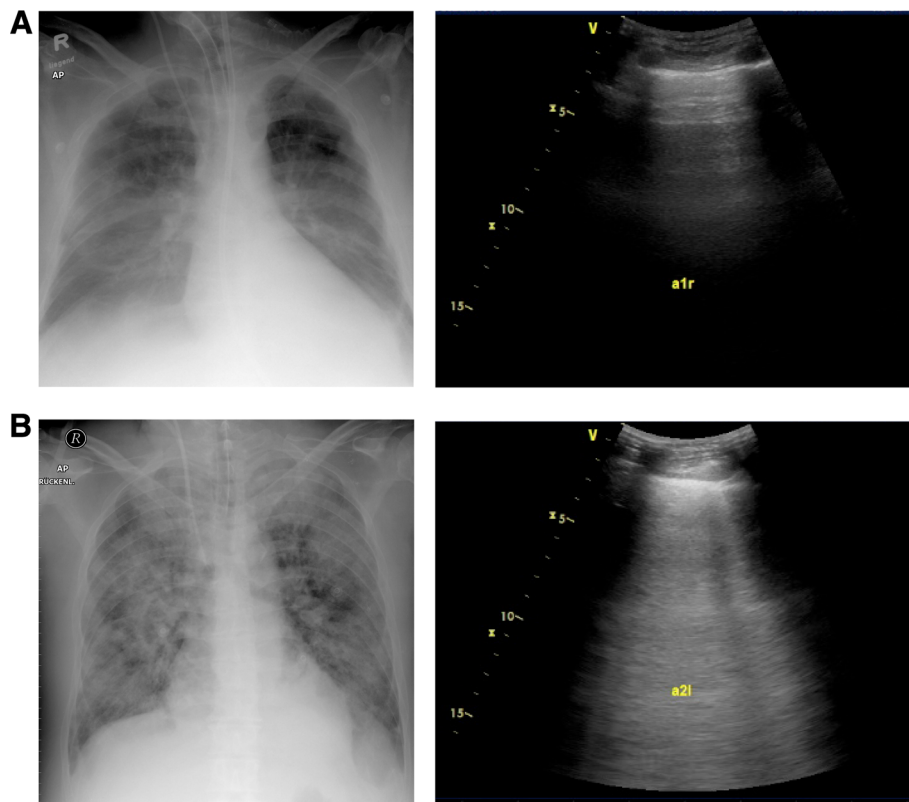


**Figure 2** Chest radiographs (left) and corresponding ultrasound screenshots (right) of two study patients. **(A)** Dry lung with a normal extravascular lung water index (EVLWI) and predominant A lines. **(B)** Severe, non-cardiac pulmonary edema with a high EVLWI and confluent B lines.

Scanning time was recorded for 40 of 50 patients. All included patients were successfully examined, and no dropouts caused by poor examination conditions occurred.

The ultrasound score (US score) calculated directly by the examiner performing the examination closely correlated with the EVLWI (Spearman's  $r = 0.91$ ,  $P < 0.0001$ ) (Figure 3A). To further validate B lines as a tool for assessing the lung water status, the recorded ultrasound pictures were reanalyzed in a blinded fashion by two independent examiners, and the results were averaged. Retrospective blinded assessment slightly reduced the strength of the association with EVLWI; nevertheless, the correlation remained tight and highly significant (Spearman's  $r = 0.72$ ,  $P < 0.0001$ ) (Figure 3B).

A Bland-Altman plot was calculated to assess for any potential bias by comparing the EVLWI and the US score. A bias of 2.52 (mean difference of EVLWI - US score) was observed. Additionally, the difference and average were not independent, suggesting that in patients with low fluid status, the EVLWI was relatively higher than the US score, and the converse was true with increasing lung fluid. A linear regression was calculated according to the method of Bland and Altman [14]. The

linear function- and linear regression-based 95% limits of agreement are shown in Figure 3C.

A receiver operating characteristic curve was calculated to further specify the diagnostic potential of B lines. A US score  $>1.5$  had a sensitivity and specificity of 92.1% and 91.7%, respectively, for diagnosing an EVLWI above the normal value of 7 ml/kg (area under the curve (AUC) = 0.9419). To identify patients with a severely increased EVLWI  $>15$ , a US score of  $>18.5$  had a sensitivity of 92.3% and specificity of 94.6% (AUC = 0.9636) (Figure 3D).

#### Correlation of ultrasound score and PaO<sub>2</sub>/FiO<sub>2</sub>, central venous pressure and intrathoracic blood volume index

The data indicated a significant but weak correlation between the US score and the index of arterial partial pressure of oxygen and inspiratory oxygen concentration (PaO<sub>2</sub>/FiO<sub>2</sub>) (Spearman's  $r = -0.34$ ,  $P = 0.02$ ). The correlation between the EVLWI and the PaO<sub>2</sub>/FiO<sub>2</sub> was also weak, but it was significant (Spearman's  $r = -0.37$ ,  $P = 0.01$ ) (data not shown). Neither CVP (Spearman's  $r = -0.011$ ,  $P = 0.4924$ ) nor intrathoracic blood volume index (ITBVI) (Spearman's  $r = 0.16$ ,  $P = 0.2873$ ) was significantly correlated with the presence and extent of pulmonary B lines (data not shown).

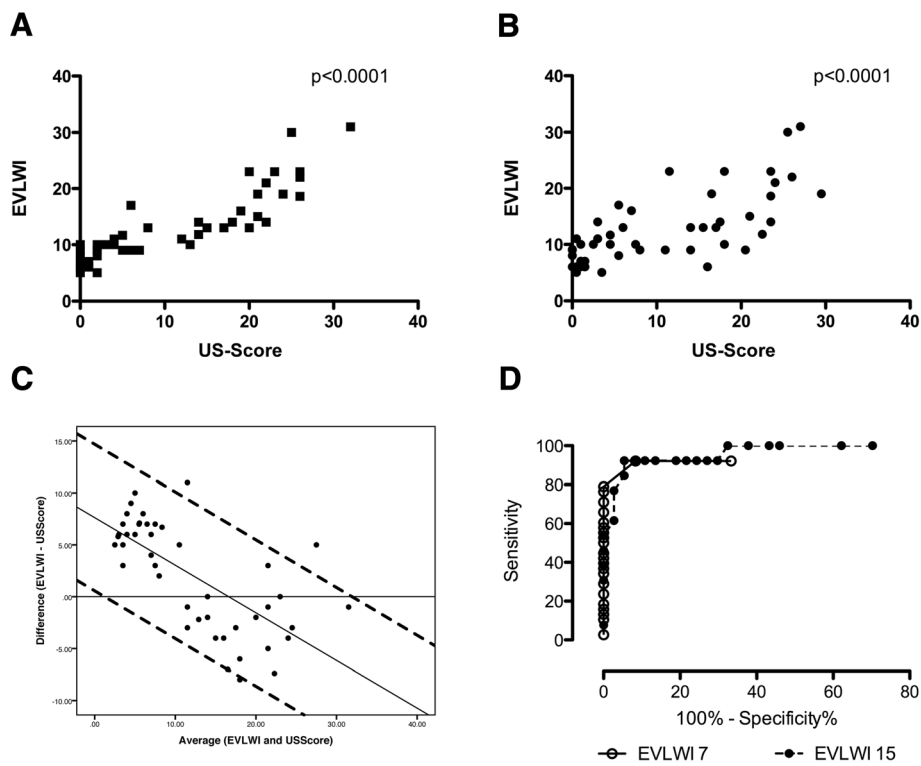


**Figure 3 Correlation of the extravascular lung water index with the ultrasound score.** (A) We found a close correlation of the ultrasound (US) score with the extravascular lung water index (EVLWI) (Spearman’s  $r = 0.91$ ,  $P < 0.0001$ ). (B) Correlation of the blinded US score as a mean of two independent examiners is shown (Spearman’s  $r = 0.72$ ,  $P < 0.0001$ ). (C) Bland-Altman plot comparing the difference (EVLWI – US score) with the average (of EVLWI and US score). Additionally, a linear regression (difference =  $7.62 - 0.46 \times$  average) and the 95% confident intervals (linear regression  $\pm 1.96 \times 3.6$ ) are plotted. (D) Receiver operating characteristic curves of the US score obtained to identify patients with EVLWIs  $>7$  and  $>15$  show excellent diagnostic performance, as indicated by the areas under the curve of 0.9419 and 0.9636.

**Comparison of chest radiography and central venous pressure with EVLWI and ITBVI**

Chest radiography and EVLWI showed a significant, but rather weak, correlation, with a Spearman coefficient of 0.33 and a  $P$ -value of 0.03. No significant correlation

was found between chest radiography and ITBVI, CVP and  $\text{PaO}_2/\text{FiO}_2$  (Figure 4).

Likewise, no significant correlation was found between CVP and the EVLWI (Spearman’s  $r = -0.24$ ,  $P = 0.11$ ). Interestingly, there was also no correlation between CVP

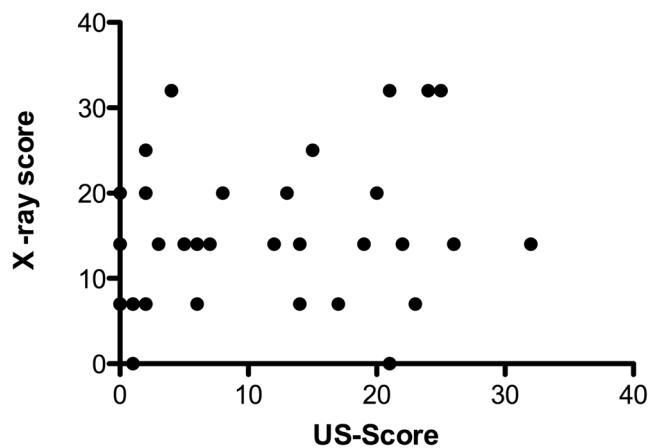


**Figure 4 Comparison of pulmonary fluid status evaluated by chest radiography and ultrasound.** US, Ultrasound.

and ITBVI (Spearman's  $r = 0.06$ ,  $P = 0.73$ ) (Figure 5 and data not shown).

**Discussion**

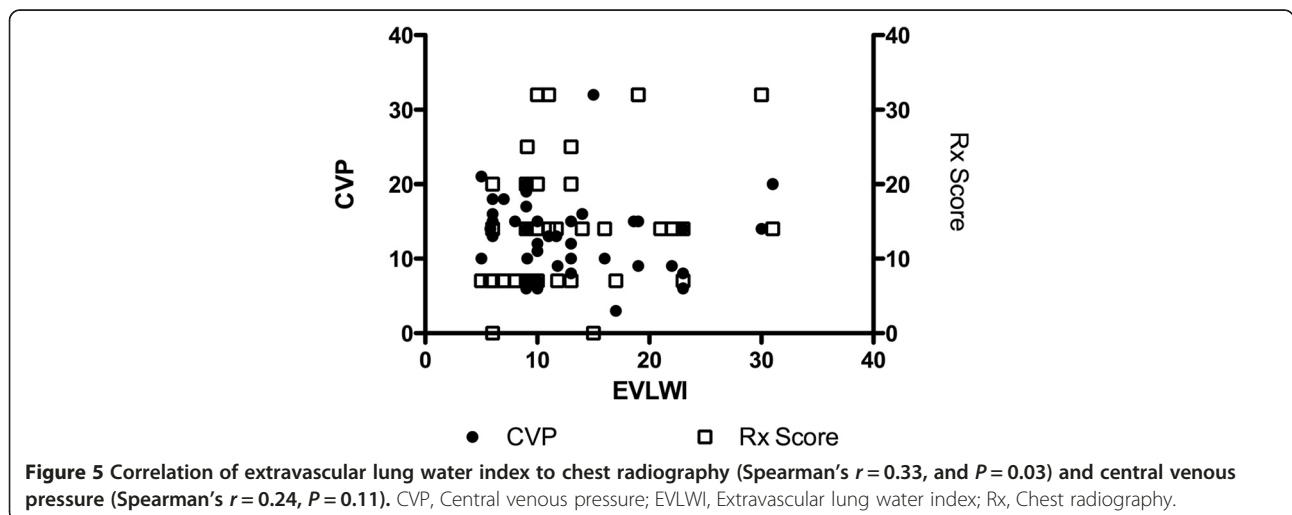
Our data suggest that lung ultrasound may be a valuable tool in assessing EVLW in patients in the ICU. Our four-sector protocol showed a tight and significant correlation with EVLWI values derived from transpulmonary thermodilution measurements. It had good sensitivity and specificity to exclude clinically relevant accumulation of EVLW and for diagnosis of severe pulmonary edema. Retrospective analysis of the screenshots by different investigators revealed a good correlation with the EVLWI. Simplified lung ultrasound performed markedly better than chest radiography for prediction of EVLWI. The ultrasound examination was easy, noninvasive and fast, making it an attractive approach for assessing pulmonary fluid status.

EVLW accumulation is a common problem in the critical ill patient in general and especially in patients with sepsis and ARDS. It is still debated which diagnostic tool is the best to use for guiding fluid therapy in regard to EVLW in the ICU. To this end, transpulmonary thermodilution or double-indicator measurement, analysis of chest radiography, CVP and pulmonary artery occlusion pressure measurement are used in different institutions [15,16]. Chest radiography is frequently used to assess EVLW, but usually its interpretation is subjective; in addition, the sensitivity and specificity of scoring systems are largely uncertain [16,17]. Measurement of CVP or the use of pulmonary artery catheters is still common, although their utility and value in guiding fluid therapy have been questioned in recent years [18,19]. The measurement of the EVLWI by transpulmonary thermodilution or a transpulmonary double-indicator (thermo-dye dilution) technique was proved to predict outcome in a general ICU population

and patients with severe ARDS [11,12]. This measurement method showed significant correlation with lung gravimetry as the standard *ex vivo* parameter for EVLW [10]. It has been shown that even small changes in EVLW can be detected by using transpulmonary thermodilution [20]. For these reasons, it has become the standard method for assessment of EVLW in many institutions and was used as the reference method in our study. However, placement of a central line and a special arterial catheter is required, generating costs and making it an invasive procedure. Possible pitfalls lie in assessment of patients with focal lung injury and vascular obstruction [21].

Using lung ultrasound to detect so-called B lines proved to be a useful diagnostic tool in diagnosing pulmonary edema in the emergency medicine setting and in animal studies, where the detection and quantification of so-called B lines showed correlation with clinical assessment, radiologic findings, natriuretic peptides and pulmonary artery occlusion pressure [1,4,9,22-26]. Other conditions that cause an acute interstitial syndrome such as pulmonary fibrosis and interstitial pneumonitis should be ruled out clinically and by assessment of the sonographic appearance of the pleural line [5,27]. Various protocols have been proposed, but, although a 28-sector approach is recommended in a cardiology outpatient setting, no consensus has been reached about the ideal lung ultrasound protocol in the ICU [5]. In our present study, we were able to demonstrate that a four-sector approach provides similar accuracy in predicting EVLW compared with more complex protocols and might be of value because rapid decision-making is key in the emergency and ICU setting.

Because blinding of the ultrasound examiner to the appearance and clinical volume status of the patient was hardly possible, we recorded screenshots of the ultrasound examination and asked two independent examiners to reassess the US score in a blinded manner. Correlation



with EVLWI remained significant as a surrogate for good reproducibility. We believe that the correlation coefficient was slightly lower in the blinded analysis because static screenshots were analyzed, whereas the dynamic real-time examination would be more sensitive in detecting B lines that move with pleural sliding images. Nevertheless, only an examination by two independent operators within a narrow time window would prove good reproducibility. This is clearly a limitation of our study.

Correlation of US score and EVLWI with the  $\text{PaO}_2/\text{FiO}_2$  was significant but rather weak. This is in agreement with earlier findings [11] and is not unexpected, given the fact that fluid overload is only one of many factors influencing the pulmonary gas exchange. Assessment of the chest radiographs using a numeric scale revealed a significant but weak correlation with the EVLWI. Given the fact that the correlation of the chest radiographs to the EVLWI was worse than that of the US score, and keeping in mind the risks to the patient associated with radiation exposure due to repeated radiologic examinations and the fact that chest radiographs are not always readily available at the bedside, we conclude that the ultrasound examination might be a better way to conduct an EVLW assessment in the ICU. Researchers in previous studies also reported conflicting results regarding the performance of chest radiographs in predicting pulmonary hyperhydration, interstitial syndrome or high cardiac filling pressures [28-30]. Our data suggest that lung ultrasound is a valuable method to use for assessing EVLW at the bedside of the ventilated ICU patient.

One of the major limitations of our study is the fact that it was done at a single center. We did not compare different protocols using, for example, an 8- or even a 28-zone approach, so no final conclusions can be drawn regarding the superiority of either protocol. We defined transpulmonary thermodilution as our standard method. No consensus has been reached so far regarding the threshold for a pathologic EVLW level. The cutoff values of 7 and 15 ml/kg used in our study were chosen on the basis of different reported mortality rates in critically ill patients associated with these values, but they remain arbitrary [12]. Nevertheless, the results of using lung ultrasound as a bedside tool in the ICU are promising and should prompt further studies to evaluate its utility for making diagnoses and guiding therapy.

## Conclusions

Assessment of EVLW by lung ultrasound using a simplified four-sector protocol shows excellent correlation with the results of transpulmonary thermodilution. The performance of lung ultrasound appears to be superior to chest radiography. The measurement of CVP does not reliably predict pulmonary hydration status in this setting.

## Key messages

- Ultrasound assessment of pulmonary fluid status can be performed by following a simplified protocol that allows rapid decision-making in the critical ill patient.
- A simplified lung ultrasound protocol shows significant correlation to EVLW measured by using a transpulmonary thermodilution technique and performs markedly better than chest radiography.
- Ventilator settings do not significantly influence the accuracy of lung ultrasound assessment of EVLW in the critical ill patient.

## Abbreviations

APACHE II: Acute Physiology and Chronic Health Evaluation II; ARDS: Acute respiratory distress syndrome; AUC: Area under the curve; CVP: Central venous pressure; EVLWI: Extravascular lung water index; ICS: Intercostal space; ICU: Intensive care unit; ITBVI: Intrathoracic blood volume index;  $\text{PaO}_2/\text{FiO}_2$ : Index of arterial partial pressure of oxygen and inspiratory oxygen concentration; PCWP: Pulmonary capillary wedge pressure; SD: Standard deviation; US: Ultrasound.

## Competing interests

The authors declare that they have no competing interests.

## Authors' contributions

PE, SR and JMK participated in the design of the study and performed the ultrasound examinations and the statistical analysis. JN, DH and AJ participated in the design of the study and helped to draft the manuscript. UE evaluated radiographic examinations and helped to draft the manuscript. All authors read and approved the final manuscript.

## Authors' information

PE and SR shared authorship. PE and UE take responsibility for all aspects of the reliability and freedom from bias of the data presented and their discussed interpretation.

## Author details

<sup>1</sup>Medizinische Klinik mit Schwerpunkt Nephrologie und Internistische Intensivmedizin, Charité-Universitätsmedizin Berlin, Augustenburger Platz 1, 13353 Berlin, Germany. <sup>2</sup>Abteilung für Radiologie, Charité Universitätsmedizin Berlin, Augustenburger Platz 1, 13353 Berlin, Germany.

Received: 12 August 2014 Accepted: 19 January 2015

Published online: 06 February 2015

## References

1. Liteplo AS, Marill KA, Villen T, Miller RM, Murray AF, Croft PE, et al. Emergency thoracic ultrasound in the differentiation of the etiology of shortness of breath (ETUDES): sonographic B-lines and N-terminal pro-brain-type natriuretic peptide in diagnosing congestive heart failure. *Acad Emerg Med*. 2009;16:201-10.
2. Noble VE, Murray AF, Capp R, Sylvia-Reardon MH, Steele DJ, Liteplo A. Ultrasound assessment for extravascular lung water in patients undergoing hemodialysis: time course for resolution. *Chest*. 2009;135:1433-9.
3. Bouhemad B, Liu ZH, Arbelot C, Zhang M, Ferarri F, Le-Guen M, et al. Ultrasound assessment of antibiotic-induced pulmonary re-aeration in ventilator-associated pneumonia. *Crit Care Med*. 2010;38:84-92.
4. Jambrik Z, Gargani L, Adamicza A, Kaszaki J, Varga A, Forster T, et al. B-lines quantify the lung water content: a lung ultrasound versus lung gravimetry study in acute lung injury. *Ultrasound Med Biol*. 2010;36:2004-10.
5. Volpicelli G, Elbarbary M, Blaivas M, Lichtenstein DA, Mathis G, Kirkpatrick AW, et al. International evidence-based recommendations for point-of-care lung ultrasound. *Intensive Care Med*. 2012;38:577-91.
6. Agricola E, Bove T, Oppizzi M, Marino G, Zangrillo A, Margonato A, et al. "Ultrasound comet-tail images": a marker of pulmonary edema: a comparative study with wedge pressure and extravascular lung water. *Chest*. 2005;127:1690-5.

7. Volpicelli G, Skurzak S, Boero E, Carpinteri G, Tengattini M, Stefanone V, et al. Lung ultrasound predicts well extravascular lung water but is of limited usefulness in the prediction of wedge pressure. *Anesthesiology*. 2014;121:320–7.
8. Mallamaci F, Benedetto FA, Tripepi R, Rastelli S, Castellino P, Tripepi G, et al. Detection of pulmonary congestion by chest ultrasound in dialysis patients. *JACC Cardiovasc Imaging*. 2010;3:586–94.
9. Lichtenstein DA, Mézière GA, Lagoueyte JF, Biderman P, Goldstein I, Gepner A. A-lines and B-lines: lung ultrasound as a bedside tool for predicting pulmonary artery occlusion pressure in the critically ill. *Chest*. 2009;136:1014–20.
10. Rossi P, Wanecek M, Rudehill A, Konrad D, Weitzberg E, Oldner A. Comparison of a single indicator and gravimetric technique for estimation of extravascular lung water in endotoxemic pigs. *Crit Care Med*. 2006;34:1437–43.
11. Jozwiak M, Silva S, Persichini R, Anguel N, Osman D, Richard C, et al. Extravascular lung water is an independent prognostic factor in patients with acute respiratory distress syndrome. *Crit Care Med*. 2013;41:472–80.
12. Sakka SG, Klein M, Reinhart K, Meier-Hellmann A. Prognostic value of extravascular lung water in critically ill patients. *Chest*. 2002;122:2080–6.
13. World Medical Association. Declaration of Helsinki. 2008. <http://www.wma.net/en/30publications/10policies/b3/17c.pdf>. Accessed 8 Feb 2015.
14. Bland JM, Altman DG. Measuring agreement in method comparison studies. *Stat Methods Med Res*. 1999;8:135–60.
15. Bethlehem C, Groenwold FM, Buter H, Kingma WP, Kuiper MA, de Lange F, et al. The impact of a pulmonary-artery-catheter-based protocol on fluid and catecholamine administration in early sepsis. *Crit Care Res Pract*. 2012;2012:161879.
16. Brown LM, Calfee CS, Howard JP, Craig TR, Matthay MA, McAuley DF. Comparison of thermodilution measured extravascular lung water with chest radiographic assessment of pulmonary oedema in patients with acute lung injury. *Ann Intensive Care*. 2013;3:25.
17. Halperin BD, Feeley TW, Mihm FG, Chiles C, Guthaner DF, Blank NE. Evaluation of the portable chest roentgenogram for quantitating extravascular lung water in critically ill adults. *Chest*. 1985;88:649–52.
18. Connors Jr AF, Speroff T, Dawson NV, Thomas C, Harrell Jr FE, Wagner D, et al. The effectiveness of right heart catheterization in the initial care of critically ill patients. *JAMA*. 1996;276:889–97.
19. Marik PE, Baram M, Vahid B. Does central venous pressure predict fluid responsiveness? A systematic review of the literature and the tale of seven maids. *Chest*. 2008;134:172–8.
20. Dres M, Teboul JL, Guerin L, Anguel N, Amilien V, Clair MP, et al. Transpulmonary thermodilution enables to detect small short-term changes in extravascular lung water induced by a bronchoalveolar lavage. *Crit Care Med*. 2014;42:1869–73.
21. Michard F. Bedside assessment of extravascular lung water by dilution methods: temptations and pitfalls. *Crit Care Med*. 2007;35:1186–92.
22. Gargani L, Lionetti V, Di Cristofano C, Bevilacqua G, Recchia FA, Picano E. Early detection of acute lung injury uncoupled to hypoxemia in pigs using ultrasound lung comets. *Crit Care Med*. 2007;35:2769–74.
23. Volpicelli G, Mussa A, Garofalo G, Cardinale L, Casoli G, Perotto F, et al. Bedside lung ultrasound in the assessment of alveolar-interstitial syndrome. *Am J Emerg Med*. 2006;24:689–96.
24. Gargani L, Frassi F, Soldati G, Tesorio P, Gheorghiane M, Picano E. Ultrasound lung comets for the differential diagnosis of acute cardiogenic dyspnoea: a comparison with natriuretic peptides. *Eur J Heart Fail*. 2008;10:70–7.
25. Lichtenstein D, Mézière G, Biderman P, Gepner A, Barré O. The comet-tail artifact: an ultrasound sign of alveolar-interstitial syndrome. *Am J Respir Crit Care Med*. 1997;156:1640–6.
26. Manson WC, Bonz JW, Carmody K, Osborne M, Moore CL. Identification of sonographic B-lines with linear transducer predicts elevated B-type natriuretic peptide level. *West J Emerg Med*. 2011;12:102–6.
27. Volpicelli G, Melniker LA, Cardinale L, Lamorte A, Frascisco MF. Lung ultrasound in diagnosing and monitoring pulmonary interstitial fluid. *Radiol Med*. 2013;118:196–205.
28. Chakko S, Woska D, Martinez H, de Marchena E, Futterman L, Kessler KM, et al. Clinical, radiographic, and hemodynamic correlations in chronic congestive heart failure: conflicting results may lead to inappropriate care. *Am J Med*. 1991;90:353–9.
29. Lichtenstein D, Goldstein I, Mourgeon E, Cluzel P, Grenier P, Rouby JJ. Comparative diagnostic performances of auscultation, chest radiography, and lung ultrasonography in acute respiratory distress syndrome. *Anesthesiology*. 2004;100:9–15.
30. Xirouchaki N, Magkanas E, Vaporidi K, Kondili E, Platakis M, Patrianakos A, et al. Lung ultrasound in critically ill patients: comparison with bedside chest radiography. *Intensive Care Med*. 2011;37:1488–93.

**Submit your next manuscript to BioMed Central and take full advantage of:**

- Convenient online submission
- Thorough peer review
- No space constraints or color figure charges
- Immediate publication on acceptance
- Inclusion in PubMed, CAS, Scopus and Google Scholar
- Research which is freely available for redistribution

Submit your manuscript at  
[www.biomedcentral.com/submit](http://www.biomedcentral.com/submit)



### **3.3. Welche Rolle spielt die Gerinnungskaskade im COVID-ARDS?**

#### 3.3.1 Hypofibrinolyse bei Patienten mit schwerer COVID-19-Erkrankung

Neben Ventilations-Perfusionsfehlverteilungen und kapillärer Leckage als Ausdruck der endothelialen Dysfunktion wird die Perfusion der Lungen und damit auch der pulmonale Gasaustausch vor allem auch durch die Interaktion des vaskulären Endothels und der Gerinnungskaskaden beeinflusst. Hierbei spielt eine komplexe Interaktion von Inflammationsmediatoren, Endothel und Gerinnungssystem die entscheidende Rolle <sup>32</sup>. Letztlich kommt es im ARDS zu unterschiedlichen Schweregraden einer disseminierten intravasalen Gerinnung (DIC) und Mikrothrombenbildung in der pulmonalen Strombahn. <sup>33</sup>

Mit Ausbruch der Pandemie durch SARS-CoV2 und der sich rasch entwickelnden Evidenz für eine Alteration des Gerinnungssystems von Patienten, die schwer an COVID-19 erkrankten mit einer deutlichen Häufung thromboembolischer Ereignisse, rückten diese pathophysiologischen Zusammenhänge wieder stärker in den Fokus.

Wir untersuchten die Kohorte der Patienten die auf unseren internistischen Intensivstationen während der ersten Welle der SARS-CoV-2 Pandemie im Jahre 2020 aufgrund eines C-ARDS behandelt wurden in Hinblick auf eine mögliche Häufung thromboembolischer Ereignisse und versuchten mittels viskoelastischer Testung unter Nutzung des ROTEM®-Systems die Veränderungen in der Gerinnungskaskade näher zu charakterisieren.

Wir fanden thromboembolische Komplikationen bei 23 von 40 Patienten (58%).

Die systematische Analyse der Ergebnisse der viskoelastischen Testung ergab neben einer deutlich erhöhten Gerinnselfestigkeit eine deutlich eingeschränkte

Fibrinolyseaktivität der kritisch kranken COVID-19 Patienten als mögliche Erklärung der Thromboseneigung in diesem Patientenkollektiv.

In der Subgruppe der Patienten die thrombembolische Komplikationen entwickelte, war die Maximum lysis (ML) als Parameter der Fibrinolyseaktivität in der ROTEM-Untersuchung noch einmal deutlich niedriger als im Gesamtkollektiv, was einen kausalen Zusammenhang möglich erscheinen lässt.

Analog zu anderen Gruppen fanden wir ein signifikant höheres Niveau der D-Dimere in der Gruppe der Patienten mit thrombembolischen Komplikationen. Während die ML des ROTEM in der ROC-Kurvenanalyse eine area under the curve (AUC) von 0,8 zur Vorhersage thrombembolischer Ereignisse zeigte, lag die AUC für die D-Dimere mit 0,71 deutlich darunter.

Eine Kombination beider Parameter erbrachte eine AUC  $>0,9$ , ein Wert der diese Parameterkombination als einen aussichtsreichen Kandidaten für eine prognostische Einschätzung hinsichtlich des Risikos einer Entwicklung thrombembolischer Komplikationen bei COVID-19 erscheinen lässt.

Die klinischen Empfehlungen hinsichtlich eines Antikoagulationszieles für Patienten mit schwerem Verlauf einer COVID-19-Erkrankung sind weiterhin uneinheitlich und auch Abhängig von der Schwere des klinischen Verlaufes.

Gerade für die schwer Erkrankten ist auch eine Häufung von Blutungskomplikationen dokumentiert. Ein Parameter oder eine Parameterkombination, die eine ausreichende Sensitivität und Spezifität zur Vorhersage thromboembolischer Komplikationen bietet wurde bislang nicht gefunden. Ein Solcher könnte aber an dieser Stelle die Behandlung von Patienten mit schwerer COVID-19-Erkrankung auf der Intensivstation erheblich vereinfachen und helfen Komplikation sowohl durch Thrombosen oder Embolien als auch durch schwere Blutungsereignisse infolge einer unnötig starken Antikoagulations-behandlung zu vermeiden.

Größere Studien mit deutlich höheren Patientenzahlen müssen jedoch unsere Befunde bestätigen, bevor sie Eingang in die klinische Routine oder gar eine generelle Empfehlung finden können <sup>34</sup>.

**J M Kruse, A Magomedov, A Kurreck, F Münch, R Koerner, J Kamhieh-Milz, A Kahl, I Gotthardt, S K Piper, K-U Eckardt, T Dörner, D. Zickler:**

**Thromboembolic complications in critically ill COVID-19 patients are associated with impaired fibrinolysis; Crit Care 220; 24:676**

RESEARCH

Open Access



# Thromboembolic complications in critically ill COVID-19 patients are associated with impaired fibrinolysis

Jan Matthias Kruse<sup>1†</sup>, Abakar Magomedov<sup>2†</sup>, Annika Kurreck<sup>3</sup>, Frédéric H. Münch<sup>1</sup>, Roland Koerner<sup>1</sup>, Julian Kamhieh-Milz<sup>4,5</sup>, Andreas Kahl<sup>1</sup>, Inka Gotthardt<sup>1</sup>, Sophie K. Piper<sup>6,7</sup>, Kai-Uwe Eckardt<sup>1</sup>, Thomas Dörner<sup>8,9</sup> and Daniel Zickler<sup>1\*</sup>

## Abstract

**Background:** There is emerging evidence for enhanced blood coagulation in coronavirus 2019 (COVID-19) patients, with thromboembolic complications contributing to morbidity and mortality. The mechanisms underlying this pro-thrombotic state remain enigmatic. Further data to guide anticoagulation strategies are urgently required.

**Methods:** We used viscoelastic rotational thromboelastometry (ROTEM) in a single-center cohort of 40 critically ill COVID-19 patients.

**Results:** Clear signs of a hypercoagulable state due to severe hypofibrinolysis were found. Maximum lysis, especially following stimulation of the extrinsic coagulation system, was inversely associated with an enhanced risk of thromboembolic complications. Combining values for maximum lysis with D-dimer concentrations revealed high sensitivity and specificity of thromboembolic risk prediction.

**Conclusions:** The study identifies a reduction in fibrinolysis as an important mechanism in COVID-19-associated coagulopathy. The combination of ROTEM and D-dimer concentrations may prove valuable in identifying patients requiring higher intensity anticoagulation.

**Keywords:** COVID-19, Coagulopathy, Hypofibrinolysis, ROTEM, D-dimers

## Background

The novel severe acute respiratory syndrome coronavirus 2 (SARS-CoV-2) causing coronavirus disease 2019 (COVID-19) has led to a global pandemic posing a major threat to humans [1]. More than 500 000 deaths related to COVID-19 have been so far reported [2].

SARS-CoV-2 primarily affects the respiratory system with a widely heterogeneous clinical presentation, ranging from none or minimal symptoms to significant hypoxia with viral pneumonia, potentially leading to severe acute respiratory distress syndrome (ARDS) and cytokine storm [3]. ARDS with related lung injury is considered one of the main causes of death in COVID-19 patients [4].

However, there is emerging evidence that involvement of other pathomechanisms contributes to morbidity and mortality. Both clinical and autopsy studies have revealed a high incidence of venous and arterial thromboembolic events, including pulmonary embolism, even in patients receiving therapeutic anticoagulation [5–7]. These

\*Correspondence: [daniel.zickler@charite.de](mailto:daniel.zickler@charite.de)

<sup>†</sup>Jan Matthias Kruse and Abakar Magomedov have contributed equally to this work

<sup>1</sup> Department of Nephrology and Medical Intensive Care, Charité – Universitätsmedizin Berlin, Augustenburger Platz 1, 13353 Berlin, Germany

Full list of author information is available at the end of the article



findings have led to recommendations for higher anti-coagulation targets; however, it remains unclear which patients are at increased risk and require anticoagulation [8]. While fibrinogen and D-dimer levels are frequently elevated, neither parameter reliably identifies patients at an increased risk of thromboembolic complications [8]. Although different markers of hypercoagulation have been reported among COVID-19 patients [6, 9], the exact mechanisms underlying the prothrombotic state in these patients remain unclear so far [10, 11]. In particular, it has not been clarified to which extent increased procoagulation and/or impaired fibrinolysis is involved.

In addition to conventional laboratory parameters, rotational thromboelastometry (ROTEM) provides evidence for net coagulation capacity and insight into clot formation time, clot firmness and fibrinolysis in the critically ill patients [12]. Here we report ROTEM data in 40 consecutive, severely ill COVID-19 patients treated in two tertiary intensive care units (ICUs) and assessed the association with thromboembolic complications.

## Methods

### Coagulation tests

After admission to our ICUs, blood samples were drawn and viscoelastic tests were performed once with citrated blood using a ROTEM sigma point-of-care device (Tem International, Munich, Germany) [13]. In each patient, intrinsically (contact activation, INTEM) and extrinsically (tissue factor activation, EXTEM) activated test assays were performed to analyze the clot dynamics in both coagulation pathways. Furthermore, FIBTEM and HEPTEM were performed. In the FIBTEM, platelets are inactivated with cytochalasin D to enable isolated evaluation of fibrinogen in clot firmness. The heparin effect was determined by comparing the clotting time of the INTEM with the clotting time of the HEPTEM, where heparinase is added.

The following ROTEM variables were analyzed: clotting time defined as the time until initiation of clotting; clot formation time (seconds until a clot strength reaches 20 mm), reflecting the kinetics of clot formation; maximum clot firmness (MCF) defined as the maximum amplitude of clot firmness; maximum lysis (ML; %) defined as the difference between MCF and the lowest clot amplitude after MCF, reflecting fibrinolytic activity (Fig. 1).

Additional routine laboratory tests performed according to standardized protocols comprised hemoglobin concentration, white blood cell count, platelet count, prothrombin time (PT), international normalized ratio (INR), activated partial thromboplastin time (aPTT) and inflammatory parameters (see Table 2). The levels of tissue-type plasminogen activator (t-PA), plasminogen activator inhibitor-1 (PAI-1) and plasminogen were

determined using commercial ELISA Kits (t-PA Antigen ELISA Kit, PAI-1 Antigen ELISA Kit, Glu-Plasminogen, TECHNOZYM®/Technoclone).

To combine the parameters maximum D-dimers (mg/l) and ML (%), the difference (maximum D-dimers—ML EXTEM) was calculated and analyzed.

### Anticoagulation therapy

In our Intensive care units, all patients included in this trial were treated with either low molecular weight heparin or in the case of ECMO therapy with argatroban. We aimed for a PTT of 50–55 s (normal 26–40 s), and in patients with thromboembolic events we aimed for a PTT of 60–80 s.

### Ultrasound

We performed ultrasound examinations in all patients (GE Vivid S70 ultrasound machine with a 9L-D probe) to screen for venous thrombosis, focusing on the jugular, subclavian, brachial, femoral and popliteal veins upon admission to our ICU and subsequently at least once weekly.

### Ethics

The study was approved by the ethics committees of Charité – Universitätsmedizin Berlin (EA4/115/20).

### Statistics

Statistical analyses were performed using IBM® SPSS® Statistics version 26 (New York, USA). The descriptives are provided as median with limits of the interquartile range (IQR) for continuous variables or as absolute and relative frequencies for categorical variables.

Continuous data were primarily right skewed. Therefore, the Mann–Whitney *U* test was used to compare differences between patient groups in continuous variables, while Chi-square test was used for categorical data. A two-sided significance level of 0.05 was applied without adjustment for multiple comparison. All *p* values constitute exploratory data analyses and do not allow for confirmatory generalization of results. To evaluate the strength of different ROTEM variables to distinguish between patients with and without thromboembolic events, receiver operating characteristic (ROC) analysis was carried out including area under the curve measures (AUC) with 95% confidence intervals (CI). Sensitivity, specificity and accuracy (percentage of correctly classified patients) are reported.

## Results

### Characteristics of the cohort

Forty consecutive patients with COVID-19 confirmed by polymerase chain reaction in throat swabs were admitted

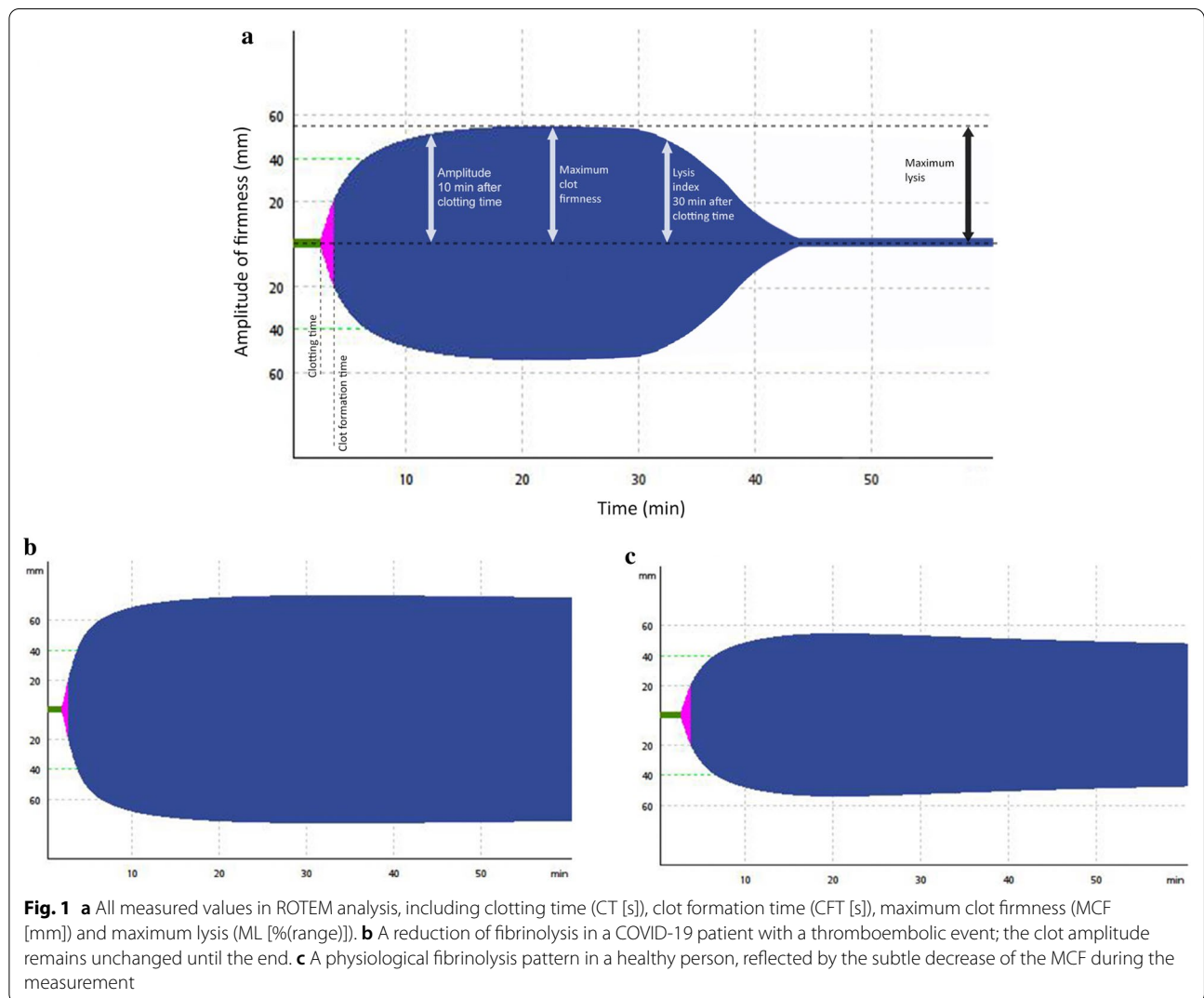
to two ICUs within our department between March 25th and May 11th. All patients received viscoelastic testing using the ROTEM system and were included in the analysis, which was censored on May 11th.

Table 1 shows baseline characteristics of the study cohort. As most patients were referred from community hospitals within a regional network, patients were mostly severely ill with a median sequential organ failure assessment (SOFA) score of 9 and a mean acute physiology and chronic health evaluation (APACHE) II of 28 points. Mechanical ventilation via either endotracheal tube or tracheostomy was administered to 78% of patients, whereas extracorporeal membrane oxygenation was required for 25% and kidney replacement therapy for 53% of patients. Evidence for macrothromboembolic events was found in 23 of 40 patients (58%). In five patients, we identified thromboembolic events upon admission to our

ICUs ( $N=3$  prediagnosed pulmonary emboli,  $N=2$  deep venous thrombosis). Nineteen patients developed thromboembolic complications during the ICU stay, comprising deep vein thrombosis ( $N=14$ ), pulmonary embolism ( $N=4$ ), ischemic stroke ( $N=3$ ), complete thrombosis of the ECMO-circuit requiring emergency circuit-change ( $N=1$ ) and a clotted ECMO cannula ( $N=1$ ).

**Laboratory parameters**

Table 2 shows laboratory parameters for the study cohort and in patients with and without thromboembolic events. Hematological parameters were similar in both patient groups. Patients with thromboembolic events had a significantly higher maximum C-reactive protein (CRP) value, with a median value of 341 mg/l [IQR 261.1–370.7] versus 261.1 mg/l [IQR 175.3–312.9], respectively ( $p=0.002$ ). Other markers of inflammation



such as procalcitonin (PCT), ferritin and interleukin-6 did not differ significantly between groups.

Analyses of the coagulation parameters revealed no significant differences between the groups with the exception of a prolonged PTT in the group with thromboembolic events. Patients had significantly elevated levels of fibrinogen without significant differences between groups.

Moreover, the median initial D-dimer levels were 4.84 mg/l [IQR 3.5–7.2] in the group with thromboembolic complications in comparison with 3.06 mg/l [IQR 2.3–3.9] in the group without thromboembolic complications ( $p=0.003$ ).

### ROTEM parameters

Substantial abnormalities in the ROTEM analysis were found in the overall cohort. Maximum clot firmness in INTEM, EXTEM, FIBTEM and HEPTEM was markedly elevated in the entire cohort compared to reference values with median values of 74 mm [IQR 69–77], 75 mm [IQR 70.3–78], 34.5 mm [IQR 27.3–39.5] and 73 mm [IQR 67.5–75.3], respectively. Of note, there was no significant difference in these parameters between the subgroups with and without thromboembolic complications. However, the median clotting time detected in INTEM was significantly longer in the group of patients with thromboembolic complications: 215 s [IQR 197–251] versus 189 s [IQR 171.5–212];  $p=0.005$ . Clotting times in FIBTEM, EXTEM and HEPTEM showed no significant differences between groups.

Figure 2 depicts ML in INTEM and EXTEM. Under both conditions, ML was reduced and significantly lower in the group with thromboembolic complications (INTEM median 2% [IQR 0–3.0] versus 6% [IQR 2.5–6];  $p=0.001$ ; EXTEM median 3% [IQR 0–5] versus 5% [IQR 3.5–8],  $p=0.001$ ), indicating substantially impaired fibrinolysis in both groups. This was observed to be more pronounced in patients with thromboembolic complications.

### ROC analysis to distinguish patients with and without thromboembolic complications

Based on the above findings, we evaluated the potential of different ROTEM variables to distinguish between patients with and without thromboembolic events using ROC analysis (Fig. 3). Maximum lysis in EXTEM resulted in an area under the curve (AUC) of 0.8 [95% CI 0.7–0.9] for thromboembolic events ( $p=0.001$ ), while the ML in INTEM resulted in an AUC of 0.79 [95% CI 0.6–0.9] ( $p=0.002$ ). D-dimers showed an AUC of 0.78 [95% CI 0.6–0.9], and maximum D-dimers had an AUC of 0.82 [95% CI 0.7–1.0]. Combined analysis showed that the difference in D-dimers and ML EXTEM resulted in an AUC of 0.92 [95% CI 0.8–1].

### Discussion

This study provides evidence that hypofibrinolysis is an important contributor to the hypercoagulable state in COVID-19 patients. Maximum lysis assessed in ROTEM analysis, especially in the EXTEM analysis, was reduced more profoundly in patients with thromboembolic events. Based on these observations, we propose that ROTEM analysis is useful for patient stratification according to their prothrombotic risk. In particular, combined consideration of ROTEM maximum lysis and D-dimers may identify patients that benefit from therapeutic anticoagulation.

In this small cohort of severely ill COVID-19 patients, we observed thromboembolic complications in more than 50% of patients. Analysis of routine coagulation parameters should be interpreted with caution, as many of the patients were treated with therapeutic anticoagulation. However, in accordance with previous studies, fibrinogen and factor VIII were elevated in our cohort and D-dimers were significantly elevated in the subgroup with thromboembolic complications [14]. Other conventional markers of the coagulation system showed no significant differences between the two groups.

In contrast to individual parameters, viscoelastic methods, such as thromboelastography and ROTEM, permit functional evaluations by recording most components of the coagulation process in vitro in the presence of cellular blood components. This provides insight into the different coagulation phases, including the initiation, formation and stabilization of a clot, and finally, clot lysis. The influence of the endothelium as an important cofactor of coagulation, however, is not directly reflected in ROTEM assessment. In several studies, hypercoagulable conditions were identified using ROTEM in disease states with an increased risk of thromboembolic events [15, 16]. Moreover, viscoelastic systems, such as ROTEM and thromboelastography, were successfully established to detect hypo- or hyperfibrinolysis in patients with traumatic injury or severe septic shock [17, 18].

Panigada *et al.* used thromboelastography in 20 patients with COVID-19 in addition to plasmatic tests of coagulation [19]. Similar to our study, they also found increased levels of fibrinogen and factor VIII, and almost normal routine coagulation tests. Thromboelastography data showed elevated clot firmness as reflected by maximal amplitude and reduced fibrinolysis measured as reduced clot lysis at 30 min (Lys 30), consistent with our observations. Spiezia and colleagues and Pavoni and co-workers also recently showed severe hypercoagulopathy in critically-ill COVID-19 patients using ROTEM [20, 21]. They found a significantly higher maximal clot firmness in INTEM, EXTEM and FIBTEM, and shorter INTEM clot formation time in comparison with a healthy control

**Table 1 Patient characteristics of total cohort and subcohorts with and without thromboembolic events**

	Cohort (n = 40)		Thromboembolic events (N = 23)		No thromboembolic events (N = 17)		p value
Age (years, (median, [IQR]))	67	[57.3–76.6]	66	[56–76]	68	[62–77.5]	ns
Gender, male (n, %)	35	87.5%	20	87%	15	88%	ns
BMI, kg/m <sup>2</sup> (median, [IQR])	28.1	[24.8–32.8]	27.8	[24.2–33]	28.7	[25.7–32.3]	ns
Duration of ICU stay, days (median, [IQR])	39.5	[24–54.25]	42	[28–58]	25	[8.5–47.5]	0.05
Death during ICU stay (n, %)	11	27.5%	9	39.1%	2	11.8%	0.58
Intubation (n, %)	31	77.5%	20	87%	11	65%	ns
ECMO (n, %)	10	25%	9	39.1%	1	6%	ns
CRRT (n, %)	21	52.5%	16	69.6%	5	29.4%	0.013
SOFA score (median, [IQR])	9	[6.3–11.8]	10	[6–11]	8	[4.5–11]	ns
SIC score (median, [IQR])	3	[2–4]	3	[2–4]	3	[2–4]	ns
APACHE score (median, [IQR])	28	[22–33]	29	[23–34]	26	[19–31.8]	ns
Preexisting conditions							
Coronary artery disease (n, %)	9	22.5%	6	26%	3	18%	ns
Hypertension (n, %)	25	62.5%	14	61%	11	65%	ns
Diabetes mellitus/insulin resistance (n, %)	13	32.5%	10	43%	3	18%	ns
Chronic kidney disease (n, %)	7	17.5%	6	26%	1	6%	ns
Chronic dialysis (n, %)	1	2.5%	1	4%	0	0%	ns
Lung disease (n, %)	7	17.5%	6	26%	1	6%	ns

ECMO Extracorporeal membrane oxygenation, SOFA sequential organ failure assessment, CRRT continuous renal replacement therapy, SIC sepsis-induced coagulopathy, APACHE acute physiology and chronic health evaluation

group. However, they observed no differences between COVID-19 patients with and without thrombosis [20]. In a cohort of 19 patients, Ibañez et al. noted markedly reduced fibrinolysis in COVID-19 patients; however, no distinction with respect to the presence of thromboembolic events was made [23].

While our findings confirm these results, we noted not only a markedly reduced fibrinolysis in the whole cohort but a significantly reduced ML in the group with thromboembolic complications. The clot lysis parameter ML provides information on the fibrinolytic activity, with low values providing evidence for hypofibrinolysis. In the current study, we found the ML in both EXTEM and INTEM to be markedly below normal values. Furthermore, the ML under both conditions was even lower in the group with thromboembolic complications. Therefore, we conclude that a severely impaired fibrinolysis plays an important role in the hypercoagulable state and thromboembolic risk in COVID-19 patients [23].

It is, however, somewhat surprising that highly elevated levels of D-dimers were found in a state of hypofibrinolysis. As a hypothesis, it has been suggested that intra-alveolar fibrin deposition accounts for local activation of fibrinolysis in ARDS.

The mechanisms leading to hypofibrinolysis in COVID-19 remain to be defined. Complex interactions between inflammation and the coagulation and fibrinolytic system

have been examined and controversially discussed for decades [24–26]. One potential mechanism may be the production of alpha defense in neutrophils, which are known to promote fibrin polymerization and block fibrinolysis in vitro [27].

In our cohort, we found markedly elevated markers of inflammation, including interleukin-6, CRP and ferritin; however, only the maximum CRP level differed significantly between patients with and without thromboembolic complications. We could not detect significant differences among additional individual analytes (i.e., tPA or PAI concentrations) between both groups; however, we did not evaluate the effect of the complement or bradykinin system, which are both known to play crucial roles in connecting the inflammatory response and fibrinolytic activity. Future clinical trials should also focus on the role of thrombin-activatable fibrinolysis inhibitor (TAFI), plasmin-alpha-2-antiplasmin (PAP) complexes and antiplasmin, which would give valuable insights into the mechanisms of COVID-19-induced hypofibrinolysis. Furthermore, endothelial dysfunction is likely involved but was not assessed.

ROC analyses provided an AUC for ML in EXTEM of 0.8. As such, it might be a candidate as prediction marker of future thromboembolic complications. Zhou et al. reported D-dimers to be one of the most sensitive and specific factors predicting mortality in a large cohort

**Table 2 Laboratory parameters of total cohort and subcohorts with and without thromboembolic events**

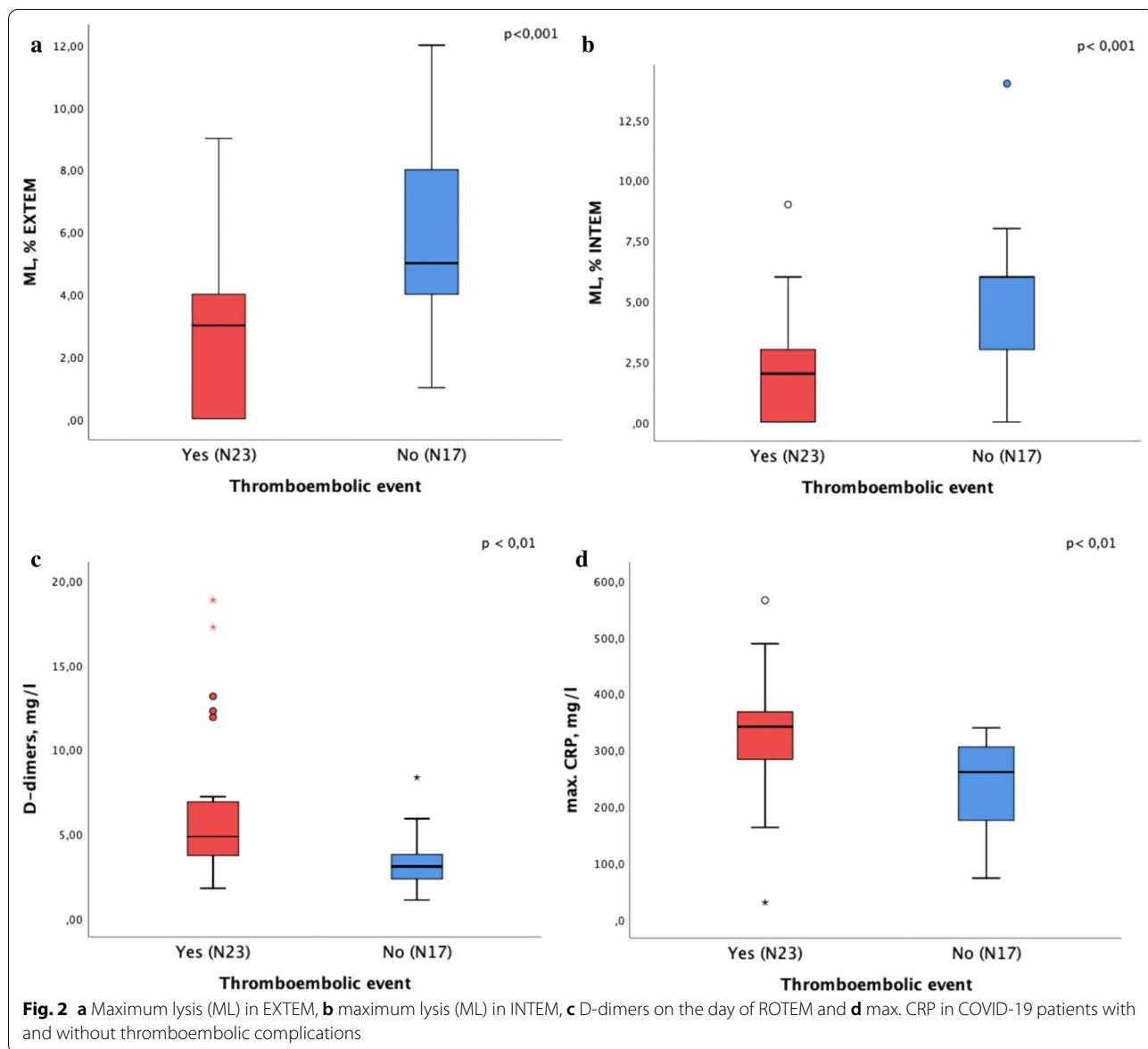
	Cohort (N = 40)		Thromboembolic event				p value
	Median	[IQR]	Yes (N = 23)		No (N = 17)		
			Median	[IQR]	Median	[IQR]	
Laboratory variables (normal values)							
Haemoglobin (12.5–17.2 g/dL)	10.1	[8.5–11.2]	9.70	[8.3–10.8]	10.4	[9.3–11.9]	ns
White blood cells (3.5–10.5/nl)	10.13	[7.5–13.7]	10.63	[7.4–16]	9.58	[6.6–12.1]	ns
Platelet count (150–370/nl)	193.5	[131.3–316.3]	181	[116–306]	209	[178–325.5]	ns
Prothrombin time (70–130%)	74.5	[62.8–86]	79	[61–83]	71	[63.5–87.5]	ns
INR (0.9–1.25)	1.2	[1.1–1.4]	1.18	[1.1–1.4]	1.26	[1.1–1.4]	ns
PTT (26–40 s)	45.65	[39.4–56.1]	51.10	[40.8–57.4]	41.1	[38.7–54.2]	ns
Fibrinogen (1.6–4 g/l)	6.67	[4.7–7.7]	6.72	[5.0–7.8]	6.1	[4.6–7.9]	ns
D-dimers (< 0.5 mg/l)	3.95	[2.6–5.9]	4.84	[3.5–7.2]	3.06	[2.3–3.9]	0.003
max. D-dimers (< 0.5 mg/l)	8.25	[3.6–16.2]	11.57	[8.2–18.4]	3.98	[2.6–6.4]	< 0.001
Procalcitonin (0.5 µg/l)	0.57	[0.2–2.5]	0.81	[0.4–4.7]	0.24	[0.2–1.3]	ns
CRP (< 0.5 mg/l)	123.8	[84.3–216.5]	130	[86–273.7]	111	[79.3–185]	ns
max. CRP (< 0.5 mg/l)	312.9	[208.3–343.9]	341.4	[261.1–370.7]	261.05	[175.3–312.9]	0.002
IL-6 (< 7 ng/l)	103	[35.6–230]	88	[27.7–340]	153	[53.7–206.5]	ns
max. IL-6 (< 7 ng/l)	558.6	[178.8–1792.3]	550	[174–2475]	567.2	[186.5–1196.5]	ns
Ferritin (30–400 µg/l)	1636	[1067.8–4028.5]	1663	[1218.5–4655]	1567	[720–3662]	ns
max. Ferritin (30–400 µg/l)	2523.2	[1536.7–6635.1]	2781.5	[1854.7–7996.2]	2028.4	[922.9–4893.4]	ns
tPA (2–8 µg/l)	1	[0.9–5.5]	1	[0.9–3.6]	2	[0.9–9.9]	ns
PAI-1 (7–43 ng/ml)	36	[17–70]	31	[12–61]	42.50	[25.3–87]	ns
tPA/PAI-1	0.053	[0.02–0.18]	0.05	[0.02–0.14]	11	[0.03–0.24]	ns
Antithrombin III (80–120%)	79	[58.5–96.5]	75.5	[56.8–84]	94	[66.5–110]	ns
Factor VIII (50–150%)	258	[190.5–319.5]	260	[219.5–355]	222	[149.5–289.5]	ns
Plasminogen (80–120%)	88	[72.8–114]	82	[72.8–109.8]	101	[70.8–129.8]	ns
ROTEM variables							
FIBTEM CT (s)	88.5	[78–97.8]	89	[78–102]	88	[75.5–96]	ns
FIBTEM CFT (s)	68	[51–104]	64.5	[54–95.8]	71	[47–165]	ns
FIBTEM MCF (mm)	34.5	[27.3–39.5]	35	[27–38]	34	[27–40]	ns
EXTEM CT (s)	86	[69.5–99.8]	84	[69–96]	86	[70.5–107.5]	ns
EXTEM CFT (s)	46.5	[40–60.5]	47	[40–61]	45	[40.5–56.5]	ns
EXTEM MCF (mm)	75	[70.3–78]	75	[69–78]	76	[72.5–78.5]	ns
INTEM CT (s)	208	[181.3–227.5]	215	[197–251]	189	[171.5–212]	0.005
INTEM CFT (s)	50.5	[39.5–61.8]	56	[39–63]	45	[39.5–60.5]	ns
INTEM MCF (mm)	74	[69–77]	74	[65–77]	73	[69.5–78]	ns
HEPTTEM CT (s)	188.5	[170.5–208.3]	193	[173–209]	173	[159–206]	ns
HEPTTEM CFT (s)	41	[35.5–56.5]	40	[34–60]	42	[37–51]	ns
HEPTTEM MCF (mm)	73	[67.5–75.3]	73	[66–76]	71	[71–75]	ns
ML, EXTEM (%)	3	[1.3–5.8]	3	[0–5]	5	[3.5–8]	0.001
ML, INTEM (%)	3	[1–6]	2	[0–3]	6	[2.5–6]	0.001

Unless values are designated as maximum values during the ICU stay, these parameters were determined on the day, when ROTEM analysis was performed, after admission to our ICUs

CT clotting time, CFT clot formation time, MCF maximum clot firmness, ML maximum lysis

of COVID-19-patients in China [14]. Cui et al. found a good sensitivity and specificity using a cutoff of 1.5 ng/ml for predicting thrombotic events in COVID-19 patients [8]. D-dimers were also markedly elevated in our cohort

and were found to be significantly higher in the subgroup with thromboembolic events. ROC analysis for D-dimers revealed an AUC of 0.78. The combination of the maximum D-dimer and ML in EXTEM (D-dimer—ML)

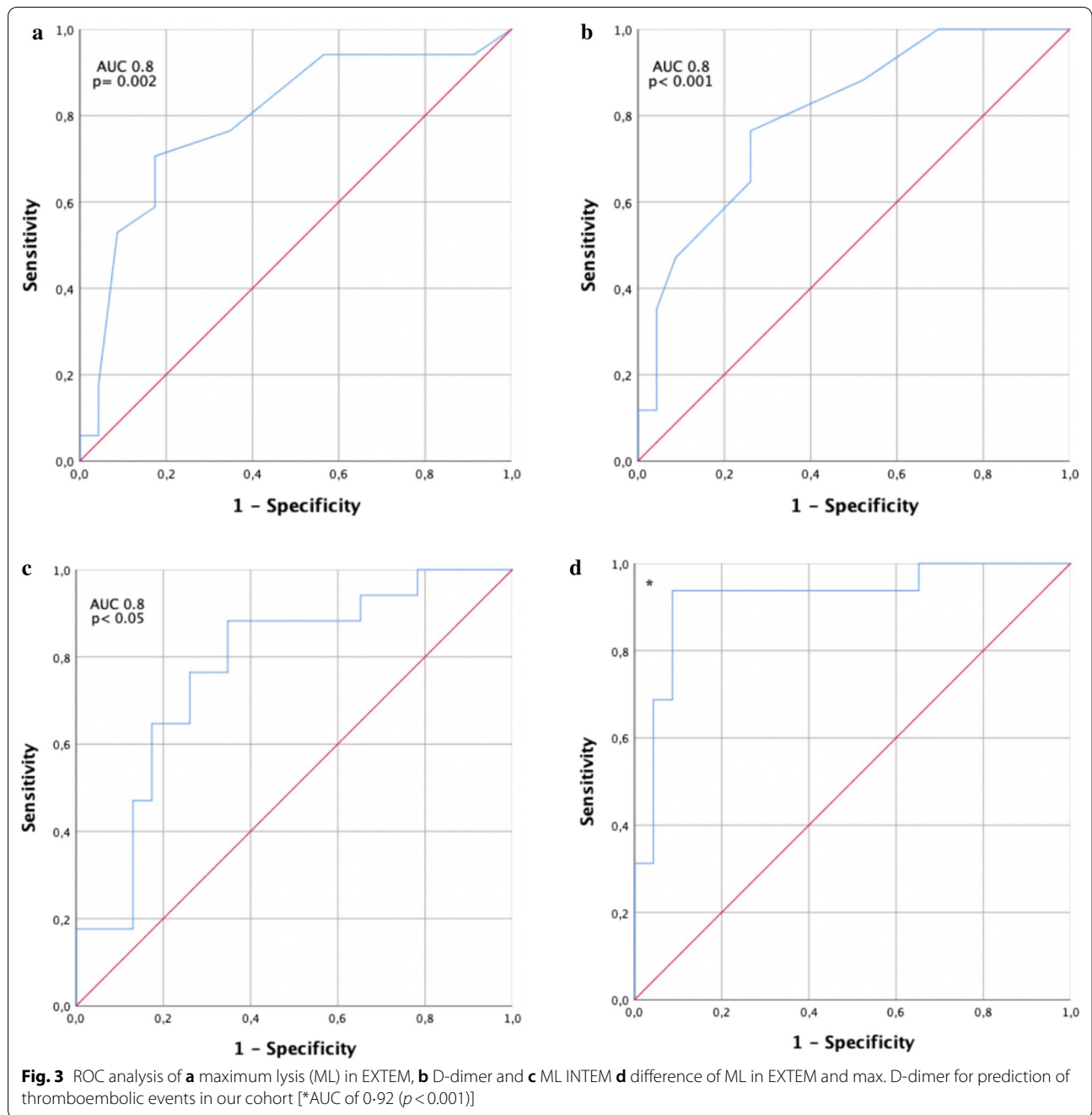


improved the AUC to 0.92, with a cutoff of 3.7 for a sensitivity of 94% and specificity > 90%. The predictive value of this D-dimer–ML parameter, however, requires validation in a second cohort.

In addition to providing insights in the mechanism of thrombus formation, our results may underline the possible therapeutic option of specific fibrinolytic therapy for ARDS caused by COVID-19. Administration of recombinant t-PA has already been suggested as a potential treatment and has shown promising results in a previous study independent of COVID-19 [28]. Currently, a phase IIa trial is underway to examine the effect of thrombolytics in COVID-19 patients

with hypoxemic lung injury (ClinicalTrials.gov, NCT 04357730) [29].

There are several limitations to our study. First, ROTEM measurements were performed when patients were transferred to our ICUs after different treatment periods in other hospitals. Thus, the ROTEM results reflect different stages of the disease. Also, many, but not all patients, were previously treated with heparin when thromboelastometry measurements were performed. Second, the study is monocentric, performed in a tertiary care center, and the generalizability to other settings and patients with a less severe course and earlier stages of the disease needs to be tested. Third,



our prediction models based on associations between poor clot lysis, D-dimers and the presence of thromboembolic events are hypotheses and require validation in independent patient cohorts and prospective observational studies. Fourth, thromboembolic events may have been underdiagnosed, as only ultrasound was routinely performed, while CT scans to exclude pulmonary embolism were only performed in some patients. Fifth,

our results are descriptive in nature and do not provide explanatory models for the observed hypofibrinolysis. Future studies should focus on the examination of possible mechanisms.

Sixth, 25% of patients of our cohort received ECMO therapy, which may itself have had a thrombogenic effect and in part may have contributed to the high rates of thrombosis. However, the current literature points into

the direction that in some cases ECMO rather leads to hyperfibrinolysis [30]. An ECMO-side effect as an explanation for a systematic hypofibrinolysis as observed in our cohort thus appears rather unlikely. Seventh, even though the statistical analysis showed robust values for our analysis, it may be difficult to guide clinical decision based on these values, as the difference in maximum lysis is 2%.

In summary, we found substantially reduced fibrinolysis in COVID-19 patients, which was more pronounced in patients with thromboembolic events. Clot ML time, as assessed by ROTEM as a single parameter, or in combination with D-dimers may prove valuable for thromboembolic risk stratification in COVID-19 patients and aid in decision-making regarding anticoagulation strategies.

## Conclusions

ROTEM revealed severe hypofibrinolysis in COVID-19 patients. Maximum lysis, especially following stimulation of the extrinsic coagulation system, was inversely associated with an enhanced risk of thromboembolic complications. The combination of maximum lysis with D-dimer concentrations revealed high sensitivity and specificity of thromboembolic risk prediction. Hence, ROTEM may help to identify patients benefiting from therapeutic anticoagulation.

## Abbreviations

ROTEM: Rotational thromboelastometry; COVID-19: Coronavirus 2019; SARS-CoV-2: Severe acute respiratory syndrome coronavirus 2; ARDS: Acute respiratory distress syndrome; ICU: Intensive care units; MCF: Maximum clot firmness; ML: Maximum lysis; PT: Prothrombin time; INR: International normalized ratio; aPTT: Activated partial thromboplastin time; t-PA: Tissue-type plasminogen activator; PAI-1: Plasminogen activator inhibitor-1; IQR: Interquartile range; ROC: Receiver operating characteristic; AUC: Area under the curve; CI: Confidence intervals; PCT: Procalcitonin; CRP: C-reactive protein.

## Acknowledgements

Not applicable.

## Authors' contributions

The study was designed by Dr. Zickler and Dr. Kruse. Dr. Magomedov, Dr. Kamhieh-Milz, Dr. Körner and Dr. Kahl contributed to study design, data collection, data analyses and interpretation, Dr. Münch and Dr. Kurreck performed data collection. Dr. Piper performed statistical analyses. Dr. Dörner contributed to study design and interpretation. Drs. Zickler, Eckardt and Gotthardt wrote the first draft of the manuscript and revised subsequent versions. All authors read and approved the final manuscript.

## Funding

Open Access funding enabled and organized by Projekt DEAL. This research received no specific grant from any funding agency in the public, commercial, or not-for-profit sectors.

## Availability of data and materials

The data that support the findings of this study are available from the corresponding author upon reasonable request.

## Ethics approval and consent to participate

The study was approved by the ethics committees of Charité – Universitätsmedizin Berlin (EA4/115/20).

## Consent for publication

Not applicable.

## Competing interests

Dr. Kruse, Dr. Magomedov, Dr. Kurreck, Dr. Münch, Dr. Koerner, Dr. Kamhieh-Milz, Dr. Kahl, Dr. Piper and Dr. Dörner have nothing to disclose. Dr. Eckardt reports personal fees from Akebia, grants from Amgen, grants from Astra Zeneca, grants and personal fees from Bayer, grants from Fresenius, from Genzyme, from Shire and grants and personal fees from Vifor, outside the submitted work. Dr. Zickler reports grants and personal fees from Baxter, outside the submitted work.

## Author details

<sup>1</sup> Department of Nephrology and Medical Intensive Care, Charité – Universitätsmedizin Berlin, Augustenburger Platz 1, 13353 Berlin, Germany. <sup>2</sup> Department of Hepatology and Gastroenterology, Charité – Universitätsmedizin Berlin, Berlin, Germany. <sup>3</sup> Department of Hematology and Oncology, Charité – Universitätsmedizin Berlin, Berlin, Germany. <sup>4</sup> Institute for Transfusion Medicine, Charité – Universitätsmedizin Berlin, Berlin, Germany. <sup>5</sup> Wimedko GmbH, Berlin, Germany. <sup>6</sup> Institute of Biometry and Clinical Epidemiology, Charité – Universitätsmedizin Berlin, Berlin, Germany. <sup>7</sup> Berlin Institute of Health (BIH), Berlin, Germany. <sup>8</sup> Department of Rheumatology and Clinical Immunology, Charité – Universitätsmedizin Berlin, Berlin, Germany. <sup>9</sup> Deutsches Rheumaforschungszentrum (DRFZ), Berlin, Germany.

Received: 23 August 2020 Accepted: 20 November 2020

Published online: 07 December 2020

## References

1. Jin Y, Yang H, Ji W, et al. Virology, epidemiology, pathogenesis, and control of COVID-19. *Viruses*. 2020;12:372.
2. Dong E, Du H, Gardner L. An interactive web-based dashboard to track COVID-19 in real time. *Lancet Infect Dis*. 2020;20:533–4.
3. Huang C, Wang Y, Li X, et al. Clinical features of patients infected with 2019 novel coronavirus in Wuhan. *China Lancet*. 2020;395:497–506.
4. Zangrillo A, Beretta L, Scandroglio AM, et al. Characteristics, treatment, outcomes and cause of death of invasively ventilated patients with COVID-19 ARDS in Milan, Italy. *Crit Care Resusc*. 2020.
5. Lodigiani C, Iapichino G, Carenzo L, et al. Venous and arterial thromboembolic complications in COVID-19 patients admitted to an academic hospital in Milan, Italy. *Thromb Res*. 2020;191:9–14.
6. Helms J, Tacquard C, Severac F, et al. High risk of thrombosis in patients with severe SARS-CoV-2 infection: a multicenter prospective cohort study. *Intensive Care Med*. 2020;4:1–10.
7. Llitjos JF, Leclerc M, Chochois C, et al. High incidence of venous thromboembolic events in anticoagulated severe COVID-19 patients. *J Thromb Haemost*. 2020;18:1743–6.
8. Cui S, Chen S, Li X, Liu S, Wang F. Prevalence of venous thromboembolism in patients with severe novel coronavirus pneumonia. *J Thromb Haemost*. 2020;18:1421–4.
9. Zhang Y, Xiao M, Zhang S, et al. Coagulopathy and antiphospholipid antibodies in patients with Covid-19. *N Engl J Med*. 2020;382:e38.
10. Tang N, Li D, Wang X, Sun Z. Abnormal coagulation parameters are associated with poor prognosis in patients with novel coronavirus pneumonia. *J Thromb Haemost*. 2020;18:844–7.
11. Becker RC. COVID-19 update: Covid-19-associated coagulopathy. *J Thromb Thrombolysis*. 2020;50:54–67.
12. Fletcher TE, Leblebicioglu H, Bozkurt I, et al. Rotational thromboelastometry alongside conventional coagulation testing in patients with Crimean-Congo haemorrhagic fever: an observational cohort study. *Lancet Infect Dis*. 2019;19:862–71.
13. Gørlinger K, Bhardwaj V, Kapoor PM. Simulation in coagulation testing using rotational thromboelastometry: a fast emerging, reliable point of care technique. *Ann Card Anaesth*. 2016;19:516–20.
14. Zhou F, Yu T, Du R, et al. Clinical course and risk factors for mortality of adult inpatients with COVID-19 in Wuhan, China: a retrospective cohort study. *Lancet*. 2020;395:1054–62.

15. Hincker A, Feit J, Sladen RN, Wagener G. Rotational thromboelastometry predicts thromboembolic complications after major non-cardiac surgery. *Crit Care*. 2014;18:549.
16. Akay OM, Ustuner Z, Canturk Z, Mutlu FS, Gulbas Z. Laboratory investigation of hypercoagulability in cancer patients using rotation thrombelastography. *Med Oncol*. 2009;26:358–64.
17. Schmitt FCF, Manolov V, Morgenstern J, et al. Acute fibrinolysis shutdown occurs early in septic shock and is associated with increased morbidity and mortality: results of an observational pilot study. *Ann Intensive Care*. 2019;9:19.
18. Schochl H, Frietsch T, Pavelka M, Jambor C. Hyperfibrinolysis after major trauma: differential diagnosis of lysis patterns and prognostic value of thrombelastometry. *J Trauma*. 2009;67:125–31.
19. Panigada M, Bottino N, Tagliabue P, et al. Hypercoagulability of COVID-19 patients in intensive care unit. A report of thrombelastography findings and other parameters of hemostasis. *J Thromb Haemost*. 2020;18:1738–42.
20. Spiezia L, Boscolo A, Poletto F, et al. COVID-19-related severe hypercoagulability in patients admitted to intensive care unit for acute respiratory failure. *Thromb Haemost*. 2020;120:998–1000.
21. Pavoni V, Giansello L, Pazzi M, Stera C, Meconi T, Frigieri FC. Evaluation of coagulation function by rotation thromboelastometry in critically ill patients with severe COVID-19 pneumonia. *J Thromb Thrombolysis*. 2020;50:1–6.
22. Ibanez C, Perdomo J, Calvo A, et al. High D dimers and low global fibrinolysis coexist in COVID19 patients: what is going on in there? *J Thromb Thrombolysis*. 2020;15:1–5.
23. Roberts I. Fibrinolytic shutdown: fascinating theory but randomized controlled trial data are needed. *Transfusion*. 2016;56(Suppl 2):S115–8.
24. Lupu F, Keshari RS, Lambris JD, Coggeshall KM. Crosstalk between the coagulation and complement systems in sepsis. *Thromb Res*. 2014;133(Suppl 1):S28–31.
25. Degen JL, Bugge TH, Goguen JD. Fibrin and fibrinolysis in infection and host defense. *J Thromb Haemost*. 2007;5(Suppl 1):24–31.
26. Gando S, Wada H, Thachil J. Scientific, Standardization Committee on DICot/SoT, Haemostasis. Differentiating disseminated intravascular coagulation (DIC) with the fibrinolytic phenotype from coagulopathy of trauma and acute coagulopathy of trauma-shock (COT/ACOTS). *J Thromb Haemost*. 2013;11:826–35.
27. Abu-Fanne R, Stepanova V, Litvinov RI, et al. Neutrophil alpha-defensins promote thrombosis in vivo by altering fibrin formation, structure, and stability. *Blood*. 2019;133:481–93.
28. Hardaway RM, Harke H, Tyroch AH, Williams CH, Vazquez Y, Krause GF. Treatment of severe acute respiratory distress syndrome: a final report on a phase I study. *Am Surg*. 2001;67:377–82.
29. Barrett CD, Moore HB, Moore EE, et al. Fibrinolytic therapy for refractory COVID-19 acute respiratory distress syndrome: Scientific rationale and review. *Res Pract Thromb Haemost*. 2020;4:524–31.
30. Durila M, Smetak T, Hedvicak P, Berousek J. Extracorporeal membrane oxygenation-induced fibrinolysis detected by rotational thromboelastometry and treated by oxygenator exchange. *Perfusion*. 2019;34:330–3.

### Publisher's Note

Springer Nature remains neutral with regard to jurisdictional claims in published maps and institutional affiliations.

Ready to submit your research? Choose BMC and benefit from:

- fast, convenient online submission
- thorough peer review by experienced researchers in your field
- rapid publication on acceptance
- support for research data, including large and complex data types
- gold Open Access which fosters wider collaboration and increased citations
- maximum visibility for your research: over 100M website views per year

At BMC, research is always in progress.

Learn more [biomedcentral.com/submissions](https://biomedcentral.com/submissions)



### 3.3.2. Die Hypofibrinolyse nach schwerer COVID 19-Erkrankung ist reversibel

Mit der Erkenntnis, dass eine schwere COVID-19 Erkrankung und insbesondere ein C-ARDS zu einem hyperkoagulablem Zustand führen und immer wieder über eine Häufung thromboembolischer Ereignisse berichtet wurde, stellte sich neben der Frage nach Zielen einer Antikoagulation während der akuten Phase aber auch das Problem, dass unklar blieb, ob das erhöhte thromboembolische Risiko auch nach Abklingen der klinischen Symptomatik persistiert und ob sich daraus eine Indikation zur prothrombotischen systemischen Antikoagulation ergibt.

Kompliziert wird das Problem durch Berichte über eine Häufung von Blutungskomplikationen bei Patienten mit schwerer COVID-19 Erkrankung.<sup>35</sup>

Um einen Beitrag zur Klärung dieser Problematik zu bringen, luden wir alle Patienten, die von unserer Intensivstation nach einer kritischen COVID-19 Erkrankung entlassen worden waren, zu einer Follow-Up-Untersuchung in unsere Post-Intensivstationssprechstunde ein.

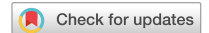
Von den während der ersten Welle behandelten Patienten konnten wir 13 in unserer Sprechstunde nach 12 Wochen nachuntersuchen. Es ergab sich klinisch und sonographisch kein Anhalt für neuhinzugetretene thromboembolische Ereignisse bei den Patienten.

Die jetzt erneut durchgeführte viskoelastische Untersuchung mittel des ROTEM®-Systems zeigte bei allen Patienten eine normalisierte Gerinnselfestigkeit und auch die Fibrinolyseaktivität, gemessen an der Maximum Lysis, hatte sich bei allen Patienten normalisiert.

Desweiteren lagen bei allen Patienten die Blutwerte für die D-Dimere und das Fibrinogen wieder im Normbereich<sup>36</sup>.

Man kann aus diesen Daten folgern, dass wahrscheinlich das erhöhte thrombembolische Risiko der Patienten sich nach Überwinden der klinischen Symptome normalisiert und vorbehaltlich größerer klinischer Studien, unabhängig von möglichen anderen Gründen, keine Indikation zur systemischen Antikoagulation jenseits der ersten drei Monate besteht.

**A Magomedov, D Zickler, S Karaivanov, A Kurreck, , F  
Münch, J Kamhieh-Milz, Caroline Ferse, A Kahl, S K Piper,  
K-U Eckardt, T Dörner, J M Kruse: Viscoelastic testing  
reveals normalization of the coagulation profile 12 weeks  
after severe COVID-19; Sci Rep 2201; 11:13325**



OPEN

## Viscoelastic testing reveals normalization of the coagulation profile 12 weeks after severe COVID-19

Abakar Magomedov<sup>1,9</sup>, Daniel Zickler<sup>1,9</sup>, Stoyan Karaivanov<sup>1</sup>, Annika Kurreck<sup>2</sup>, Frédéric H. Münch<sup>1</sup>, Julian Kamhieh-Milz<sup>3,4</sup>, Caroline Ferse<sup>1</sup>, Andreas Kahl<sup>1</sup>, Sophie K. Piper<sup>5,6</sup>, Kai-Uwe Eckardt<sup>1</sup>, Thomas Dörner<sup>7,8</sup> & Jan Matthias Kruse<sup>1</sup>✉

COVID 19 is associated with a hypercoagulable state and frequent thromboembolic complications. For how long this acquired abnormality lasts potentially requiring preventive measures, such as anticoagulation remains to be delineated. We used viscoelastic rotational thrombelastometry (ROTEM) in a single center cohort of 13 critical ill patients and performed follow up examinations three months after discharge from ICU. We found clear signs of a hypercoagulable state due to severe hypofibrinolysis and a high rate of thromboembolic complications during the phase of acute illness. Three month follow up revealed normalization of the initial coagulation abnormality and no evidence of venous thrombosis in all thirteen patients. In our cohort the coagulation profile was completely normalized three months after COVID-19. Based on these findings, discontinuation of anticoagulation can be discussed in patients with complete venous reperfusion.

### Abbreviations

ROTEM	Rotational thrombelastometry
COVID-19	Coronavirus 2019
SARS-CoV-2	Severe acute respiratory syndrome coronavirus 2
ARDS	Acute respiratory distress syndrome
ICU	Intensive care units
MCF	Maximum clot firmness
ML	Maximum lysis
PT	Prothrombin time
INR	International normalized ratio
aPTT	Activated partial thromboplastin time
t-PA	Tissue-type plasminogen activator
PAI-1	Plasminogen activator inhibitor-1
IQR	Interquartile range
ROC	Receiver operating characteristic
AUC	Area under the curve
CI	Confidence intervals
PCT	Procalcitonin
CRP	C-reactive protein

<sup>1</sup>Department of Nephrology and Medical Intensive Care, Charité-Universitätsmedizin Berlin, Augustenburger Platz 1, 13353 Berlin, Germany. <sup>2</sup>Department of Hematology and Oncology, Charité-Universitätsmedizin Berlin, Berlin, Germany. <sup>3</sup>Department of Transfusion Medicine, Universitätsmedizin Berlin, Berlin, Germany. <sup>4</sup>Wimedko GmbH, Manfred-von-Richthofen Str. 15, 12101 Berlin, Germany. <sup>5</sup>Institute of Biometry and Clinical Epidemiology, Charité-Universitätmedizin Berlin, Berlin, Germany. <sup>6</sup>Berlin Institute of Health (BIH), Anna-Louisa-Karsch 2, 10178 Berlin, Germany. <sup>7</sup>Department of Rheumatology und Clinical Immunology, Charité-Universitätsmedizin Berlin, Berlin, Germany. <sup>8</sup>Deutsches Rheumaforschungszentrum (DRFZ) Berlin, Berlin, Germany. <sup>9</sup>These authors contributed equally: Abakar Magomedov and Daniel Zickler. ✉email: jan-matthias.kruse@charite.de

SARS-CoV-2 is a single stranded RNA virus belonging to the coronavirus family. It causes coronavirus disease 2019 (COVID-19) which often can take an asymptomatic course but can also result in substantial severe manifestations, such as acute respiratory failure, acute kidney failure, multi-organ dysfunction and death. It has led to a global pandemic with over 2.9 million attributable death toll to date<sup>1,2</sup>.

While severe respiratory failure seems to be the most frequent cause of death, other complications like acute kidney injury, cardiac and neurologic involvement seem to occur more frequent than initially expected<sup>3–6</sup>.

From the beginning of the pandemic, a high incidence of thromboembolic complications was reported in patients with COVID-19 and autopsy findings confirmed a high rate of local thrombosis and embolic events in the pulmonary and systemic circulation associated with the disease<sup>7–11</sup>. Laboratory markers revealed hyperinflammation linked to a hypercoagulable status with markedly elevated levels of fibrinogen, d-dimers and thrombocytosis. Numerous haemostatic tests performed in ICU patients with COVID-19 have shown, namely viscoelastic tests (ROTEM, TEG), Thrombin Generation (reference 1, 2, 3) and Clot Waveform analysis (reference 4, 5) have demonstrated a hypercoagulable state<sup>12–16</sup>.

In our intensive care units we performed viscoelastic testing and noted severely impaired fibrinolysis as a characteristic of procoagulation in COVID-19<sup>17</sup>. In this context the term fibrinolytic shutdown has been proposed<sup>18</sup>.

These findings led to intensive discussions about the pros and cons of systemic anticoagulation, use of available drugs and intensity of systemic anticoagulation<sup>19–23</sup>. The question for how long survivors of the disease should receive subsequent anticoagulation as secondary prophylaxis is unclear so far. Long term data regarding the question whether the hypercoagulable state persists after clinical cure of the disease are currently lacking<sup>23</sup>.

Here we present observational data of 13 critically ill patients with COVID-19 who presented at the post Intensive Care clinic of a tertiary care university hospital 3 months after discharge from ICU.

## Methods

**Follow-up cohort.** Out of 41 Covid-19 patients admitted to our ICUs between March 25th and May 11th 2020, 29 patients survived<sup>17</sup>. All of these were invited for a follow-up visit. Thirteen patients came back to the follow-up visit after 3 months.

**Anticoagulation.** Upon admission on the ICU, all COVID patients were treated with therapeutic anticoagulation using intermediate doses of unfractionated heparin or argatroban with a aPTT goal of 50–55 s. Nevertheless, nine out of thirteen patients developed thromboembolic complications during their stay on the intensive care unit (ICU). These patients were then anticoagulated using higher doses of unfractionated heparin or argatroban with a targeted partial thromboplastin time of 60–80 s, respectively. Upon transfer to rehabilitation units the continuation of this therapy regimen was recommended followed Rivaroxaban 20 mg per day until the first visit to the follow up clinic 12 weeks after discharge from the ICU.

**Coagulation tests.** After admission to our ICUs, routine viscoelastic tests were performed with citrated blood by using a ROTEM sigma point-of-care device (Tem International, Munich, Germany)<sup>24</sup>. In each patient, intrinsically (contact activation, INTEM) and extrinsically (tissue factor activation, EXTEM) activated test assays were performed to analyze the clot dynamics in both coagulation pathways. Furthermore, FIBTEM and HEPTEM were performed. For FIBTEM thrombocytes are inactivated with Cytochalasin D to allow isolated evaluation of fibrinogen in clot firmness. For HEPTEM heparinase is added. The heparin effect was determined by comparing the clotting time of the INTEM with the clotting time of the HEPTEM.

The following ROTEM variables were analyzed: clotting time defined as the time until initiation of clotting; clot formation time (seconds until a clot strength reaches 20 mm), reflecting the kinetics of clot formation; maximum clot firmness (MCF) defined as the maximum amplitude of clot firmness; maximum lysis (ML) in percent (%) defined as the difference between MCF and the lowest clot amplitude after MCF, reflecting fibrinolytic activity (Fig. 1).

Additional routine laboratory tests carried out according to standardized protocols comprised haemoglobin concentration, white blood cell count, platelet count, prothrombin time (PT), International Normalized Ratio (INR), activated partial thromboplastin time (aPTT), d-dimers, fibrinogen, Interleukin 6, CRP and Ferritin (see Table 2).

**Ultrasound assessments.** During the ICU stay we performed ultrasound examinations in all patients (GE Vivid S70 ultrasound machine with a 9L-D probe) to screen for deep venous thrombosis, focusing on the jugular, subclavian, brachial, femoral and popliteal veins upon admission to our ICU and subsequently at least once a week.

The same examinations were performed as part of the 3 months follow-up visit.

**Post-ICU-follow-up evaluations.** All patients were invited for follow-up visits scheduled 3 months after discharge from the ICU. Follow-up visits took place at our post-ICU outpatient department and followed a standardized procedure including a medical consultation, ultrasound examination of the large vessels as described above and routine laboratory work up, including viscoelastic tests.

**Ethics.** The study was approved by the ethics committees of Charité—Universitätsmedizin Berlin (EA4/115/20) and was in compliance with the Declaration of Helsinki. Consent to participate was not applicable due to the retrospective nature of the study. Informed consent was exempted by the ethics committee of the Charite Universitätsmedizin Berlin (EA4/115/20).

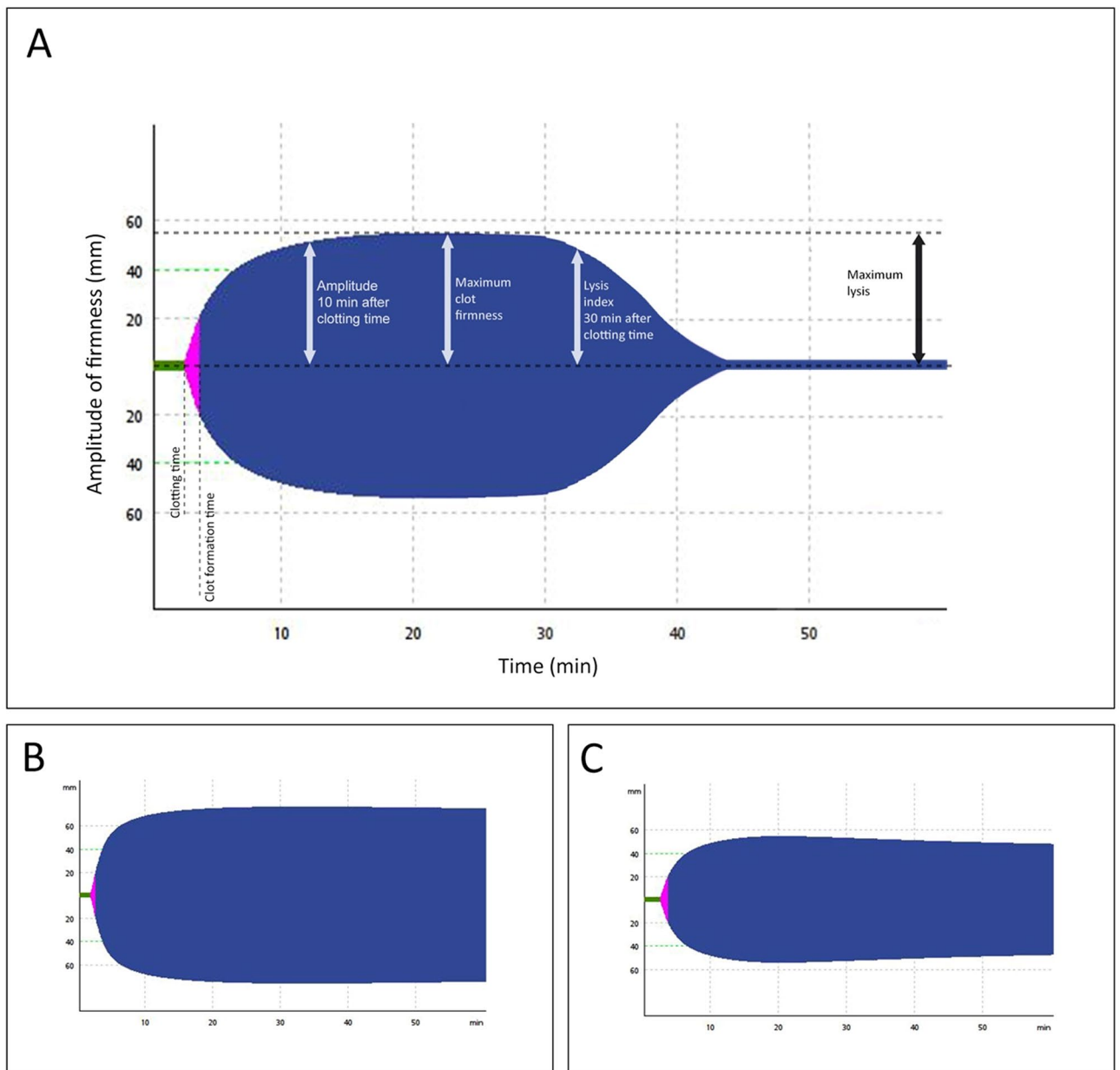


**Figure 1.** (A) Shows all measured values in ROTEM analysis, including clotting time (CT [s]), clot formation time (CFT [s]), maximum clot firmness (MCF [mm]) and maximum lysis (ML [%range]). (B) Describes a fibrinolysis shutdown pattern (increased MCF, low ML) in a COVID-19 patient with a thromboembolic event; the clot amplitude remains unchanged until the end. (C) Shows a clot profile with reduced MCF and increased ML in a patient during the follow-up presentation.

**Statistics.** Statistical evaluations were performed with IBM SPSS Statistics Version 26 (New York, USA) and GraphPad Prism (version 8.4.3; GraphPad Software, San Diego, CA, USA). Descriptive variables were given as median with limits of the interquartile range (IQR) for continuous variables or as absolute and relative frequencies for categorical variables.

Continuous data were mostly right skewed. Therefore, Wilcoxon signed rank test was used to compare changes in continuous variables between ICU stay and 3 months follow-up evaluation. A two-sided significance level of 0.05 was applied without adjustment for multiple comparison. All p-values constitute exploratory data analyses and do not allow for confirmatory generalization of results.

## Results

Out of 41 Covid-19 patients admitted to our ICUs between March 25th and May 11th 2020, thirteen patients came back to the follow-up visit after three months. Out of 13 patients, 9 were male with a median age of 60 [IQR 53–67] years and a median BMI of 29.6 [IQR 27.8–33.9].

	Whole cohort (n = 41)		No follow-up- cohort (n = 28)		Follow-up cohort (n = 13)		P follow-up vs. no follow-up
Age (years, (median, [IQR]))	67	[56.5–76.5]	69.5	[59–78]	60	[53–66.5]	0.019
Gender, male (n, %)	35	85.4%	26	92.9%	9	69.2%	ns
BMI, kg/m <sup>2</sup> (median, [IQR])	28.0	[25–32.7]	27.8	[24.3–31.1]	29.6	[27.8–33.5]	ns
Duration of ICU stay, days (median, [IQR])	39.0	[24–52.5]	28.5	[24–47.5]	46	[30–62]	ns
Death during ICU stay (n, %)	11	26.8%	11	39.3%			
Thromboembolic events (n, %)	24	58.5%	15	53.6%	9	69.2%	ns
Intubation (n, %)	36	87.8%	25	89.3%	11	84.6%	ns
ECMO (n, %)	10	24.4%	5	17.9%	5	38.5%	ns
CRRT (n, %)	22	53.7%	13	46.4%	9	69.2%	ns
SOFA-Score (median, [IQR])	9	[6.5–11.5]	8.5	[6.25–11]	10	[6.25–12.0]	ns
SIC-Score (median, [IQR])	3	[2–4]	3	[2–4]	3	[2–4]	ns
APACHE-Score (median, [IQR])	28	[22–33]	26	[22–32]	31.0	[25.5–34]	ns
Follow up days					100	[63.5–108.50]	
<b>Preexisting conditions</b>							
Coronary artery disease (n, %)	9	22%	7	25%	2	15.4%	ns
Hypertension (n, %)	28	68.3%	18	64.3%	10	76.9%	ns
Diabetes mellitus/insulin resistance (n, %)	13	31.7%	8	28.6	5	38.5%	ns
Chronic kidney disease (n, %)	7	17.1%	5	17.9%	2	15.4%	ns
Chronic dialysis (n, %)	1	2.4%	1	3.6%	0	0%	ns
Lung disease (n, %)	10	24.4%	7	25%	3	23.1%	ns

**Table 1.** Baseline characteristics of patients with COVID-19 infection. *ECMO* Extracorporeal membrane oxygenation, *SOFA* sequential organ failure assessment, *CRRT* continuous renal replacement therapy, *SIC* Sepsis-Induced Coagulopathy Score, *APACHE* acute physiology and chronic health evaluation.

Their median SOFA score was 10.0 [IQR 5.3–11.8] points and their median APACHE II was 32.5 [IQR 25.3–34.0] points. Eleven patients required mechanical ventilation (85%), whereas extracorporeal membrane oxygenation was required in five (39%). Nine patients developed acute renal failure requiring continuous renal replacement therapy (69%). Median length of stay in the intensive care unit was 45 [IQR 30–65] days. (Table 1).

**Laboratory parameters.** The laboratory values are displayed in Table 2 and showed distinctive changes between the ICU and post-discharge timepoints regarding inflammatory and coagulation parameters.

In terms of the measurements of coagulation values, patients during their initial ICU admission had significantly elevated levels of d-dimers (4.8 mg/l [IQR 3.9–7.8] vs. 0.4 mg/l [IQR 0.3–0.8],  $p=0.001$ ) and fibrinogen (6.7 mg/l [IQR 4.7–8.3] vs. 3.6 mg/l [IQR 2.9–4.5],  $p=0.006$ ) compared to their follow-up measurements (Fig. 2). Moreover, the median of fibrinogen and d-dimers levels returned to a normal level at the follow-up visit (Table 2). aPTT was significantly prolonged during the ICU stay (56.4 s [IQR 47.6–62.0] vs. 36.8 s [IQR 34.4–43.7],  $p=0.033$ ), whereas prothrombin time and INR revealed no significant difference between measurement time points. CRP (191.0 mg/l [IQR 121.0–314.4] vs. 2.9 mg/l [IQR 2.1–6.3],  $p=0.001$ ), Ferritin (2408.7  $\mu$ g/l [IQR 1441.5–5280.5] vs. 190.4  $\mu$ g/l [IQR 108.6–288.2],  $p=0.002$ ) and IL-6 (177 ng/l [IQR 68.0–358.0] vs. 2.9 ng/l [IQR 2.1–6.3],  $p=0.02$ ) were significantly elevated during the ICU stay.

Notably, ROTEM analyses showed substantial changes between the measurements between the ICU stay and follow-up visit. (Fig. 3) Maximum clot firmness decreased significantly with median values from 73 mm [IQR 70.0–76.5] to 63.0 mm [IQR 59.5–67.5] ( $p=0.003$ ), in INTEM; from 73 mm [IQR 71.5–76] to 66.0 mm [IQR 63.5–70.0] ( $p=0.004$ ) in EXTEM and from 32 mm [IQR 27.0–39] to 16 mm [IQR 14–24] ( $p=0.002$ ), in FIBTEM.

Clot formation time in EXTEM und INTEM were longer at the follow up visit compared to ICU measurements, but these changes were not statistically significant. In contrast to the ICU values, the maximum Lysis (ML) in INTEM and EXTEM increased significantly until 3 months follow-up (ML INTEM from 2% [IQR 2–4] to 8% [IQR 6–13] at Follow-Up;  $p=0.002$ ; ML EXTEM median from 3% [IQR 3–5] to 8% [IQR 6–12] at Follow-Up;  $p=0.002$ ) marking a substantial normalization of the fibrinolytic capacity which was markedly impaired at the initial assessments.

**Thromboembolic events.** During ICU stay, nine patients developed thromboembolic complications. In this regard, two patients developed pulmonary embolisms, while lower-extremity deep venous thrombosis was found in seven patients.

At 3 month follow-up, there was no sonographic evidence of thrombosis in any of the patients indicating complete recanalization of the prior occluded veins (see Table 3).

	ICU (N = 13)		Follow-up (N13)		p value
	Median	[IQR]	Median	[IQR]	
<b>Laboratory variables (normal values)</b>					
Haemoglobin (12.5–17.2 g/dL)	9.9	[8.7–11.0]	13.6	[10.6–14.1]	0.006
White blood cells (3.5–10.5/nl)	12.8	[8.0–13.6]	7.1	[5.3–9.1]	0.023
Platelet count (150–370/nl)	142.0	[116.0–271.5]	224.0	[193.5–237.0]	0.263
Prothrombin time (70–130%)	79.0	[64.0–86.5]	85.0	[78.5–96.5]	0.196
INR (0.9–1.25)	1.2	[1.1–1.4]	1.1	[1.0–1.2]	0.173
aPTT (26–40 s)	56.4	[49.2–62.0]	36.8	[34.4–43.7]	0.033
D-dimers (<0.5 mg/l)	4.8	[3.9–7.8]	0.4	[0.3–0.8]	0.001
Fibrinogen (1.6–4 g/l)	6.7	[4.7–8.3]	3.6	[2.9–4.5]	0.006
IL-6 (<7 ng/l)	173.0	[68.0–358.0]	2.9	[2.1–6.3]	0.002
CRP (<0.5 mg/l)	191.0	[121.0–314.4]	3.0	[1.6–5.4]	0.001
Ferritin (30–400 µg/l)	2408.7	[1441.5–5280.5]	190.4	[108.6–288.2]	0.002
<b>ROTEM variables (reference ranges)</b>					
FIBTEM CT (43–69 s)	92.0	[86.5–104.5]	99.0	[68.0–110.5]	0.463
FIBTEM CFT (n/a s)	101.0	[54.5–200.5]	198.0	[57.5–559.0]	0.225
FIBTEM A10 (9–24 mm)	29.0	[24.0–35.5]	15.0	[13.0–21.5]	0.002
FIBTEM MCF (9–25 mm)	32.0	[27.0–39.0]	16.0	[14.0–24.0]	0.002
EXTEM CT (42–74 s)	88.0	[83.5–101.0]	79.0	[62.5–100.5]	0.039
EXTEM CFT (46–148 s)	54.0	[42.0–64.5]	64.0	[48.5–82.5]	0.208
EXTEM A10 (43–65 mm)	66.0	[63.0–68.5]	59.0	[54.5–62.5]	0.033
EXTEM MCF (49–71 mm)	73.0	[71.5–76.0]	66.0	[63.5–70.0]	0.004
INTEM CT (137–246 s)	215.0	[187.5–258.0]	189.0	[176.5–201.5]	0.019
INTEM CFT (40–100 s)	56.0	[50.5–60.5]	71.0	[52.5–79.5]	0.075
INTEM A10 (44–68 mm)	64.0	[60.0–70.5]	57.0	[53.5–59.5]	0.006
INTEM MCF (52–72 mm)	73.0	[70.0–76.5]	63.0	[59.5–67.5]	0.003
ML EXTEM (0–18%)	3.0	[3.0–5.0]	8.0	[6.0–12.0]	0.002
ML INTEM (0–12%)	2.0	[2.0–4.0]	8.0	[6.0–13.0]	0.002

**Table 2.** The laboratory and ROTEM values at ICU presentation and 3 months follow-up. Unless values are designated as maximum values during the ICU stay, these parameters were determined on the day, when ROTEM analysis was performed, after admission to our ICUs. *CT* Clotting time, *CFT* clot formation time, *MCF* maximum clot firmness, *ML* maximum lysis<sup>55</sup>.

## Discussion

We report the data of thirteen critically ill patients with COVID-19, who initially required ICU admission with a severely hyperinflammatory and hypercoagulable state characterized by high levels of d-dimers and fibrinogen and a markedly increased clot firmness consistent with impaired fibrinolysis. While a hypercoagulable state was noted during their stay on the ICU, on their first visit in the ICU-follow-up clinic three months after discharge, they presented with normalized markers of inflammation and coagulation. Fibrinolytic activity and clot firmness had returned to normal values consistent with the reversible nature of the initial hypofibrinolysis. All patients analyzed showed normal d-dimer levels reflecting normalized turnover of the coagulation system also taken as surrogate of recurrence risks. Following normalization of laboratory values and viscoelastic parameters anticoagulation has been discontinued in all patients.

Venous and arterial thrombembolism contribute significantly to morbidity and mortality in COVID-19<sup>7–11,25,26</sup>. The nature of COVID-19 coagulopathy appears to be complex and the exact mechanisms still have to be elucidated. In contrast to septic coagulopathy thrombocytopenia seems to be a rare finding and only few patients with COVID-19 meet the criteria for disseminated intravascular coagulation<sup>27</sup>.

Ranucci and Panagida performed comprehensive coagulation analyses in critical ill patients with COVID-19 including viscoelastic testing and demonstrated increased clot firmness beside significant elevations in levels of d-dimers and fibrinogen-levels as reported by various other authors<sup>28–30</sup>. The amplitude of the d-dimer level was associated with increased mortality in several studies<sup>30,31</sup>. Spiezia et al. and Pavoni et al. have also recently shown severe hypercoagulopathy in critical-ill COVID-19 patients using viscoelastic testing<sup>32,33</sup>. Microthrombus formation in the lungs and various other organs has been described in autopsy series<sup>11,34</sup>. Microvascular injury associated with complement deposition might serve as a possible explanation as Magro et al. reported in their study<sup>35</sup>.

SARS-CoV2 can infect endothelial cells through the ACE2-receptor and cause endothelial damage and apoptosis<sup>36</sup>. Endothelial injury resulting in substantial endothelitis together with dysfunction seems to play a crucial role in the induction of microvascular thrombosis in COVID-19<sup>37</sup>.

Panagida et al. found diminished activity of fibrinolysis in their ROTEM-analysis<sup>28</sup>. Similar changes have been reported in septic patients and might indicate protective mechanisms employed to isolate intruding

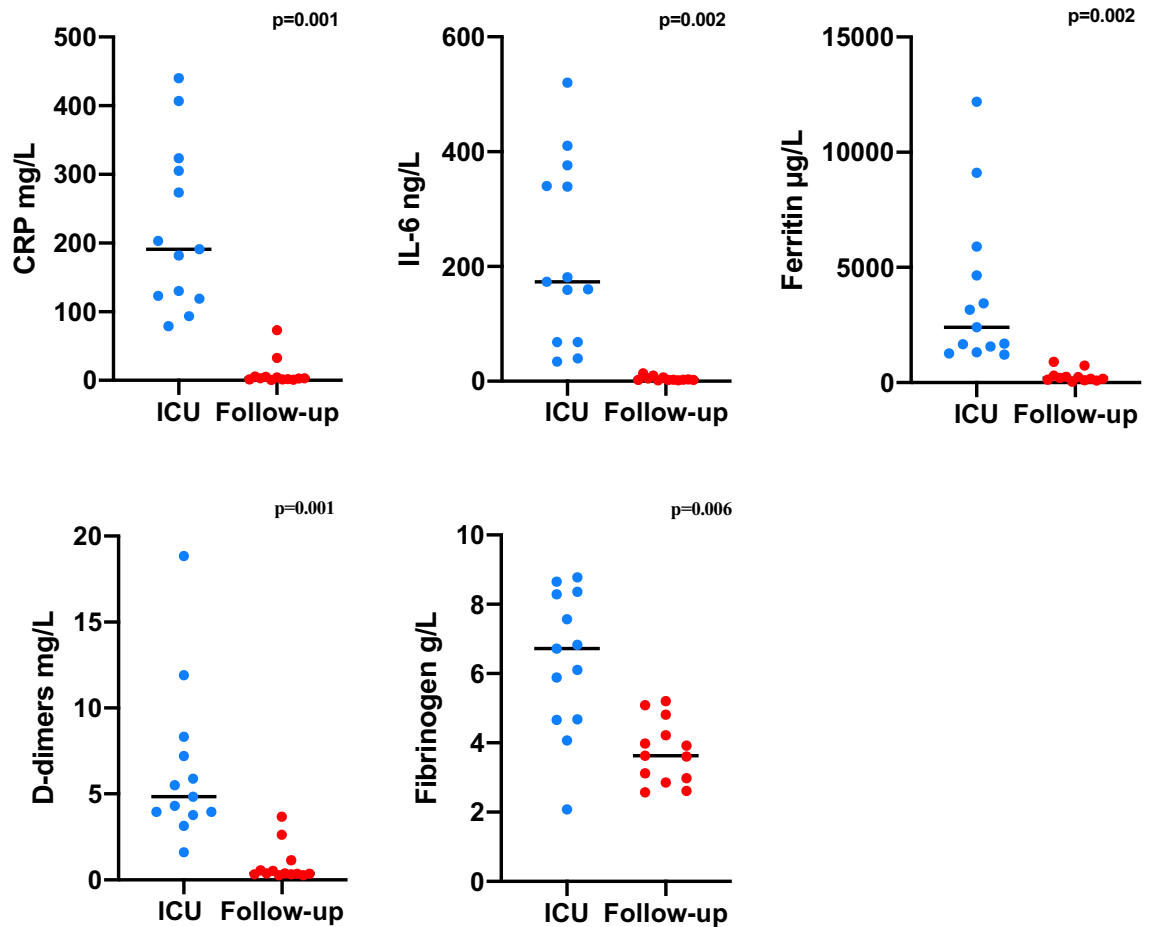


**Figure 2.** Comparison of inflammatory markers during ICU stay and follow-up visit ( $n = 13$ , Wilcoxon signed rank test).

pathogens<sup>38,39</sup>. One might interpret the persisting fibrinolytic shutdown in COVID-19 as a consequence of the fact that there is no effective therapeutic agent to influence viremia until today and to protect the endothelial cells that are not only the target of SARS-Cov2 but also the key tissue regulating fibrinolysis. Impaired fibrinolysis has also been linked to the pathogenesis of ARDS in general<sup>40,41</sup>.

Continuously reported high levels of inflammatory cytokines and infiltration of tissues with granulocytes and monocytes as demonstrated for lung tissue in autopsy using caspase-3 immunostaining probably also play an important role in the pathogenesis of coagulopathy and thrombophilia in COVID-19<sup>37,42</sup> with a particular impact on endothelial damage.

Tang et al. demonstrated decreased mortality in COVID-19 patients with coagulopathy who were treated with either unfractionated heparin or low molecular weight heparin (LMWH) for 7 days or longer compared to those who did not receive heparin<sup>43</sup>. Heparin has anti-inflammatory effects and might mitigate capillary leakage and favorably influence the toxic effect of damage associated molecular patterns (DAMPs) and histones on the endothelium<sup>44,45</sup>.

The American College of chest physicians (ACCP) and the American Society of hematology (ASH) recommended low molecular weight heparin (LMWH) in prophylactic doses in critical ill COVID-19 patients and in therapeutic dose if venous thromboembolism (VTE) occurred<sup>19</sup>.

Recent guidelines of the International society on thrombosis and hemostasis (ISTH) recommend either prophylactic or intermediate dosing of LMWH or UFH<sup>46</sup>.

Given the high incidence of thromboembolic events many centers switched to intermediate dosing of anti-coagulation instead of standard prophylaxis<sup>26,47</sup>.

As a consequence, our patients received unfractionated heparin with a target PTT of 50–55 (normal range aPTT 39 s) seconds as long as there were no thromboembolic complications. Patients with thromboembolic events received therapeutic doses of unfractionated heparin with a target PTT of 60–80 s. We decided against routine measurements of AT-III-levels in all patients, instead patients who received more than 1800 U of unfractionated heparin per hour and still did not reach their target PTT were classified as heparin resistant and switched to Argatroban. The reason for this being the fear of increasing the risk of enhancing bleeding episodes by substitution of AT-III while at the same time further uptitrating the dose of unfractionated heparin, given the difficult situation of frequent thromboembolic complications on the one hand and reported enhanced risk of bleeding episodes on the other. We decided to use Argatroban and not Bivalirudin due to the greater experience in our

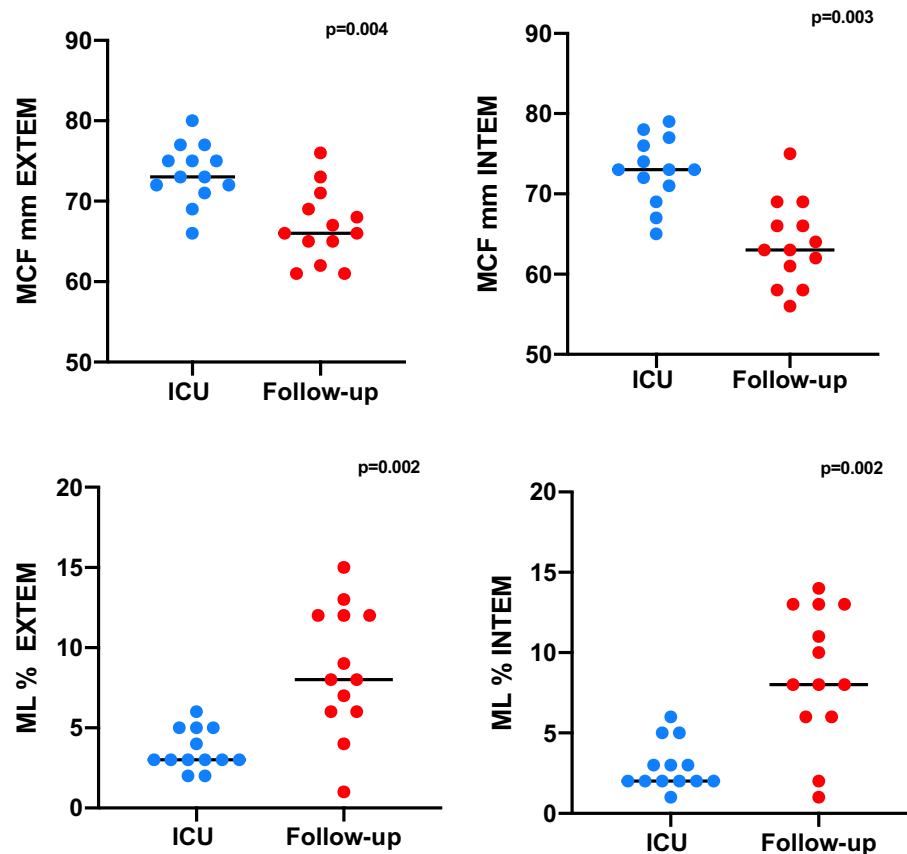


**Figure 3.** Comparison of coagulation parameters during ICU stay and follow-up visit (n = 13, Wilcoxon signed rank test).

Age	Gender	Thromboembolic event	Follow-up sonogram
51	F	Left femoral vein	No evidence of thrombosis
59	M	Left femoral vein	No evidence of thrombosis
60	M	Left popliteal vein	No evidence of thrombosis
67	M	Left and right popliteal vein	No evidence of thrombosis
64	F	Bilateral central pulmonary embolism	No evidence of thrombosis
56	M	Right femoral and external iliac vein	No evidence of thrombosis
47	M	Bilateral central pulmonary embolism	No evidence of thrombosis
38	F	Femoral vein and ecmo cannula clotting	No evidence of thrombosis
75	M	Right internal jugular vein	No evidence of thrombosis
68	M	No thromboembolic event	No evidence of thrombosis
62	M	No thromboembolic event	No evidence of thrombosis
55	F	No thromboembolic event	No evidence of thrombosis
66	M	No thromboembolic event	No evidence of thrombosis

**Table 3.** Results of the ultraononographic examinations at 3 month follow up.

department with the use of Argatroban. We did not encounter spontaneous prolonging of the aPTT and did not routinely check for lupus anticoagulans. Since the turnaround time for the anti-Xa-activity is about 12 h at our institution, we decided against its use for guiding our anticoagulation management.

In contrast to individual parameters, viscoelastic methods like thrombelastography and ROTEM permit functional evaluations of whole blood aggregometry. Thus it allows evaluation of the different and complex coagulation phases including the initiation, formation and stabilization of a clot, and finally, clot lysis. Still endothelial function and the influence of soluble tissue factor have to be taken into account as they will not be represented in the results of the test. Not only bleeding diathesis as the classical indication for viscoelastic testing but also hypercoagulable conditions due to different diseases were examined in the past using ROTEM and states of hyper- and hypofibrinolysis could be reliably detected and characterized by viscoelastic tests<sup>38,48–50</sup>.

Our cohort presented with a significantly increased clot firmness on the one hand and severely impaired fibrinolytic activity represented by a maximum lysis of < 3% during their ICU-stay on the other.

The clot lysis parameter ML provides information on the fibrinolytic capacity and was successfully used in several studies to assess hyper-, or hypofibrinolysis. Lower values of ML provide evidence of existing hypofibrinolysis, while values above 15% are suggestive for hyperfibrinolysis. Other groups already demonstrated that global haemostatic tests in critical ill patients with COVID-19, tests revealed a hypercoagulable state. That holds true for viscoelastic tests like TEG and ROTEM as well as Thrombin Generation (14, 15, 16) and Clot Generation Waveform analysis (17, 18). Nouigier et al. reported in their recent study that critical ill patient with COVID pneumonia have an impaired fibrinolytic capacity which was associated with increased levels of PAI-1 and TAFI<sup>14</sup>. It has also been proposed that decreased activity of urokinase-type plasminogen activator and increased release of plasminogen activator inhibitor-1 might be the mediating mechanism of hypofibrinolysis, but data to support this further are scarce<sup>51</sup>.

On their 12-week follow up visit, clot firmness and fibrinolytic activity had normalized in all patients. The significant increase of ML in the follow-up assessment indicates an appropriate regeneration or reversibility of physiologic fibrinolytic capacity.

To the best of our knowledge, this is a first study reporting follow-up data on the reversibility of thrombelastometry abnormalities after COVID-19. We found normalized fibrinolytic activity and normalized clot firmness. In contrast, von Meijenfeldt et al. found sustained prothrombotic changes in COVID-19 patients 4 months after hospital discharge. 53 Hemostasis exams showed enhanced thrombin-generating capacity and decreased plasma fibrinolytic potential. Further studies will be necessary to clarify this contradictory data situation.

ACCP recommends to evaluate patients for extended prophylaxis after their hospital stay depending on their risk of bleeding<sup>19</sup>. ISTH states, that post discharge prophylaxis for 2–6 weeks should be considered<sup>46</sup>. For patients after VTE, current guidelines recommend therapeutic anticoagulation for at least 3 months<sup>46</sup>.

Especially patients with high d-dimer values were found to be at high risk of post-discharge VTE independent of COVID-19<sup>32</sup>. Around 60% of all VTE in medical patients occur in the post-hospital discharge period with a more than 5 times increased risk in fatal pulmonary embolism<sup>53</sup>. Newer studies reported favorable risk–benefit ratios for extended prophylaxis in medical patients<sup>54</sup>.

In conclusion our patients who suffered from thromboembolic events during their course of COVID-19 received therapeutic anticoagulation during their ICU stay and continuation was recommended for the first 3 months thereafter. Taking into account the grade of immobilization and the high levels of d-dimers, increased clot firmness and severely impaired fibrinolysis on viscoelastic testing, we recommended to evaluate therapeutic anticoagulation in the patients without thromboembolic complications at least until reassessment during their first visit on the post-ICU-clinic. On the other hand, proper patient selection to identify patients at higher risk for bleeding while at the same time weighing it against the risk of thrombosis is crucial.

On their 3 months follow-up visit all patients presented with normalized values of d-dimer, fibrinogen and viscoelastic testing. Inflammatory markers were also normalized. Since there were no signs of a persistent hypercoagulable state left and none of the patients suffered from a thromboembolic event after discharge the discontinuation of anticoagulation can be discussed and future clinical trials are needed.

Our study has several limitations. We report the data of a relatively small single center cohort of critically ill patients which may limit generalizability. Due to its retrospective nature it can only be hypothesis generating. Our presumptions have to be verified in a clinical trial focusing not only on coagulation profiles but also on clinical data such as rate of thromboembolic events and ideally survival.

Furthermore, in the meantime between ICU discharge and follow-up, no control follow-ups were routinely performed or analyzed.

Moreover, we only performed anamnesis, clinical examination and screening ultrasound examinations as follow-up exams. There were no clinical or anamnestic hints for pulmonary embolism but routine tests regarding asymptomatic events were performed so no statements regarding asymptomatic pulmonary embolism can be made.

In summary, we found substantially limited fibrinolysis in acutely ill COVID-19 patients with normalization after three months.

## Conclusion

In our cohort of critically ill COVID-19 patients, the coagulation profile and inflammatory markers were completely normalized three months after discharge from the ICU. It thus appears reasonable that anticoagulation can be discontinued beyond this timepoint in patients with complete venous reperfusion.

## Data availability

The datasets analyzed during the current study are available from the corresponding author upon reasonable request.

Received: 14 January 2021; Accepted: 14 June 2021

Published online: 25 June 2021

## References

1. Jin, Y. et al. Virology, epidemiology, pathogenesis, and control of COVID-19. *Viruses* **12**, 372 (2020).
2. Dong, E., Du, H. & Gardner, L. An interactive web-based dashboard to track COVID-19 in real time. *Lancet Infect. Dis.* **20**, 533–534 (2020).
3. Ronco, C., Reis, T. & Husain-Syed, F. Management of acute kidney injury in patients with COVID-19. *Lancet Respir. Med.* **8**, 738–742 (2020).

4. Chan, L. *et al.* AKI in hospitalized patients with COVID-19. *J. Am. Soc. Nephrol.* **32**, 151–160 (2020).
5. Akhmerov, A. & Marban, E. COVID-19 and the heart. *Circ. Res.* **126**, 1443–1455 (2020).
6. Mao, L. *et al.* Neurologic manifestations of hospitalized patients with coronavirus disease 2019 in Wuhan, China. *JAMA Neurol.* **77**, 683–690 (2020).
7. Lodigiani, C. *et al.* Venous and arterial thromboembolic complications in COVID-19 patients admitted to an academic hospital in Milan, Italy. *Thromb. Res.* **191**, 9–14 (2020).
8. Helms, J. *et al.* High risk of thrombosis in patients with severe SARS-CoV-2 infection: A multicenter prospective cohort study. *Intensive Care Med.* **46**, 1089–1098 (2020).
9. Klok, F. A. *et al.* Incidence of thrombotic complications in critically ill ICU patients with COVID-19. *Thromb. Res.* **191**, 145–147 (2020).
10. Menter, T. *et al.* Post-mortem examination of COVID-19 patients reveals diffuse alveolar damage with severe capillary congestion and variegated findings of lungs and other organs suggesting vascular dysfunction. *Histopathology* **77**, 198–209 (2020).
11. Wichmann, D. *et al.* Autopsy findings and venous thromboembolism in patients with COVID-19: A prospective cohort study. *Ann. Intern. Med.* **173**, 1030 (2020).
12. Ranucci, M. *et al.* Covid-19-associated coagulopathy: Biomarkers of thrombin generation and fibrinolysis leading the outcome. *J. Clin. Med.* **9**, 3487 (2020).
13. Campello, E., Bulato, C., Spiezia, L. *et al.* Thrombin generation in patients with COVID-19 with and without thromboprophylaxis. *Clin. Chem. Lab. Med.* (2021). (Online ahead of print)
14. Nougier, C. *et al.* Hypofibrinolytic state and high thrombin generation may play a major role in SARS-CoV2 associated thrombosis. *J. Thromb. Haemost.* **18**, 2215–2219 (2020).
15. Fan, B. E. *et al.* COVID-19 associated coagulopathy in critically ill patients: A hypercoagulable state demonstrated by parameters of haemostasis and clot waveform analysis. *J. Thromb. Thrombolysis* **51**, 663–674 (2021).
16. Tan, C. W. *et al.* Critically ill COVID-19 infected patients exhibit increased clot waveform analysis parameters consistent with hypercoagulability. *Am. J. Hematol.* **95**, E156–E158 (2020).
17. Kruse, J. M. *et al.* Thromboembolic complications in critically ill COVID-19 patients are associated with impaired fibrinolysis. *Crit. Care* **24**, 676 (2020).
18. Wright, F. L. *et al.* Fibrinolysis shutdown correlation with thromboembolic events in severe COVID-19 infection. *J. Am. Coll. Surg.* **231**, 193–203 (2020).
19. Moores, L. K. *et al.* Prevention, diagnosis, and treatment of VTE in patients with coronavirus disease 2019: CHEST guideline and expert panel report. *Chest* **158**, 1143–1163 (2020).
20. McGlynn, F. *et al.* Argatroban for therapeutic anticoagulation for heparin resistance associated with Covid-19 infection. *J. Thromb. Thrombolysis* **51**, 243–245 (2020).
21. Aliter, K. F. & Al-Horani, R. A. Thrombin inhibition by argatroban: Potential therapeutic benefits in COVID-19. *Cardiovasc. Drugs Ther.* **35**, 195–203 (2020).
22. Arachchilage, D. J. *et al.* Anticoagulation with argatroban in patients with acute antithrombin deficiency in severe COVID-19. *Br. J. Haematol.* **190**, e286–e288 (2020).
23. Barnes, G. D. *et al.* Thromboembolism and anticoagulant therapy during the COVID-19 pandemic: Interim clinical guidance from the anticoagulation forum. *J. Thromb. Thrombolysis* **50**, 72–81 (2020).
24. Gorlinger, K., Bhardwaj, V. & Kapoor, P. M. Simulation in coagulation testing using rotational thromboelastometry: A fast emerging, reliable point of care technique. *Ann. Card. Anaesth.* **19**, 516–520 (2016).
25. Llitjos, J. F. *et al.* High incidence of venous thromboembolic events in anticoagulated severe COVID-19 patients. *J. Thromb. Haemost.* **18**, 174–1746 (2020).
26. Middeldorp, S. *et al.* Incidence of venous thromboembolism in hospitalized patients with COVID-19. *J. Thromb. Haemost.* **18**, 1995–2002 (2020).
27. Deng, Y. *et al.* Clinical characteristics of fatal and recovered cases of coronavirus disease 2019 in Wuhan, China: A retrospective study. *Chin. Med. J. (Engl.)* **133**, 1261–1267 (2020).
28. Panigada, M. *et al.* Hypercoagulability of COVID-19 patients in Intensive Care Unit. A report of thromboelastography findings and other parameters of hemostasis. *J. Thromb. Haemost.* **18**, 1738–1742 (2020).
29. Ranucci, M. *et al.* The procoagulant pattern of patients with COVID-19 acute respiratory distress syndrome. *J. Thromb. Haemost.* **18**, 1747–1751 (2020).
30. Zhou, F. *et al.* Clinical course and risk factors for mortality of adult inpatients with COVID-19 in Wuhan, China: A retrospective cohort study. *Lancet* **395**, 1054–1062 (2020).
31. Zhang, L. T. *et al.* D-dimer levels on admission to predict in-hospital mortality in patients with Covid-19. *J. Thromb. Haemost.* **18**, 1324–1329 (2020).
32. Spiezia, L. *et al.* COVID-19-related severe hypercoagulability in patients admitted to intensive care unit for acute respiratory failure. *Thromb. Haemost.* **120**, 998–1000 (2020).
33. Pavoni, V., Gianesello, L., Pazzi, M., Stera, C., Meconi, T., Frigieri, F. C. Evaluation of coagulation function by rotation thromboelastometry in critically ill patients with severe COVID-19 pneumonia. *J. Thromb. Thrombolysis* **50**(2), 281–286 (2020).
34. Zhang, Y. *et al.* Clinical and coagulation characteristics of 7 patients with critical COVID-2019 pneumonia and acro-ischemia. *Zhonghua Xue Ye Xue Za Zhi* **41**, E006 (2020).
35. Magro, C. *et al.* Complement associated microvascular injury and thrombosis in the pathogenesis of severe COVID-19 infection: A report of five cases. *Transl. Res.* **220**, 1–13 (2020).
36. Zhang, H., Penninger, J. M., Li, Y., Zhong, N. & Slutsky, A. S. Angiotensin-converting enzyme 2 (ACE2) as a SARS-CoV-2 receptor: Molecular mechanisms and potential therapeutic target. *Intensive Care Med.* **46**, 586–590 (2020).
37. Varga, Z. *et al.* Endothelial cell infection and endotheliitis in COVID-19. *Lancet* **395**, 1417–1418 (2020).
38. Schmitt, F. C. F. *et al.* Acute fibrinolysis shutdown occurs early in septic shock and is associated with increased morbidity and mortality: Results of an observational pilot study. *Ann. Intensive Care* **9**, 19 (2019).
39. Antoniak, S. & Mackman, N. Multiple roles of the coagulation protease cascade during virus infection. *Blood* **123**, 2605–2613 (2014).
40. Gunther, A. *et al.* Alveolar fibrin formation caused by enhanced procoagulant and depressed fibrinolytic capacities in severe pneumonia. Comparison with the acute respiratory distress syndrome. *Am. J. Respir. Crit. Care Med.* **161**, 454–462 (2000).
41. Glas, G. J. *et al.* Bronchoalveolar hemostasis in lung injury and acute respiratory distress syndrome. *J. Thromb. Haemost.* **11**, 17–25 (2013).
42. Xiong, Y. *et al.* Transcriptomic characteristics of bronchoalveolar lavage fluid and peripheral blood mononuclear cells in COVID-19 patients. *Emerg. Microbes Infect.* **9**, 761–770 (2020).
43. Tang, N. *et al.* Anticoagulant treatment is associated with decreased mortality in severe coronavirus disease 2019 patients with coagulopathy. *J. Thromb. Haemost.* **18**, 1094–1099 (2020).
44. Liu, Y. *et al.* Unfractionated heparin alleviates sepsis-induced acute lung injury by protecting tight junctions. *J. Surg. Res.* **238**, 175–185 (2019).
45. Thachil, J. The versatile heparin in COVID-19. *J. Thromb. Haemost.* **18**, 1020–1022 (2020).

46. Spyropoulos, A. C. *et al.* Scientific and Standardization Committee communication: Clinical guidance on the diagnosis, prevention, and treatment of venous thromboembolism in hospitalized patients with COVID-19. *J. Thromb. Haemost.* **18**, 1859–1865 (2020).
47. Connors, J. M. & Levy, J. H. COVID-19 and its implications for thrombosis and anticoagulation. *Blood* **135**, 2033–2040 (2020).
48. Hincker, A., Feit, J., Sladen, R. N. & Wagener, G. Rotational thromboelastometry predicts thromboembolic complications after major non-cardiac surgery. *Crit. Care* **18**, 549 (2014).
49. Akay, O. M., Ustuner, Z., Canturk, Z., Mutlu, F. S. & Gulbas, Z. Laboratory investigation of hypercoagulability in cancer patients using rotation thrombelastography. *Med. Oncol.* **26**, 358–364 (2009).
50. Schochl, H., Frietsch, T., Pavelka, M. & Jambor, C. Hyperfibrinolysis after major trauma: Differential diagnosis of lysis patterns and prognostic value of thrombelastometry. *J. Trauma* **67**, 125–131 (2009).
51. D'Alonzo, D., De Fenza, M. & Pavone, V. COVID-19 and pneumonia: A role for the uPA/uPAR system. *Drug Discov. Today* **25**, 1528–1534 (2020).
52. Spyropoulos, A. C. *et al.* Modified IMPROVE VTE risk score and elevated D-dimer identify a high venous thromboembolism risk in acutely ill medical population for extended thromboprophylaxis. *TH Open* **4**, e59–e65 (2020).
53. Spyropoulos, A. C. *et al.* Predictive and associative models to identify hospitalized medical patients at risk for VTE. *Chest* **140**, 706–714 (2011).
54. Hull, R. D. *et al.* Extended-duration venous thromboembolism prophylaxis in acutely ill medical patients with recently reduced mobility: A randomized trial. *Ann. Intern. Med.* **153**, 8–18 (2010).
55. Lang, T. *et al.* Multi-centre investigation on reference ranges for ROTEM thromboelastometry. *Blood Coagul. Fibrinolysis* **16**, 301–310 (2005).

### Author contributions

J.M.K., D.Z., A.M., S.K., S.P., J.K.-M., I.G., A.K., F.H.M., C.F., T.D. and K.U.E. collected and interpreted clinical data. J.M.K., D.Z. and A.M. wrote the first manuscript draft, all authors revised and approved the manuscript.

### Funding

Open Access funding enabled and organized by Projekt DEAL. This research received no specific grant from any funding agency in the public, commercial, or not-for-profit sectors.

### Competing interests

The authors declare no competing interests.

### Additional information

**Correspondence** and requests for materials should be addressed to J.M.K.

**Reprints and permissions information** is available at [www.nature.com/reprints](http://www.nature.com/reprints).

**Publisher's note** Springer Nature remains neutral with regard to jurisdictional claims in published maps and institutional affiliations.



**Open Access** This article is licensed under a Creative Commons Attribution 4.0 International License, which permits use, sharing, adaptation, distribution and reproduction in any medium or format, as long as you give appropriate credit to the original author(s) and the source, provide a link to the Creative Commons licence, and indicate if changes were made. The images or other third party material in this article are included in the article's Creative Commons licence, unless indicated otherwise in a credit line to the material. If material is not included in the article's Creative Commons licence and your intended use is not permitted by statutory regulation or exceeds the permitted use, you will need to obtain permission directly from the copyright holder. To view a copy of this licence, visit <http://creativecommons.org/licenses/by/4.0/>.

© The Author(s) 2021

### **3.4. Wie beeinflusst die Gerinnungs- und Perfusionsstörung der Lungen Morphologie und Verlauf des ARDS? Lungenkavitationen im C-ARDS**

Wie im Vorhergehenden dargelegt besitzt die Lungenperfusion über verschiedene Pathomechanismen einen großen Einfluss auf die Pathogenese und damit auch den klinischen Verlauf. Sowohl lokale Fehlverteilungen der Lungenperfusion im Verhältnis zur Lungenventilation als auch endotheliale Dysfunktion mit folgender Schrankenstörung und die Aktivierung der Gerinnungskaskaden sind in diesem Zusammenhang als wesentliche Morbiditätsfaktoren anzusehen.

Wir untersuchten Anhand der Computertomographien der Thoraxorgane von allen Patienten mit schwerer COVID-19 Erkrankung, die auf unserer Intensivstation behandelt wurden in Hinblick auf die beschriebenen Phänomene.

Es zeigte sich neben bereits erwähnten thromboembolischen Komplikationen in über 50% der Patienten im Sinne von Lungenembolien eine deutliche Häufung von kavitären Lungenveränderungen in ebenfalls mehr als der Hälfte der Patienten. Desweiteren zeigten sich in einem hohen Prozentsatz die typischen milchglasartigen Infiltrate, die letztlich zumindest auch durch die endotheliale Schädigung und das folgende Kapillarleck bedingt sind.

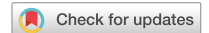
In zwei von drei durchgeführten Obduktionen konnte dann eine in-situ Thrombosierung des zur Kaverne hinführenden Blutgefäßes dokumentiert werden, so dass wir schlossen, dass die kavernösen Veränderungen die das radiologische und klinische Bild entscheidend mitprägen, zum Großteil als durch in-situ Thrombosen bedingt und damit Folge der Aktivierung der Gerinnungskaskaden und der folgenden Perfusionsstörungen zu werten sind.<sup>37</sup>

Wir fanden keine Häufung von bakteriellen Superinfektionen oder gehäufte Keimnachweise in der Gruppe der Patienten die pulmonale Kavernen entwickelten.

Auch die Beatmungsparameter waren in beiden Gruppen nicht signifikant unterschiedlich, so dass auch ein Barotrauma als alleinige Ursache für die gefundenen morphologischen Veränderungen unwahrscheinlich erscheint.

Unsere Ergebnisse unterstreichen die große Bedeutung die der Perfusion in Entwicklung und Verlauf des COVID-assoziierten akuten Lungenversagens zukommt.

**J M Kruse, D Zickler, W M Lüdemann, S K Piper, I  
Gotthardt, J Ihlow, S Greuel, D Horst, A Kahl, K-U Eckardt,  
S Elez Kurtaj: Evidence for a thromboembolic pathogenesis  
of lung cavitations in severely ill COVID-19 patients; Sci  
Rep 2201; 11:16039**



OPEN

## Evidence for a thromboembolic pathogenesis of lung cavitations in severely ill COVID-19 patients

Jan Matthias Kruse<sup>1</sup>, Daniel Zickler<sup>1</sup>, Willie M. Lüdemann<sup>2</sup>, Sophie K. Piper<sup>4</sup>, Inka Gotthardt<sup>1</sup>, Jana Ihlow<sup>3</sup>, Selina Greuel<sup>3</sup>, David Horst<sup>3</sup>, Andreas Kahl<sup>1</sup>, Kai-Uwe Eckardt<sup>1</sup> & Sefer Elezkurtaç<sup>3</sup>

Severe acute respiratory syndrome coronavirus 2 (SARS-CoV-2) causing coronavirus disease 2019 (COVID-19) induces lung injury of varying severity, potentially causing severe acute respiratory distress syndrome (ARDS). Pulmonary injury patterns in COVID-19 patients differ from those in patients with other causes of ARDS. We aimed to explore the frequency and pathogenesis of cavitory lung lesions in critically ill patients with COVID-19. Retrospective study in 39 critically ill adult patients hospitalized with severe acute respiratory syndrome coronavirus 2 including lung injury of varying severity in a tertiary care referral center during March and May 2020, Berlin/Germany. We observed lung cavitations in an unusually large proportion of 22/39 (56%) COVID-19 patients treated on intensive care units (ICU), including 3/5 patients without mechanical ventilation. Median interquartile range (IQR) time between onset of symptoms and ICU admission was 11.5 (6.25–17.75) days. In 15 patients, lung cavitations were already present on the first CT scan, performed after ICU admission; in seven patients they developed during a subsequent median (IQR) observation period of 48 (35–58) days. In seven patients we found at least one cavitation with a diameter > 2 cm (maximum 10 cm). Patients who developed cavitations were older and had a higher body mass index. Autopsy findings in three patients revealed that the cavitations reflected lung infarcts undergoing liquefaction, secondary to thrombotic pulmonary artery branch occlusions. Lung cavitations appear to be a frequent complication of severely ill COVID-19 patients, probably related to the prothrombotic state associated with COVID-19.

### Abbreviations

ACE-2	Angiotensin converting enzyme 2
APACHE	Acute Physiology And Chronic Health Evaluation
ARDS	Acute respiratory distress syndrome
BMI	Body mass index
COVID-19	Coronavirus disease 2019
CRP	C-reactive protein
CRRT	Continuous renal replacement therapy
CT	Computer tomography
ECMO	Extracorporeal membrane oxygenation therapy
HE	Hematoxylin and eosin staining
ICU	Intensive care unit
IQR	Interquartile range
PAS	Periodic acid Schiff's reaction
PCR	Polymerase chain reaction
PEEP	Positive endexpiratory pressure

<sup>1</sup>Department of Nephrology and Medical Intensive Care, Charité – Universitätsmedizin Berlin, Augustenburger Platz 1, 13353 Berlin, Germany. <sup>2</sup>Institute of Radiology, Charité – Universitätsmedizin Berlin, Berlin, Germany. <sup>3</sup>Institute of Pathology, Charité – Universitätsmedizin Berlin, corporate member of Freie Universität Berlin and Humboldt-Universität zu Berlin, Charitéplatz 1, 10117 Berlin, Germany. <sup>4</sup>Institute of Biometry and Clinical Epidemiology, Charité – Universitätsmedizin Berlin, corporate member of Freie Universität Berlin and Humboldt-Universität zu Berlin, Charitéplatz 1, 10117 Berlin, Germany. ✉email: jan-matthias.kruse@charite.de; sefer.elezkurtaç@charite.de

PIP	Peak inspiratory pressure
PTT	Partial thromboplastin time
SARS-CoV-2	Severe acute respiratory syndrome coronavirus 2
SOFA	Sequential Organ Failure Assessment
UFH	Unfractionated heparin
VT	Tidal volume
VTE	Venous thromboembolic

The novel severe acute respiratory syndrome coronavirus 2 (SARS-CoV-2), a beta coronavirus is causing coronavirus disease 2019 (COVID-19). In the past months, its spread to most countries of the world has led to a global pandemic<sup>1</sup>, causing more than 1,600,000 deaths to date<sup>2</sup>.

Severe hypoxemic respiratory failure due to acute lung injury is the most common complication leading to admission to intensive care units (ICU) and one of the main causes of death<sup>3,4</sup>. The precise etiology of the impaired gas exchange and optimal treatment strategies remain a matter of debate<sup>5</sup>. Of note, some clinical aspects seem to differentiate COVID-19 from other forms of acute respiratory distress syndrome (ARDS). In particular, in many COVID-19 patients with ARDS the pulmonary compliance is not significantly altered, in contrast to classic ARDS<sup>5</sup>.

Besides lung injury a prothrombotic state has emerged as an important characteristic of COVID-19. Data from both clinical studies and postmortem case series demonstrate a high incidence of thromboembolic events<sup>6–9</sup>. These events include pulmonary artery occlusions, which may have a thrombotic or thromboembolic origin<sup>10</sup>. Massive pulmonary embolism has been suggested to cause out-of-hospital mortality<sup>11</sup>. Whether pulmonary artery occlusion contributes to hypoxemic respiratory failure due to impaired lung perfusion and dead space ventilation is controversial<sup>12</sup>.

To clarify the etiology of the seemingly high incidence of cavitory lesions was the purpose of the retrospective analysis of our cohort of severely ill COVID-19 patients.

## Material and methods

Since we conducted a retrospective analysis the materials and methods section describes the standard of care of COVID-19 patients in our institution. We screened the electronic records for possible discriminating factors between patients who did and did not develop cavitory lesions with special consideration of markers of the coagulation and inflammatory cascades.

**Patients.** We retrospectively analyzed clinical patient data of 39 COVID-19 patients admitted to ICU between March and May 2020 who received at least one chest CT shortly before or during their ICU stay. All patients were tested positive for SARS-CoV-2 by polymerase chain reaction (PCR). Five patients were admitted through the emergency department, one patient was directly admitted to our ICU from an outpatient setting, two patients had worsened during their stay on regular wards and 31 patients were secondary referrals from other ICUs.

**Anticoagulation.** All patients received unfractionated heparin (UFH) with a targeted partial thromboplastin time (PTT) of 50–55. Patients who suffered from venous thromboembolic (VTE) complications or who had other indications for therapeutic anticoagulation were dosed for a target PTT of 60–80 s.

Patients who did not reach the target PTT with usual doses of UFH were switched to Argatroban. Patients were also switched to Argatroban when they required extracorporeal membrane oxygenation therapy (ECMO).

**Mechanical ventilation.** All mechanically ventilated patients received pressure controlled ventilation. Positive endexpiratory pressure (PEEP) was titrated to reach best possible oxygenation index. Patients received low tidal volume ventilation with a target tidal volume (VT) of 6 ml/kg/PBW and a driving pressure below 15 mmHg was targeted.

**Data collection.** CT scans were analyzed independently by two of us (JMK, WML) for parenchymal cavities, defined as a lucency within a zone of pulmonary consolidation, a mass, or a nodule; hence, a lucent area within the lung that may or may not contain a fluid level and that was surrounded by a wall of varied thickness<sup>13</sup>.

Screening for venous thrombosis was performed using ultrasound (GE Vivid S70 ultrasound machine with a 9L-D probe) in all patients after ICU admission and repeated at least weekly.

Laboratory parameters included viscoelastic coagulation testing after ICU admission using the ROTEM Sigma System (Tem International, Munich, Germany)<sup>14</sup>. Maximum values of C-reactive protein (CRP), d-dimers, fibrinogen, leukocytes, interleukin-6 and procalcitonin were compared between patient groups.

Microbiology reports of all of the collected specimens from the respiratory tract and blood cultures were analyzed for pneumopathogenic species.

The highest levels of PEEP, peak inspiratory pressure and driving pressure during the ICU stay were recorded and analyzed in ventilated patients.

The highest values for SOFA and APACHE II during the course of therapy were recorded and analyzed.

Five patients (13%) had died during their ICU stay, 22 patients (56%) had been discharged alive and 12 patients (31%) were still treated on ICU. On three of the five patients who succumbed, autopsies were performed on days 31, 37 and 47 after ICU admission. The study was approved by the Ethics Committee of the Charité (EA4/115/20) and was in compliance with the Declaration of Helsinki.

**Autopsy procedure.** Complete autopsies and tissue sampling were performed by opening all luminal structures and lamellar incisions of all parenchymatous organs. The lung was dissected by a combination of lamellar incision and subsequent selective preparation of the airways and blood vessels to allow for visualization of pulmonary lesions in the context of vascular supply and airways. For histopathology, representative tissue samples of all organs were fixed in 4% buffered formalin, dehydrated, paraffin embedded and sectioned with a thickness of 4  $\mu\text{m}$ . Paraffin sections were stained with hematoxylin and eosin (HE), periodic acid Schiff's reaction (PAS), Van Gieson's elastic stain, Prussian blue stain and Kongo-red stain. Two pathologists (DH and SE) examined all slides by light microscopy.

**Statistics.** Statistical evaluations were performed with IBM SPSS Statistics Version 26 (New York, USA). The descriptives are given as median and limits of the interquartile range [IQR] for continuous variables or as absolute and relative frequencies for categorical variables.

Due to the retrospective nature of the study no sample-size or power calculations were performed. We conducted a post-hoc power calculation as a substitute.

Mann–Whitney  $U$  tests were used to compare differences between patient groups in continuous variables while Chi-squared tests were used for categorical data. A two-sided significance level of 0.05 was applied without adjustment for multiple comparison. All  $p$ -values constitute exploratory data analysis and do not allow for confirmatory generalization of results.

**Ethics approval and consent to participate.** The study was approved by the ethics committees of Charité – Universitätsmedizin Berlin (EA4/115/20) and was in compliance with the Declaration of Helsinki. Informed consent was waived by the ethics committees of Charité – Universitätsmedizin Berlin due to the retrospective nature of the study.

## Results

**Chest CT findings.** 64 CT scans were analyzed, of which 39 were performed shortly before or after ICU admission and 25 during the course of the ICU stay. In 37/39 (95%) of patients we found ground glass opacities of the lung parenchyma, characterized as “mosaic pattern”. Cavitory lung lesions were found in 22 patients (56; 95% confidence interval 41–72%), of which 15 patients presented with cavitations in the initial CT while seven patients exhibited cavitory lesions in a subsequent CT scan.

Among patients with cavitations the number of cavities between left and right lung were similar. Cavitations were evenly distributed between central and peripheral parts of the lungs. Eleven patients presented with peripherally and 11 patients with centrally located cavitations. Thirteen patients showed involvement of the lower parts, while in 9 patients cavitations were found in the upper parts of the lung. Figure 1 shows typical characteristics of cavitory lesions on representative CT scans. The spectrum ranges from unilateral peripheral cavitations (Fig. 1A) to well-separated lesions in both lungs (Fig. 1B) and extensive bilateral cavitating destructions of the lung parenchyma (Fig. 1C). Maximum cavitation size in the two patients with the largest cavities was approximately 10 cm. Repetitive CT scans had been performed in 13/22 patients. In these patients a comparison between first and last CT scan showed an increase in cavity number in eight patients, no change in four patients and a decline in one patient. In 18/22 patients, cavities were identified in opaque lung areas (example in Fig. 1D). Among patients with lung cavities 19 were on mechanical ventilation, while three patients required no mechanical ventilation.

**Clinical characteristics.** Table 1 shows demographics, preexisting comorbidities and treatment parameters of the patient cohort and the two subgroups with and without lung cavitations. Most parameters were similar between groups, except that patients in the group with cavitations were older and had a higher body mass index (BMI) than those without cavitations.

Fifteen patients (38%) developed deep vein thrombosis. Pulmonary emboli were identified by CT imaging in five patients (12% of the whole group), four with and one without lung cavitations. Two patients had an ischemic stroke (5%). One patient required urgent extracorporeal membrane oxygenation (ECMO)-circuit change due to fulminant clotting and one patient showed acute thrombotic obstruction of the venous drainage cannula on ECMO. There was no statistically significant difference when considering all these thromboembolic complications combined between the group of patients with and without lung cavities.

**Ventilation parameters.** 34 patients (87%) were mechanically ventilated via endotracheal tube or tracheostomy using a pressure controlled mode. The median peak inspiratory pressure (PIP) was 31 mbar [IQR 28.7–35.0], the median positive endexpiratory pressure was 17 mbar [IQR 15–18.2]. The median driving pressure was 15 mbar [IQR 11.7–17.2]. There were no significant differences in these parameters between the group of patients with and without cavitory lesions on CT. 25 patients were prone (64%), 12 patients in the group with and 13 patients in the group without lung cavitations. Ten Patients received nitric oxide (26%), six and four patients with and without cavitations, respectively. Ten patients were treated with veno-venous ECMO (26%), four and six patients with and without cavitations, respectively.

**Laboratory and microbiology findings.** Table 2 shows markers of inflammation and coagulation. These parameters did not differ significantly between the patients with and without cavitations.

Positive cultures of respiratory secretions were found in 32 of our patients (82%), 16 (73%) patients with and 16 patients (94%) without pulmonary cavities. The microbial spectrum appeared typical for ventilated patients. Bacterial species known to be able to induce pulmonary abscesses, such as *Klebsiella spp.* and *Staphylococcus aureus*

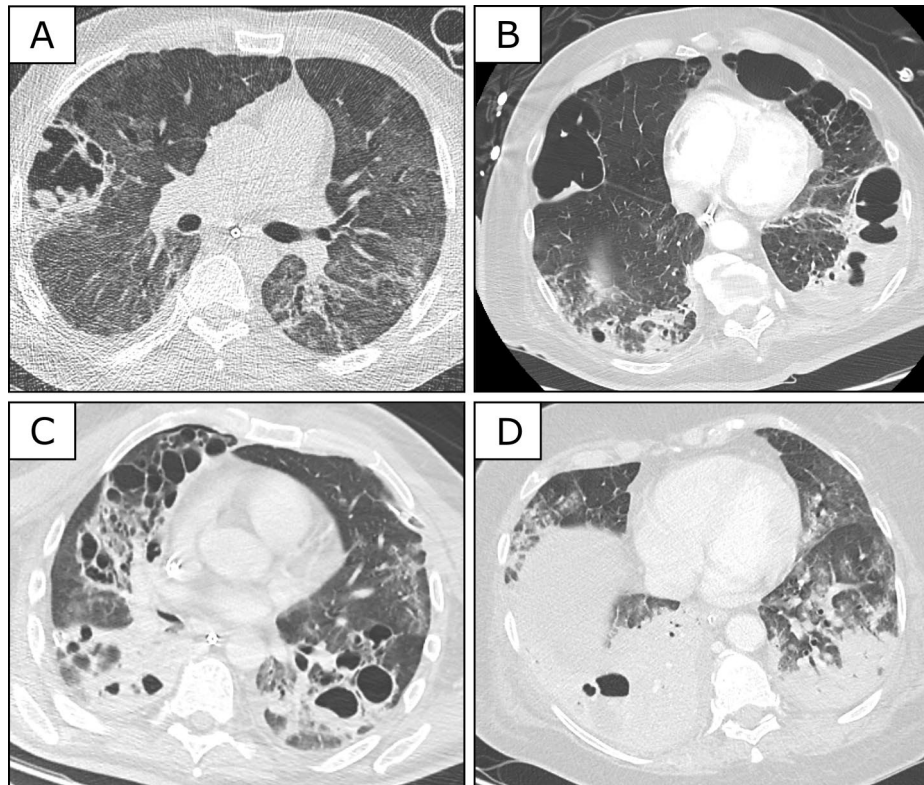


**Figure 1.** CT scans in COVID-19 patients receiving long term ICU care. CT scans showing typical cavitary lesions in four COVID-19 patients. (A) Single cavity in a 49-year old male patient 29 days after symptom onset; (B) bilateral cavitations in a 77-year old male patient 39 days after onset of symptoms; (C) extensive bilateral cavities in a 57-year old male patient on day 36 after symptom onset; (D) right-sided cavitation in a large lower lobe consolidation in a 69-year old female patient 29 days after onset of symptoms. Only open source software (GIMP 2.10.18 <https://www.gimp.org/> and Inkscape, Version 1.0 (4035a4fb49, 2020–05-01) ) were used to generate the figure.

were cultivated in 13 and 11 of the patients with or without lung cavities, respectively. All bronchoalveolar lavage specimens were tested for *Mycobacterium tuberculosis* and none of them revealed a positive result.

**Autopsy findings.** In all three patients in whom an autopsy was performed, lung cavities had previously been identified on CT scans. External examination of the lungs showed pronounced pleural fibrin deposits and sunken lung areas, which corresponded to bullous transformations of lung parenchyma. Findings in two patients are presented in Fig. 2. Upon opening the cavities appeared as areas of liquefied necrosis (Fig. 2B). Careful dissection revealed connections between cavities and bronchial system (Fig. 2C). Moreover, preparation of the pulmonary vessels on frontally oriented cross-sections yielded unequivocal associations of cavitary lesions with thrombotic occlusion of the supplying pulmonary artery branches (Fig. 2D, E). Microscopy of adjacent lung tissue revealed numerous thrombotic vascular occlusions and extended, partially hemorrhagic and partially anemic infarct zones in spatial association with vascular occlusions (Fig. 2F). The border zone of the infarct areas showed pronounced neutrophil infiltrations, but there was morphologic evidence for bacterial colonization. In summary, macro- and microscopic findings in combination suggested extensive vascular occlusions of different duration with multiple pulmonary infarctions of different size, some of which had transformed into liquefying necrosis, corresponding to large cavities. Table 3 shows markers of coagulation, inflammation and ventilation of the patients, who underwent autopsy.

## Discussion

We noted extensive lung cavitations in single cases of COVID-19, which prompted us to perform a systematic analysis of a cohort of 39 critically ill COVID-19 patients consecutively admitted to two ICUs in a tertiary care referral center. This analysis revealed a high incidence of cavitary lung lesions. Computer tomography (CT) morphology and the results of postmortem macro- and micropathological examination point to an ischemic etiology of these lesions due to thrombotic obstruction of pulmonary artery branches. Our findings indicate that lung cavitations of variable size, at least in part a consequence of liquefying ischemic lung infarcts, contribute to lung pathology and loss of functional lung parenchyma in COVID-19 patients. These observations extend the reported spectrum of lung CT findings that is considered as typical for COVID-19, including ground glass opacities, consolidations and a “crazy paving pattern” of the lung parenchyma<sup>15,16</sup>.

	Cohort (N = 39)		Lung cavitations (N = 22)		No cavitations (N = 17)		<i>p</i> -value
Age (years, (median, [IQR]))	67	[58–76]	69.5	[60.5–77.3]	62	[61.5–67.75]	0.047
Gender, male (n, %)	34	(87%)	19	(86%)	15	(88%)	0.86 s
BMI, kg/m <sup>2</sup> (median, [IQR])	28	[25–33]	27.8	[24.2–33]	25.2	[24.32–28.7]	0.009
Days between symptom onset and ICU admission	11	[25–33]	12	[6–17]	11	[6–19]	0.49
Duration ICU stay, days (median, [IQR])	28	[15.5–39.8]	30.9	[27.07–34.25]	25	[8.5–30.5]	0.25
Intubation (n, %)	34	(87.2%)	18	(81%)	16	(94%)	0.47
ECMO (n, %)	10	(25.6%)	5	(22%)	5	(29.4%)	0.22
CRRT* (n, %)	19	(48.7%)	12	(54.5%)	7	(50%)	0.19
SOFA-Score (median, [IQR])	9	[7–12]	10	[6–11]	9	[7–11]	0.49
APACHE-Score (median, [IQR])	28	[22–33]	28	[24–34]	26	[22–34]	0.65
Secondary ICU referral	23	(59.0%)	11	(48%)	12	(52%)	0.32
PEEP (median, [IQR])	17	[15–18]	17	[15–18]	17	[15–19]	0.58
PIP (median, [IQR])	31	[29–35]	32	[27–35]	31	[29–34]	0.90
Delta P (median, [IQR])	15	[12–17]	17	[15–18]	15	[12–16]	0.86
<b>Preexisting conditions</b>							
Coronary artery disease (n, %)	9	(23.1%)	7	(31.2%)	2	(11.7%)	0.44
Hypertension (n, %)	27	(74.0%)	14	(63.63%)	13	(76.5%)	0.12
Diabetes mellitus/insulin resistance (n, %)	14	(35.9%)	8	(36.4%)	6	(35.3%)	0.62
Chronic kidney disease (n, %)	7	(17.9%)	3	(13.6%)	4	(23.5%)	0.42
Chronic dialysis (n, %)	1	(2.5%)	0	(0%)	1	(5.9%)	0.30
COPD (n, %)	10	(25.6%)	7	(31.8%)	3	(17.6%)	0.32

**Table 1.** Patient characteristics of total cohort and the groups with and without cavitory lesions on CT scan. ECMO, Extracorporeal Membrane Oxygenation; SOFA, Sequential Organ Failure Assessment; CRRT, Continuous Renal Replacement Therapy; APACHE, Acute Physiology And Chronic Health Evaluation. PEEP, positive endexpiratory pressure, PIP, Peak inspiratory pressure, deltaP, driving pressure. \*Until the time point, when the study was censored.

	Cohort (N = 39)						
	Median	[IQR]	Cavitations				<i>p</i> -value
			Yes (N = 22)		No (N = 17)		
			Median	[IQR]	Median	[IQR]	
<b>Laboratory variables (normal values)</b>							
Haemoglobin (12.5–17.2 g/dL)	10.1	[8.5–11.2]	10.1	[8.7–11.9]	9.50	[8.1–10.9]	0.34
White blood cells (3.5–10.5/nl)	19.3	[16.3–28.8]	21.4	[17–30.6]	19.3	[14.9–28.8]	0.63
Platelet count (150–370/nl)	186	[131.3–314]	190	[128–254.0]	186	[121–324]	0.68
Prothrombin time (70–130%)	71	[62–82.7]	70	[51–82.5]	74.5	[67.25–85]	0.27
INR (0.9–1.25)	1.35	[1.2–1.6]	1.5	[1.3–1.7]	1.29	[1.1–1.4]	0.12
PTT (26–40 s)	45.7	[40–56.1]	45.1	[40.3–58.5]	46.1	[39.1–56]	0.75
Fibrinogen (1.6–4 g/l)	6.6	[4.7–7.8]	6.4	[4.7–7.2]	6.1	[4.6–7.9]	0.38
D-dimers (<0.5 mg/l)	8.4	[3.9–17.2]	10	[3.6–18.6]	8.2	[3.9–11.6]	0.48
Procalcitonin (0.5 µg/l)	7.6	[1.9–15.7]	7.9	[1–16.9]	7.6	[3.1–18.9]	0.86
CRP (<0.5 mg/l)	312.9	[207.1–344.1]	305.6	[181.8–352.5]	333.9	[215.6–344.4]	0.56
IL-6 (<7 ng/l)	558.6	[180.2–1921.7]	567.2	[163.8–18600]	550	[179.5–1894.5]	0.97
Ferritin (30–400 µg/l)	2619.8	[1557–7111.9]	2621	[1155.7–8068.8]	2113.3	[1710.9–6392.2]	0.50
Ristocetin-Co-factor (%)	349	[204–404]	349	[179.5–429.5]	291	[259–401.5]	0.78
vWillebrand antigen (%)	391	[283.5–400]	394	[266.5–400]	368.5	[278.7–400]	0.96
Factor VIII (50–150%)	258	[190.5–319.5]	259	[212.2–293.5]	245	[153.2–340]	0.71
EXTEM MCF (mm)	75	[70–78]	74.5	[69.7–78.2]	76	[70.5–77.5]	0.89

**Table 2.** Coagulation, inflammatory and ROTEM parameters of total cohort and sub cohorts with and without cavitory lesions on CT-scan.

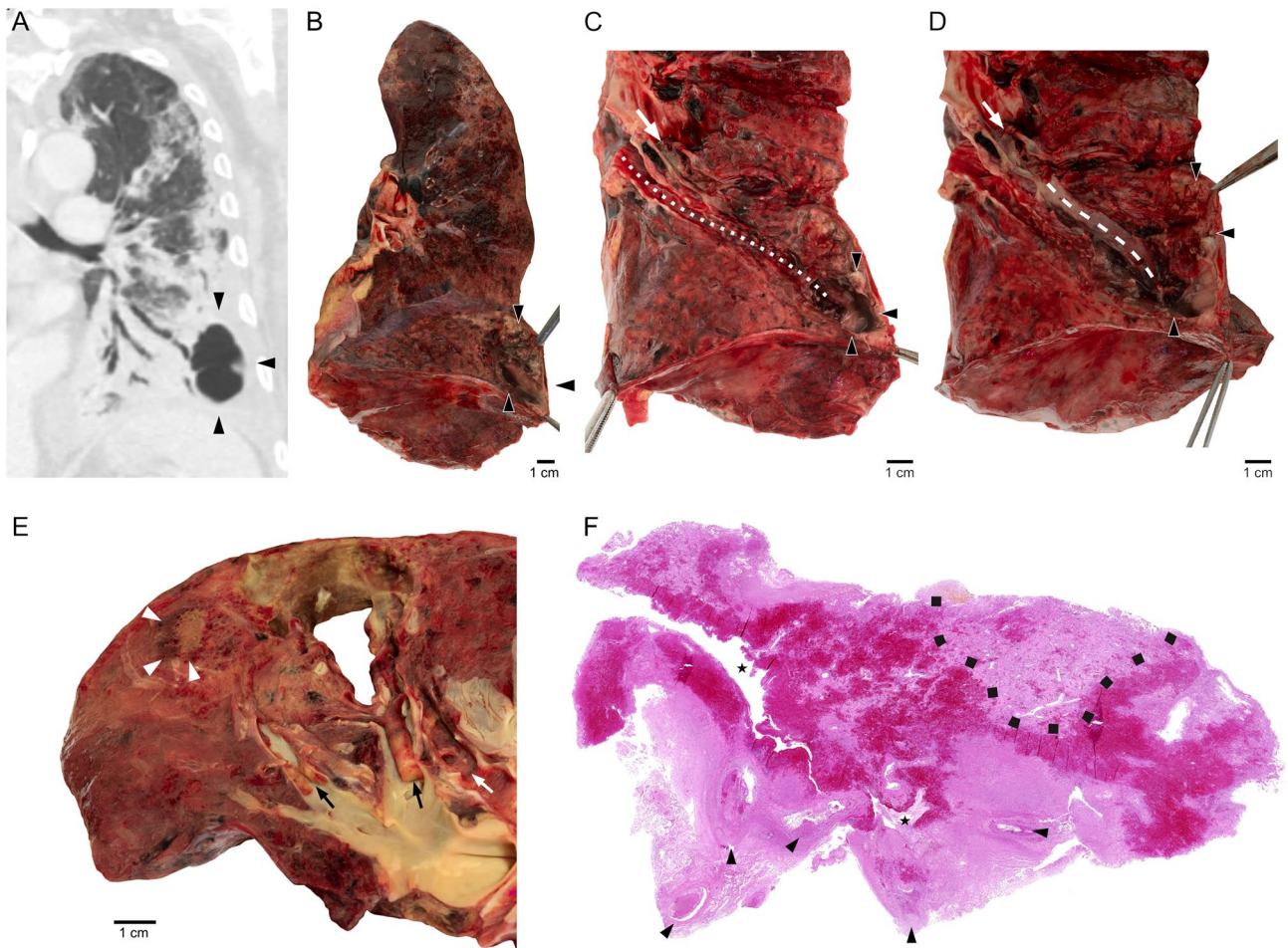


**Figure 2.** Postmortem findings in two patients. (A)–(D) show findings in a 77-year old patient who died 42 days after ICU admission. (A) Frontal reconstruction of lung CT showing large basal, left-sided cavity (corresponding to cross-sectional CT scan in Fig. 1B). Macroscopic findings during subsequent preparation steps show (B) opened lung cavity with necrotic lining (arrowheads), (C) direct connection of an opened bronchus with the cavity (dotted line), corresponding to positive aerogram on CT (A) and (D) a pulmonary artery branch (stippled line), directly connected with the necrotic cavity. A thrombotic vessel occlusion is indicated by white arrows. (E) and (F) show macro- and microscopic findings in a 69-year old patient, who died 33 days after ICU admission. (E) Opened pulmonary artery branches with subtotal (left) and total (right) occlusion of the vessel lumen (black arrows), and a directly adjacent lung cavity, suggesting that the large thrombus on the right has caused liquefactive infarct necrosis of the lung parenchyma. The necrotic area has gained access to the bronchial system (white arrow). The adjacent lung parenchyma shows a combined anemic and hemorrhagic infarct (arrowheads) that has not undergone cavitory transformation. (F) Histological sectioning (HE) shows multiple thrombotic occlusions (arrowheads) of pulmonary artery branches with consecutive anemic infarct necrosis (light red zones) with entrapment of bronchial airways (asterisks). Dark red zones around the bronchial airways represent hemorrhagic necrosis. The black dotted line delineates a small area of vital lung parenchyma.

In general, infectious causes and ventilator induced lung injury are recognized as the main etiologies of lung cavities in critically ill patients<sup>17</sup>. Ischemia is less commonly considered as a cause, although cavitations are described in up to 32% of patients with pulmonary embolism and are a common finding in patients suffering from chronic thromboembolic pulmonary hypertension<sup>18,19</sup>. While the precise pathogenesis is difficult to ascertain in individual cases in our study, we believe that several lines of evidence indicate that an ischemic pathogenesis rather than alternative causes play a major role.

First, several of our findings are not consistent with primarily ventilator induced lung injury. Ventilator settings were chosen to minimize lung trauma and did not differ significantly between the groups with and without lung cavities. The distribution of the cavities with a significant proportion of central lesions and involvement of the lower parts of the lung argues against ventilator induced lung injury, since from our experience one would expect mainly peripheral lesions in the upper lobes, if mechanical overdistension played the main role. The observation that a high percentage of lesions occurred in preexisting opacities also seems rather untypical for classical ventilator induced lung alterations. Due to higher compliance of the less affected regions, overdistension tends to occur preferentially in non-opaque regions of the lung. Most striking is the fact, that three of five patients,

Patient	1	2	3
Prothrombin time (70–130%)	69	50	71
INR (0.9–1.25)	1.2	2	1.2
PTT (26–40 s)	46	64	38
Fibrinogen (1.6–4 g/l)	5.36	6.2	5.2
D-dimers (<0.5 mg/l)	13.1	6.6	3.0
Procalcitonin (0.5 µg/l)	0.6	1.8	0.2
CRP (<0.5 mg/l)	157	255	133
IL-6 (<7 ng/l)	142	224	104
Ferritin (30–400 µg/l)	2633	4078	1490
EXTEM MCF (mm)	58	78	78
PEEP (mmHg)	17	18	16
PIP (mmHg)	35	41	31
deltaP (mmHg)	18	23	15

**Table 3.** Coagulation, inflammatory and ventilatory parameters of three patients who underwent autopsy. PEEP, positive endexpiratory pressure, PIP, Peak inspiratory pressure, deltaP, driving pressure, CRP, C-reactive-protein, IL-6, Interleukin-6, INR, International normalized ratio, PTT Partial Thromboplastin Time.

who did not need mechanical ventilation, also developed cavitations. Still mechanical ventilation might play an important role in the development of the cavitory lesions in that it aggravates the damage done by microvascular and macrovascular thrombosis. We therefore think that sticking to the principles of lung-protective ventilation is of great importance in this group of patients to minimize pulmonary destructions even if the lung compliance does not seem to be altered in every case.

Second, patients who developed cavitations did not exhibit positive cultures more often than the patients without, nor did we find typical abscess inducing species more frequently in the patients with lung cavities. However, a secondary bacterial infection of infarcted areas, transforming into cavitations cannot be ruled out.

Third, we found evidence for a prothrombotic state both in terms of coagulation parameters and thromboembolic complications. Although thromboembolic complications were evenly distributed between patients with and without lung cavities, notably pulmonary embolism was more frequent in patients with cavities (4 vs. 1). Patients who developed cavitations during the course of their disease were significantly older and had a higher BMI. Obesity has been associated with a prothrombotic state and hypofibrinolysis<sup>20–24</sup>. The “mosaic pattern” of the lung-parenchyma that we observed in accordance with previous publications and the lung cavities strikingly resemble findings in patients with chronic thromboembolic pulmonary hypertension<sup>15,18,19</sup>.

During the time of this observational study critical care resources for COVID-19 patients were in no way compromised in our regional setting, enabling long-term ICU therapy. Together with a very large proportion of secondary referrals this might explain why others have to the best of our knowledge not yet reported similar observations. However, several other observations support the concept of impaired lung perfusion in COVID-19 patients. Ackermann et al. found a high incidence of microvascular thrombi and signs of endothelitis during autopsy of seven COVID-19 patients<sup>6</sup>. Lang et al., using dual source computer tomography, discovered severe perfusion abnormalities in the lungs of three COVID-19 patients and postulated a significant contribution of altered perfusion to the etiology of respiratory failure in COVID-19<sup>12</sup>.

In terms of the mechanisms potentially causing pulmonary hypoperfusion, SARS-CoV-2 binds to the angiotensin converting enzyme 2 (ACE-2) receptor of alveolar epithelial cells<sup>25</sup>. There is evidence for consecutive downregulation of ACE-2 leading to increased levels of angiotensin II<sup>25</sup>. High levels of angiotensin II in the pulmonary circulation may lead to endothelial activation and vasoconstriction and promote a prothrombotic state<sup>26</sup>. Hypoperfusion of pulmonary artery branches either due to vasoconstriction or due to thromboembolic occlusion will lead to increased dead space ventilation and impaired gas exchange, consistent with the ventilation pattern observed in COVID-19<sup>5,27</sup>. Selective perfusion of the pulmonary circulation through anastomoses between the bronchial and the pulmonary circulation might further contribute to respiratory failure due to an increased right-to left shunt fraction<sup>28</sup>.

By implying a link between a prothrombotic stage, pulmonary hypoperfusion and structural lung changes, our data add to the considerations for therapeutic anticoagulation in COVID-19 patients. Interestingly in this regard Wang et al. recently reported a positive impact of tissue plasminogen activator treatment on oxygenation in a case series<sup>29</sup>. An association of higher therapeutic targets of systemic anticoagulation and improved survival has also been reported<sup>11,30</sup>. Although our data point towards a thromboembolic etiology of the cavitory lesions, the markers of coagulation measured in our study could not discriminate between the two groups and significant differences were only found regarding age and BMI. D-Dimers for example were not significantly different between the groups. One might argue that due to the high degree of activation of the coagulation system in both groups, the d-dimers are not sensitive enough to detect a difference. Increased age and body weight might lead to structural weakness of the lung tissue facilitating the development of cavitations. Hopefully future studies will identify more sensitive and specific laboratory markers in this regard and clarify the precipitating factors that add to the development of cavitory lung destruction in certain patient populations.

Our study has several limitations. Being retrospective and non-interventional it can only be hypothesis-generating. It is monocentric and focusses on severely ill patients, many of whom received ICU treatment for several weeks and our findings may not be generalizable to less severely ill patients. Due to the relatively small sample size, the power of our study is limited. We found a high proportion of cavitory lung lesions in the CT-scan (22/39 = 56%). The 95% confidence interval is 41–72% for our finding of this high incidence of lung cavitations. We included all 39 consecutive patients who received a CT-scan and were treated in our intensive care unit during the first COVID-19 wave, so we cannot provide a larger data set.

To make a more accurate assessment of the proportion of patients with cavitation we would have to include more patient data. For a sample size of 100, a two-sided 95% confidence interval for a single proportion using the large sample normal approximation would extend 0.097 from the observed proportion for an expected proportion of 0.56.

With a sample size of 380, a two-sided 95% confidence interval for a single proportion using the large sample normal approximation would extend only 0.05 from the observed proportion for an expected proportion of 0.56.

The etiology of lung cavitations is possibly heterogeneous and multifactorial. Finally, the number of autopsies supporting our interpretation is small and although all point to the exact same pathogenesis of the cavitations we do not know whether the same results would have been found in the lungs of the other patients of the cohort.

In conclusion, we found that cavitating lung lesions occur frequently in severely ill COVID-19 patients and provide evidence that pulmonary hypoperfusion and occlusion of pulmonary arteries plays an important role in the pathogenesis of these lesions.

## Conclusion

Although the small sample size limits the power of our study, we found a high incidence of cavitory lesions in our cohort of severely ill patients with COVID-19. Our findings underline the importance of sufficient anticoagulation in the management of patients with severe COVID-19 pneumonia. Furthermore our data show, how vulnerable the malperfused lungs of these patients are, even though the compliance might not be altered in the beginning. This points to the importance of lung protective ventilation in order to avoid further damage in the poorly perfused areas of the lungs of these patients.

## Data availability

The datasets analyzed during the current study are available from the corresponding author upon reasonable request.

Received: 22 February 2021; Accepted: 29 July 2021

Published online: 06 August 2021

## References

- Jin, Y. *et al.* Virology, epidemiology, pathogenesis, and control of COVID-19. *Viruses* **12**(4), 372 (2020).
- Dong, E., Du, H. & Gardner, L. An interactive web-based dashboard to track COVID-19 in real time. *Lancet Infect. Dis.* **20**(5), 533–534 (2020).
- Huang, C. *et al.* Clinical features of patients infected with 2019 novel coronavirus in Wuhan, China. *Lancet* **395**(10223), 497–506 (2020).
- Zangrillo, A. *et al.* Characteristics, treatment, outcomes and cause of death of invasively ventilated patients with COVID-19 ARDS in Milan, Italy. *Crit. Care Resusc.* **22**(3), 200–211 (2020).
- Gattinoni, L. *et al.* COVID-19 pneumonia: different respiratory treatments for different phenotypes?. *Intensive Care Med.* **46**(6), 1099–1102 (2020).
- Ackermann, M. *et al.* Pulmonary vascular endothelialitis, thrombosis, and angiogenesis in covid-19. *N. Engl. J. Med.* **383**(2), 120–128 (2020).
- Klok, F. A. *et al.* Confirmation of the high cumulative incidence of thrombotic complications in critically ill ICU patients with COVID-19: an updated analysis. *Thromb Res.* **191**, 148–150 (2020).
- Klok, F. A. *et al.* Incidence of thrombotic complications in critically ill ICU patients with COVID-19. *Thromb Res.* **191**, 145–147 (2020).
- Varga, Z. *et al.* Endothelial cell infection and endotheliitis in COVID-19. *Lancet* **395**(10234), 1417–1418 (2020).
- Lax, S. F. *et al.* Pulmonary arterial thrombosis in COVID-19 with fatal outcome: results from a prospective, single-center, clinicopathologic case series. *Ann. Intern. Med.* **173**(5), 350–361 (2020).
- Wichmann, D. *et al.* Autopsy findings and venous thromboembolism in patients with COVID-19: a prospective cohort study. *Ann. Intern. Med.* **173**(4), 268–277 (2020).
- Lang, M. *et al.* Hypoxaemia related to COVID-19: vascular and perfusion abnormalities on dual-energy CT. *Lancet Infect Dis.* **20**(12), 1365–1366 (2020).
- Hansell, D. M. *et al.* Fleischner society: glossary of terms for thoracic imaging. *Radiology* **246**(3), 697–722 (2008).
- Gorlinger, K., Bhardwaj, V. & Kapoor, P. M. Simulation in coagulation testing using rotational thromboelastometry: a fast emerging, reliable point of care technique. *Ann. Card Anaesth.* **19**(3), 516–520 (2016).
- Shi, H. *et al.* Radiological findings from 81 patients with COVID-19 pneumonia in Wuhan, China: a descriptive study. *Lancet Infect Dis.* **20**(4), 425–434 (2020).
- Ding, X., Xu, J., Zhou, J. & Long, Q. Chest CT findings of COVID-19 pneumonia by duration of symptoms. *Eur. J. Radiol.* **127**, 109009 (2020).
- Parkar, A. P. & Kandiah, P. Differential diagnosis of cavitory lung lesions. *J. Belg. Soc. Radiol.* **100**(1), 100 (2016).
- Harris, H. *et al.* Cavitating lung lesions in chronic thromboembolic pulmonary hypertension. *J. Radiol. Case Rep.* **2**(3), 11–21 (2008).
- Fernandes, C. *et al.* Lung cavities in chronic thromboembolic pulmonary hypertension. *Clinics (Sao Paulo)*. **75**, e1373 (2020).
- Kakafika, A. I., Liberopoulos, E. N., Karagiannis, A., Athyros, V. G. & Mikhailidis, D. P. Dyslipidaemia, hypercoagulability and the metabolic syndrome. *Curr. Vasc. Pharmacol.* **4**(3), 175–183 (2006).
- Mao, X., Ait-Aissa, K., Lagrange, J., Youcef, G. & Louis, H. Hypertension, hypercoagulability and the metabolic syndrome: a cluster of risk factors for cardiovascular disease. *Biomed. Mater. Eng.* **22**(1–3), 35–48 (2012).

22. Mavri, A., Alessi, M. C. & Juhan-Vague, I. Hypofibrinolysis in the insulin resistance syndrome: implication in cardiovascular diseases. *J. Intern. Med.* **255**(4), 448–456 (2004).
23. Nieuwdorp, M., Stroes, E. S., Meijers, J. C. & Buller, H. Hypercoagulability in the metabolic syndrome. *Curr. Opin. Pharmacol.* **5**(2), 155–159 (2005).
24. Vague, P., Raccah, D. & Scelles, V. Hypofibrinolysis and the insulin resistance syndrome. *Int. J. Obes. Relat. Metab. Disord.* **19**(Suppl 1), S11–S15 (1995).
25. Vaduganathan, M. *et al.* Renin-angiotensin-aldosterone system inhibitors in patients with Covid-19. *N Engl J Med.* **382**(17), 1653–1659 (2020).
26. Senchenkova, E. Y., Russell, J., Esmon, C. T. & Granger, D. N. Roles of Coagulation and fibrinolysis in angiotensin II-enhanced microvascular thrombosis. *Microcirculation* **21**(5), 401–407 (2014).
27. Gattinoni, L. *et al.* COVID-19 does not lead to a “typical” acute respiratory distress syndrome. *Am. J. Respir. Crit. Care Med.* **201**(10), 1299–1300 (2020).
28. Galambos, C., Sims-Lucas, S., Abman, S. H. & Cool, C. D. Intrapulmonary bronchopulmonary anastomoses and plexiform lesions in idiopathic pulmonary arterial hypertension. *Am. J. Respir. Crit Care Med.* **193**(5), 574–576 (2016).
29. Wang, J. *et al.* Tissue plasminogen activator (tPA) treatment for COVID-19 associated acute respiratory distress syndrome (ARDS): a case series. *J. Thromb. Haemost.* **18**(7), 1752–1755 (2020).
30. Cui, S., Chen, S., Li, X., Liu, S. & Wang, F. Prevalence of venous thromboembolism in patients with severe novel coronavirus pneumonia. *J. Thromb. Haemost.* **18**(6), 1421–1424 (2020).

## Acknowledgements

We are grateful to Anistan Sebastiampillai and Juliane Plaschke for technical assistance, and to Christoph Weber for photographic illustrations.

## Author contributions

J.M.K., D.Z., W.M.L., S.K.P., I.G., A.K. and K.U.E. collected and interpreted clinical data. D.H., J.I., S.G. and S.E. performed autopsies and interpreted autopsy results. J.M.K. and K.U.E. wrote the first manuscript draft, all authors revised and approved the manuscript.

## Funding

Open Access funding enabled and organized by Projekt DEAL. This research received no specific grant from any funding agency in the public, commercial, or not-for-profit sectors.

## Competing interests

The authors declare no competing interests.

## Additional information

**Correspondence** and requests for materials should be addressed to J.M.K. or S.E.

**Reprints and permissions information** is available at [www.nature.com/reprints](http://www.nature.com/reprints).

**Publisher's note** Springer Nature remains neutral with regard to jurisdictional claims in published maps and institutional affiliations.



**Open Access** This article is licensed under a Creative Commons Attribution 4.0 International License, which permits use, sharing, adaptation, distribution and reproduction in any medium or format, as long as you give appropriate credit to the original author(s) and the source, provide a link to the Creative Commons licence, and indicate if changes were made. The images or other third party material in this article are included in the article's Creative Commons licence, unless indicated otherwise in a credit line to the material. If material is not included in the article's Creative Commons licence and your intended use is not permitted by statutory regulation or exceeds the permitted use, you will need to obtain permission directly from the copyright holder. To view a copy of this licence, visit <http://creativecommons.org/licenses/by/4.0/>.

## 4. Diskussion

Seit der Erstbeschreibung des ARDS in den 60er Jahren des zwanzigsten Jahrhunderts haben die Veränderungen der Ventilation im Vergleich zu denen der Perfusion sicherlich den größeren Teil der Aufmerksamkeit erhalten.

Dies ist wohl auch der Tatsache geschuldet, dass Intensivmedizin insbesondere in ihrer Entstehungszeit auch in großen Teilen Beatmungsmedizin war und dies den Fokus auf die ventilatorischen Aspekte des akuten Lungenversagens sicherlich begünstigte.

Auch entwickelten sich die Einsichten in die Pathophysiologie der gestörten Lungenperfusion langsamer, da die direkten Visualisierung in der üblichen Bildgebung weniger zugänglich waren und manche Einsichten in die Funktion von Gerinnungsphysiologie, Endothelfunktion und Inflammationskaskaden molekularbiologische Methoden erforderten, die erst in den der Erstbeschreibung des ARDS folgenden Jahrzehnten ausreichend weiterentwickelt werden konnten um tiefere Einsichten in diesen Bereichen zu ermöglichen.

Von „Science“ wurde Stickstoffmonoxid 1992 zum Molekül des Jahrzehnts gewählt, sicherlich auch weil in der Zwischenzeit die Einblicke in die komplexen Zusammenhänge der Perfusionsregulation gewaltige Fortschritte gemacht hatten<sup>38</sup>.

In dieser Zeit wurde durch Einsatz von Therapien wie eben der inhalativen Gabe von Stickstoffmonoxid erste Versuche unternommen, dem Rechnung zu tragen und den klinischen Verlauf von Patienten mit akutem Lungenversagen durch gezielte Verbesserung der pulmonalen Perfusionssituation positiv zu beeinflussen.

Auch die Einblicke in die komplexen Zusammenhänge von Inflammations- und Gerinnungskaskaden bei Krankheitsbildern wie Sepsis und ARDS lenkten mehr Aufmerksamkeit auf die Bedeutung des Gefäß- und Gerinnungssystems für den

klinischen Verlauf von Patienten im akuten Lungenversagen und auf die Optionen einer Therapie durch medikamentöse Beeinflussung dieser komplexen Systeme<sup>33</sup>.

Auch wenn gezielte Eingriffe in die Mediatorkaskade bislang keine überzeugenden klinischen Ergebnisse erbrachten wie vielleicht beispielhaft die Therapie mit aktiviertem Protein C nicht nur in der Sepsis sondern auch im ARDS zeigt, ist das wissenschaftliche Interesse an und in der Folge auch die Datenbasis für diese Vorgänge und ihre Bedeutung für das Atemnotsyndrom der Erwachsenen kontinuierlich angewachsen<sup>33 39</sup>.

Wie unsere Daten bezüglich der Effekte auf den Gasaustausch durch Kontamination komprimierter Luft mit niedrigen Konzentrationen von Stickstoffmonoxid zeigen, sind die Effekte einer selektiven Vasodilatation auf die Oxygenierung eindeutig vorhanden.

25

Doch wenngleich inhalatives Stickstoffmonoxid gerade in der aktuellen COVID-19 Pandemie häufig als sogenannte „Rescuetherapie“ im schweren ARDS und C-ARDS eingesetzt wird, lässt sich bis heute ein positiver Effekt auf relevante klinische Endpunkte auch in Metanalysen nicht sicher belegen<sup>24</sup>

Allerdings gilt dies auch für die meisten anderen Therapieansätze einschließlich der Beatmung mit hohen PEEP-Werten, Rekrutierungsmanöver und die extrakorporale Membranoxygenierung.<sup>7 16</sup>

Bislang ist abgesehen von der Beatmung der Patienten mit niedrigen Tidalvolumina lediglich der Effekt der Bauchlagerung als Rescuetherapie bei schwerem ARDS unwidersprochen.<sup>6</sup> Über welchen Mechanismus die Bauchlagerung ihren Effekt auf Klinik und Prognose der Patienten entfaltet, ist hingegen bis heute nicht eindeutig geklärt und es existieren überzeugende Daten, die für einen Effekt durch direkte Beeinflussung der Lungenperfusion sprechen<sup>40</sup>

In jedem Falle scheint die Verbesserung des Ventilations- Perfusionsverhältnisses der wahrscheinlichste Mechanismus für den beobachteten Effekt darzustellen.

Das nichkardiale Lungenödem ist in allen aktuell gültigen Definitionen ein Hauptkriterium für die Diagnose des akuten Atemnotsyndroms des Erwachsenen.<sup>41 42</sup> Sicherlich sind die Ursachen nicht immer eindeutig und auch Faktoren wie eine generalisierte Überwässerung spielen in vielen Fällen eine Rolle.

Im Wesentlichen wird das Kapillarleck aber durch ein „Endothelversagen“ hervorgerufen und ist somit ebenfalls dem Gefäßsystem zuzuordnen.<sup>19</sup>

Wir konnten zeigen, dass die bettseitige Ultraschalluntersuchung als nichtinvasives Verfahren zum Monitoring und ggf. auch zur Therapiesteuerung des Patienten mit ARDS einsetzbar ist.<sup>31</sup>

Möglicherweise unterscheidet sich das durch SARS-CoV-2 ausgelöste Lungenversagen substantiell von anderen Verlaufsformen des akuten Atemnotsyndroms des Erwachsenen. Dennoch sind auch für andere Formen des akuten Lungenversagens Störungen des Gerinnungssystems gut dokumentiert. Im C-ARDS konnten wir an unseren Patienten demonstrieren, dass thrombembolische Komplikationen häufig sind und mit einer verminderten fibrinolytischen Aktivität in der viskoleastischen Testung in Verbindung bringen. Wir fanden auch deutlich Hinweise darauf, dass sich die Alteration des Gerinnungssystems bei diesen Patienten nach Abklingen der akuten Erkrankung wieder normalisiert. Ob auch im ARDS aus andere Ursache diese Veränderungen des Gerinnungssystems nachgewiesen werden könne bleibt zu untersuchen.

Desweiteren konnten wir aufgetretene kavitäre Lungenparenchymveränderungen mit in-situ-Thrombosierungen in der Lungenstrombahn in Verbindung bringen. Ob auch hier Analogien zu anderen Formen des akuten Lungenversagens zu finden sind muss durch weitere Untersuchungen geklärt werden.

## 5. Zusammenfassung

In den vorgelegten Arbeiten konnte der Stellenwert der Perfusion in der Pathogenese und Klinik des akuten Lungenversagens näher beleuchtet werden.

Es wurde Anhand der Wirkung geringster Dosen von Stickstoffmonoxid in der Atemluft die Bedeutung des Gefäßtonus in der Lungenstrombahn und des Ventilations-Perfusionsverhältnisses in der Lunge gezeigt.

Desweiteren zeigten wir, dass die durch das Kapillarleck in der Lungenstrombahn verursachte pulmonale Überwässerung bettseitig mittels Ultraschall einfach und zuverlässig quantifiziert werden kann.

Wir konnten an Patienten mit durch COVID-19 ausgelöstem Lungenversagen die Häufung von thromboembolischen Ereignissen in dieser Patientengruppe zeigen und mittels viskoelastischer Testverfahren eine erhöhte Gerinnselfestigkeit und gleichzeitig eine verminderte Fibrinolyseaktivität demonstrieren.

Durch Verlaufsuntersuchungen konnten wir weiterhin darlegen, dass die gezeigten Veränderungen der Gerinnungsaktivität zwölf Wochen nach Entlassung von der Intensivstation nicht mehr nachweisbar waren.

Zuletzt konnten wir durch Analyse von Computertomographien des Thorax von Patienten im C-ARDS ein Häufiges Auftreten von kavitären Lungendestruktionen dokumentieren und mittels der Obduktionsbefunde eine ischämische Genese als wahrscheinliche Ursache feststellen und damit die Auswirkungen der Perfusionsstörung auf die Pathogenese des Lungenversagens unterstreichen.

Gemeinsam belegen die Arbeiten, dass auch Veränderungen der pulmonalen Perfusion, sei es durch Veränderungen des pulmonalen Gefäßsystems, sei es durch Alteration der Gerinnung eine große Bedeutung für die Pathogenese des akuten Lungenversagens zukommt.

## 6. Literatur

1. Ashbaugh DG, Bigelow DB, Petty TL, Levine BE. Acute respiratory distress in adults. *Lancet*. 1967;2(7511):319-323.
2. Bellani G, Laffey JG, Pham T, Fan E, Investigators LS, the ETG. The LUNG SAFE study: a presentation of the prevalence of ARDS according to the Berlin Definition! *Crit Care*. 2016;20:268.
3. Thompson BT, Chambers RC, Liu KD. Acute Respiratory Distress Syndrome. *N Engl J Med*. 2017;377(19):1904-1905.
4. Acute Respiratory Distress Syndrome N, Brower RG, Matthay MA, et al. Ventilation with lower tidal volumes as compared with traditional tidal volumes for acute lung injury and the acute respiratory distress syndrome. *N Engl J Med*. 2000;342(18):1301-1308.
5. National Heart L, Blood Institute Acute Respiratory Distress Syndrome Clinical Trials N, Wiedemann HP, et al. Comparison of two fluid-management strategies in acute lung injury. *N Engl J Med*. 2006;354(24):2564-2575.
6. Guerin C, Reignier J, Richard JC, et al. Prone positioning in severe acute respiratory distress syndrome. *N Engl J Med*. 2013;368(23):2159-2168.
7. Combes A, Hajage D, Capellier G, et al. Extracorporeal Membrane Oxygenation for Severe Acute Respiratory Distress Syndrome. *N Engl J Med*. 2018;378(21):1965-1975.
8. National Heart L, Blood Institute PCTN, Moss M, et al. Early Neuromuscular Blockade in the Acute Respiratory Distress Syndrome. *N Engl J Med*. 2019;380(21):1997-2008.
9. Papazian L, Forel JM, Gacouin A, et al. Neuromuscular blockers in early acute respiratory distress syndrome. *N Engl J Med*. 2010;363(12):1107-1116.
10. Dong E, Du H, Gardner L. An interactive web-based dashboard to track COVID-19 in real time. *Lancet Infect Dis*. 2020;20(5):533-534.
11. Gattinoni L, Chiumello D, Caironi P, et al. COVID-19 pneumonia: different respiratory treatments for different phenotypes? *Intensive Care Med*. 2020;46(6):1099-1102.
12. Klok FA, Kruip M, van der Meer NJM, et al. Incidence of thrombotic complications in critically ill ICU patients with COVID-19. *Thromb Res*. 2020;191:145-147.
13. Yao Y, Cao J, Wang Q, et al. D-dimer as a biomarker for disease severity and mortality in COVID-19 patients: a case control study. *J Intensive Care*. 2020;8:49.
14. Petersson J, Glenn RW. Gas exchange and ventilation-perfusion relationships in the lung. *Eur Respir J*. 2014;44(4):1023-1041.
15. Suter PM, Fairley B, Isenberg MD. Optimum end-expiratory airway pressure in patients with acute pulmonary failure. *N Engl J Med*. 1975;292(6):284-289.
16. Writing Group for the Alveolar Recruitment for Acute Respiratory Distress Syndrome Trial I, Cavalcanti AB, Suzumura EA, et al. Effect of Lung Recruitment and Titrated Positive End-Expiratory Pressure (PEEP) vs Low PEEP on Mortality in Patients With

- Acute Respiratory Distress Syndrome: A Randomized Clinical Trial. *JAMA*. 2017;318(14):1335-1345.
17. Brower RG, Lanken PN, MacIntyre N, et al. Higher versus lower positive end-expiratory pressures in patients with the acute respiratory distress syndrome. *N Engl J Med*. 2004;351(4):327-336.
  18. Meade MO, Cook DJ, Guyatt GH, et al. Ventilation strategy using low tidal volumes, recruitment maneuvers, and high positive end-expiratory pressure for acute lung injury and acute respiratory distress syndrome: a randomized controlled trial. *JAMA*. 2008;299(6):637-645.
  19. Gonzales JN, Lucas R, Verin AD. The Acute Respiratory Distress Syndrome: Mechanisms and Perspective Therapeutic Approaches. *Austin J Vasc Med*. 2015;2(1).
  20. Klein A, Edler C, Fitzek A, et al. [The first COVID-19 hotspot in a retirement home in Hamburg]. *Rechtsmedizin (Berl)*. 2020:1-7.
  21. Wichmann D. Autopsy Findings and Venous Thromboembolism in Patients With COVID-19. *Ann Intern Med*. 2020;173(12):1030.
  22. Rossaint R, Falke KJ, Lopez F, Slama K, Pison U, Zapol WM. Inhaled nitric oxide for the adult respiratory distress syndrome. *N Engl J Med*. 1993;328(6):399-405.
  23. Hsu CW, Lee DL, Lin SL, Sun SF, Chang HW. The initial response to inhaled nitric oxide treatment for intensive care unit patients with acute respiratory distress syndrome. *Respiration*. 2008;75(3):288-295.
  24. Gebistorf F, Karam O, Wetterslev J, Afshari A. Inhaled nitric oxide for acute respiratory distress syndrome (ARDS) in children and adults. *Cochrane Database Syst Rev*. 2016(6):CD002787.
  25. Hess W, Kannmacher J, Kruse J. Contamination of anaesthetic gases with nitric oxide and its influence on oxygenation: study in patients undergoing open heart surgery. *Br J Anaesth*. 2004;93(5):629-633.
  26. Ware LB, Matthay MA. Clinical practice. Acute pulmonary edema. *N Engl J Med*. 2005;353(26):2788-2796.
  27. Costello ML, Mathieu-Costello O, West JB. Stress failure of alveolar epithelial cells studied by scanning electron microscopy. *Am Rev Respir Dis*. 1992;145(6):1446-1455.
  28. Sartori C, Rimoldi SF, Scherrer U. Lung fluid movements in hypoxia. *Prog Cardiovasc Dis*. 2010;52(6):493-499.
  29. Lichtenstein DA. Lung ultrasound in the critically ill. *Ann Intensive Care*. 2014;4(1):1.
  30. Lichtenstein D, Meziere G, Biderman P, Gepner A, Barre O. The comet-tail artifact. An ultrasound sign of alveolar-interstitial syndrome. *Am J Respir Crit Care Med*. 1997;156(5):1640-1646.

31. Enghard P, Rademacher S, Nee J, et al. Simplified lung ultrasound protocol shows excellent prediction of extravascular lung water in ventilated intensive care patients. *Crit Care*. 2015;19:36.
32. Gando S, Kameue T, Matsuda N, Sawamura A, Hayakawa M, Kato H. Systemic inflammation and disseminated intravascular coagulation in early stage of ALI and ARDS: role of neutrophil and endothelial activation. *Inflammation*. 2004;28(4):237-244.
33. Hasegawa N, Husari AW, Hart WT, Kandra TG, Raffin TA. Role of the coagulation system in ARDS. *Chest*. 1994;105(1):268-277.
34. Kruse JM, Magomedov A, Kurreck A, et al. Thromboembolic complications in critically ill COVID-19 patients are associated with impaired fibrinolysis. *Crit Care*. 2020;24(1):676.
35. Godier A, Clausse D, Meslin S, et al. Major bleeding complications in critically ill patients with COVID-19 pneumonia. *J Thromb Thrombolysis*. 2021;52(1):18-21.
36. Magomedov A, Zickler D, Karaivanov S, et al. Viscoelastic testing reveals normalization of the coagulation profile 12 weeks after severe COVID-19. *Sci Rep*. 2021;11(1):13325.
37. Kruse JM, Zickler D, Ludemann WM, et al. Evidence for a thromboembolic pathogenesis of lung cavitations in severely ill COVID-19 patients. *Sci Rep*. 2021;11(1):16039.
38. Koshland DE, Jr. The molecule of the year. *Science*. 1992;258(5090):1861.
39. Cornet AD, Groeneveld AB, Hofstra JJ, et al. Recombinant human activated protein C in the treatment of acute respiratory distress syndrome: a randomized clinical trial. *PLoS One*. 2014;9(3):e90983.
40. Nyren S, Radell P, Lindahl SG, et al. Lung ventilation and perfusion in prone and supine postures with reference to anesthetized and mechanically ventilated healthy volunteers. *Anesthesiology*. 2010;112(3):682-687.
41. Force ADT, Ranieri VM, Rubenfeld GD, et al. Acute respiratory distress syndrome: the Berlin Definition. *JAMA*. 2012;307(23):2526-2533.
42. Bernard GR, Artigas A, Brigham KL, et al. The American-European Consensus Conference on ARDS. Definitions, mechanisms, relevant outcomes, and clinical trial coordination. *Am J Respir Crit Care Med*. 1994;149(3 Pt 1):818-824.

## 7. Danksagung

Zuerst möchte ich Herrn PD. Dr. med Philipp Enghard danken, der mich ermutigt hat, inmitten meiner klinischen Karriere noch einmal Zeit und Mühe in die klinische Forschung zu investieren. Er hat mir durch seine Begeisterung Freude an der Forschung vorgelebt und vermittelt und mir immer mit Rat und Tat zur Seite gestanden. Desweiteren schulde ich meinem Kollegen Dr. med. Daniel Zickler Dank, mit dem gemeinsam ich viele Projekte in Angriff nehmen und auch beenden konnte und der mich immer unterstützt hat.

Professor Dr. med Wolfgang Heß hat mich als mein Doktorvater überhaupt erst in die klinische Forschung eingeführt, mich gefördert und unterstützt, wofür ich ihm immer dankbar sein werde.

Außerdem gilt mein Dank Professor Dr. med Achim Jörres und Professor Dr. med Kai-Uwe Eckardt, die mich ebenfalls immer gefördert und ermutigt haben.

Meinen klinischen Vorbildern PD Dr. Dietrich Hasper, PD Dr. Michael Oppert, Lutz Nibbe, PD Dr. Frank Martens und Fabrizio Esposito und Dr. med Niko Ruge gebührt ebenso Dank, da Sie mir Freude am Beruf vermittelt, mich viel gelehrt und mich in Forschungsbemühungen immer unterstützt haben.

Desweiteren danke ich allen meinen Kollegen der Abteilung für Innere Medizin m.S. Nephrologie und Internistische Intensivmedizin, die mir stets Anregungen und Unterstützung zuteil werden ließen.

Mein letzter und größter Dank gilt meiner Frau Irina und meinen Kindern Mascha, Neva und Aaron, die zu oft auf meine Unterstützung verzichten mussten und mir trotzdem mit bedingungsloser Liebe und Verständnis immer den Rücken gestärkt haben.

## 8. Erklärung

§ 4 Abs. 3 (k) der HabOMed der Charité

Hiermit erkläre ich, Jan Matthias Kruse, dass

– weder früher noch gleichzeitig ein Habilitationsverfahren durchgeführt oder angemeldet wurde.

– die vorgelegte Habilitationsschrift ohne fremde Hilfe verfasst, die beschriebenen

Ergebnisse selbst gewonnen sowie die verwendeten Hilfsmittel, die Zusammenarbeit mit

anderen Wissenschaftlern/Wissenschaftlerinnen und mit technischen Hilfskräften sowie die

verwendete Literatur vollständig in der Habilitationsschrift angegeben wurden.

– mir die geltende Habilitationsordnung bekannt ist.

29.11.2021

Unterschrift